Regulation of cellular differentiation by the *Drosophila argos* gene product

（ショウジョウバエ *argos* 遺伝子産物による細胞分化制御機構の解析）

Kazunobu Sawamoto

澤本 和延

Regulation of cellular differentiation by the *Drosophila argos* gene product Kazunobu Sawamoto

博士論文

Regulation of cellular differentiation by the *Drosophila argos* gene product

（ショウジョウバエargos遺伝子産物による細胞分化制御機構の解析）

東京大学大学院医学系研究科
第二基礎医学専攻　博士課程
平成４年入学
（指導教官：御子柴克彦教授）

澤本和延

Preface

How different cell types are generated from a group of equipotent cells is a central question in developmental biology. Both inductive and negative mechanisms have been shown to be involved in this process. They have been extensively studied using the developing eye of an excellent model organism, *Drosophila melanogaster*. Cell to cell interactions appear to direct cell fate decisions in the developing eye.

To understand the mechanisms for the regulation of cellular differentiation, I have undertaken the study of *argos* gene, which has been identified in a screening for mutants displaying rough eye phenotype. In the chapter 1, I describe molecular cloning of the *argos* gene and phenotypic analyses of the loss-of-function mutants. In the chapter 2, I report the effect of ectopic overexpression of the *argos* gene on eye and wing development. In the chapter 3, I focus on the function of *argos* in projection of photoreceptor axons during optic lobe development. In the chapter 4, I analyze the genetic interactions between *argos* and components in the Ras/MAP kinase cascade. Results obtained from these studies suggest that *argos* is a diffusible inhibitor of signal transduction in the MAP kinase cascade for cell determination.

Contents

Chapter 1. Identification and characterization of the *Drosophila argos* locus

Abstract	4
1-1 Introduction	4
1-2 Materials and Methods	6
1-3 Results and Discussion	9
Figures and Table	17

Chapter 2. Ectopic overexpression of *argos* inhibits cellular differentiation during *Drosophila* eye and wing vein development

Abstract	27
2-1 Introduction	27
2-2 Materials and Methods	29
2-3 Results	31
2-4 Discussion	35
Figures	39

Chapter 3. The function of *argos* in projection of photoreceptor axons during optic lobe development in *Drosophila*

Abstract	46
3-1 Introduction	46
3-2 Materials and Methods	48
3-4 Results	50
3-5 Discussion	55
Figures	58

Chapter 4. *argos* inhibits signal transduction in the MAP kinase cascade

Abstract	67
4-1 Introduction	67
4-2 Materials and Methods	69
4-3 Results	70
4-4 Discussion	75
Figures and Table	79

References 87

Conclusions 99

Acknowledgments 101

Chapter 1
Identification and characterization of the *Drosophila argos* locus

Abstract

The technique of transposon P-element enhancer trapping was used to identify new genes important in *Drosophila* eye development. *Drosophila argos* was isolated as a novel visual system mutant displaying rough eye phenotype. Analyses of mutant phenotypes and the expression pattern of the gene suggested that the *argos* gene has pleiotropic functions. Mutations in the *argos* gene affect eye development, leading to irregular spacing of ommatidia, an increase in the number of photoreceptor cells, and abnormal axonal projection and disrupted structure of optic lobes in the adult fly. In addition to affecting the visual system, they cause abnormal head involution, an increased number of sensilla in the antenno-maxillary complex in the embryonic stage, and abnormal morphogenesis of labial palps and the wings in later stages. I examined the expression of the *argos* gene during development in terms of *LacZ* expression from enhancer trap elements inserted within the *argos* gene. During embryogenesis, expression of *LacZ* showed a segmental pattern in the ectoderm and in the nervous system. In the eye imaginal discs, *LacZ* began to be expressed in photoreceptor cells, a few rows posterior to the morphogenetic furrow. It was also expressed in the wing disc. In the adult, it was expressed in retinula cells and the lamina. We cloned the *argos* gene by P-element tagging. On the basis of the phenotype on loss of its function, its expression pattern, and the predicted structure of its product, a secreted peptide with a putative epidermal growth factor (EGF) motif, I propose that *argos* encodes a diffusible protein with pleiotropic functions acting as a signal involved in lateral inhibition within the developing nervous system and also as a factor involved in axonal guidance.

1-1. Introduction

There is increasing interest in analysis of the molecular and cellular mechanisms involved in determination of cell fate within the developing nervous system of both vertebrates and invertebrates. In general, cell fate is believed to be determined by cell lineage and also through the interactions, including cell-cell interactions, of a pluripotent cell with its environment. The development of the compound eye of *Drosophila* is an excellent model for study of the molecular mechanisms involved in cell fate determination and cell-cell interaction during neuronal development for several reasons. First, *Drosophila* can be examined by both molecular and classical genetic methods. Mutations in the eye can easily be generated and identified on the basis of morphological phenotypes. Cloned genes can be efficiently reintroduced into the *Drosophila* genome to allow their normal expression by the P-element mediated germ line transformation technique (Rubin and Spradling, 1982; Spradling and Rubin, 1982). Second, the structure of the compound eye of *Drosophila* is highly organized, thereby providing a convenient system for studying the mechanism of cell assembly. The compound eye of *Drosophila* is composed of 750 simple units named "ommatidia". Each of these units consists of 22 cells including eight photoreceptor cells (R1-8). Their topological arrangement within the ommatidium and synaptic connection are highly organized. The plasma membrane of the photoreceptor cells has multiply folded microvilli, forming a structure, the rhabdomere, which is a functional counterpart of the outer segment of vertebrate photoreceptor cells. These structures are arranged in a stereotypic trapezoidal pattern. Third, the gross features of cellular determination in vertebrates are similar to those in the *Drosophila* compound eye in many respects. Several lines of evidence suggest that determination of cell fate in the *Drosophila* retina is a consequence of cell-cell interactions (Ready et al., 1976). In the compound eye, a sheet of pluripotent cells is rapidly transformed into an array of identical neural units in a lineage-independent manner during pupal development. This independence from cell lineage restrictions is analogous to the regulation of differentiation of neural crest cells by local environmental cues (Le Douarin, 1980) and the determination of neuronal and/or glial cell types by nonclonal mechanisms in the vertebrate nervous system (Holt et al., 1988; Luskin et al, 1988; Vassein et al., 1987).

During the course of neural development, cells that become neural cells appear to inhibit their neighbors from adopting a neural fate by a process known as "lateral inhibition" (Doe and Goodman, 1985). Recently, proteins similar to growth factors and their receptors or secreted proteins have been found to be involved in lateral inhibition during development of the *Drosophila* nervous system (Kidd et al., 1986; Vassein et al., 1987; Kopczynsi et al., 1988; Mlodzik et al., 1990; Baker et al., 1990; Wharton et al., 1985).

The *argos* mutation was identified on screening *Drosophila* visual mutations generated by P-element insertion mutagenesis (Okano et al., 1992). Mutations in *argos* cause severe rough-eye phenotype, the production of supernumerary photoreceptor cells and irregular development of the array of ommatidia in the eye (Freeman et al., 1992; Kretzschmar et al., 1992; Okano et al., 1992). Molecular characterization of the *argos* locus revealed that it encodes a putative secreted protein with an EGF motif, the sequence of which is identical to the gene products reported recently (Freeman et al., 1992; Kretzschmar et al., 1992). Taken together, these findings suggest that *argos* encodes an inhibitory signal that regulates neuronal differentiation in eye imaginal discs. The *argos* gene is also required for normal development of cephalic regions and the wings, and for axonal guidance in the optic lobe. Thus, I concluded that the *argos* gene has pleiotropic functions in the normal development of neuronal and other systems.

1-2. Materials and Methods

Genetics

Fly culture and crosses were conducted according to standard procedures described previously (Roberts, 1986). The $argos^{sty1}$ mutant was isolated as a mutant line exhibiting a severe rough eye phenotype (see Text). We also obtained another line $argos^{sty2}$ with a P-element (P[lacW]) (Bier et al., 1989) insertion at the 73A locus (a gift from Dr. M. Scott). The $argos^{sty2}$ line also displayed a rough eye phenotype that was slightly less severe than that of $argos^{sty1}$. The $argos^{sty1e20}$ and $argos^{2e1}$ lines showing the rough eye phenotype were obtained by excising the P-element from $argos^{sty1}$ and $argos^{sty2}$ lines, respectively. Lethal stocks [*l(3)73Aa* and *l(3)73Ab*] and a series of lines with deficiencies surrounding the 73A locus [*Df(3L)st-e4, Df(3L)st-f13, Df(3L)st-j7, Df(3L)st-k10, Df(3L)st4, Df(3L)g24* and *Df(3L)TRDS*] (Belote et al., 1990) (gifts from Dr. B. Baker) were examined to determine whether they complemented $argos^{sty2}$.

Chromosomal in situ hybridization

Salivary gland polytene chromosomes from late third instar larvae of $argos^{sty1}$ heterozygotes were prepared and hybridized with a probe as described by Zuker et al. (1985). The probe was prepared by labeling P-element DNA with digoxygenin-dUTP, and hybridization of the probe was detected using an anti-digoxygenin monoclonal antibody coupled to alkaline phosphatase (Boehringer Mannheim, Mannheim, Germany).

Preparation and analysis of embryonic cuticle

Preparation and analysis of embryonic cuticle were performed as described previously (Wiechaus and Nüsslein-Volhard, 1986).

Histochemistry

The location of β-galactosidase protein was determined by X-gal staining and immunohistochemical methods with an anti-β-galactosidase monoclonal antibody [dilution 1:200 (Promega, Madison, USA)] as described previously (Fortini and Rubin, 1990; Ingham et al., 1985). Immunohistochemical analysis using antibodies against ubiquitous neuronal antigens Mab 22C10 (Fujita et al., 1982) and 44C11 (Bier et al., 1988) were also performed in the same way.

Electron microscopic analysis

Histological analysis was performed on the $argos^{sty2}$ fly. Samples were prepared for transmission electron microscopy as follows. Tissues were prefixed for 3 hours with 2% paraformaldehyde and 2% glutaraldehyde in 0.1 M cacodylate buffer pH 7.2, washed with the same buffer and dehydrated in a graded ethanol series. Then they were embedded in LR White (London Resin Co., Basingstoke, Hampshire, England), and polymerized at 50° C for 24 hours. Sections of 100 nm thickness were cut on a Sorval MT-2B ultramicrotome and were collected on copper grids. They were stained with uranyl acetate and/or lead citrate and examined with a JEM-100CX electron microscope (JEOL, Tokyo, Japan). Samples of $argos^{sty2}$ and wild-type flies were analyzed by scanning electron microscopy as follows. Flies were gradually dehydrated in an ethanol series (25%, 50%, 75%, 100%, 100%) followed by a freon series (25%, 50%, 75%, 100%, 100% Freon113 in ethanol) and dried in vacuo. Mounted flies were spatter coated with platinum and examined with an ISI DS-130 microscope.

Cloning of the *argos* locus

The plasmid rescue technique was used to recover DNA sequences flanking the P-element insertion according to the method described previously (Bier et al., 1989; Mlodzik et al., 1990). Subsequently, λEMBL3 (a gift from Drs. J. Tamukun and M. Scott) and Charon4A genomic libraries of *Drosophila* (a gift from Dr. T. Maniatis) were screened with the rescued plasmids as probes according to the standard method (Sambrook et al., 1989). A 0.7 kb cDNA clone (cStb-1) was isolated by screening a λgt10 embryonic cDNA library made by Drs. J. Tamkun and M. Scott using the 5.8 kb *Sac*II fragment including the P-element insertion site in $argos^{sty2}$ line as a probe. Subsequently, the cDNA fragment in cStb-1 was used as a probe to screen a λZAP embryonic cDNA library made in Dr. Y. Jan's laboratory (a gift from Dr. T. Uemura) and 10 cDNA clones were obtained. The cStb-b3-3 clone had the longest insert (2.0 kb).

Northern blot analysis

Total RNA was isolated from total flies, fly heads, bodies and staged embryos (5-9 or 8-22 hours) by the acid phenol method described previously (Puissant and Houdebine, 1990), and poly(A)$^+$ RNA was prepared by oligo(dT)-cellulose affinity chromatography (Sambrook et al., 1989). The probe was prepared by labeling 1.2 kb and 0.7 kb *Eco*RI cDNA fragments from cStb-b3-3 with ^{32}P-dCTP using a random primed DNA labeling kit (Boehringer Mannheim, Mannheim, Germany). Subsequent Northern blot analysis was performed according to standard protocol described by Furuichi et al.(1989).

DNA sequencing

The DNA sequence was determined by the chain termination method (Sanger et al., 1977) using Sequenase (United States Biochemical, Cleveland, USA). DNA from the cDNA clones Stb b3-3 was sequenced completely on both strands by use of Bluescript (Stratagene, La Jolla, USA) vectors containing restriction fragments from cDNA as templates. We used T3 (5' ATTAACCCTCACTAAAG 3') and T7 (5' AATACGACTCACTATAG 3') primers, and various oligonucleotides as sequencing primers. Genomic sequences immediately 5' to the P insertion site were determined by use of the rescued plasmid as a template and the 22-mer oligonucleotide (5' CTCAACAAGCAAACGTGCACTG 3') at the 5' end of the P element as a primer. Conceptual translation of the nucleotide sequence and analysis of the hydropathy profile based on the method of Kyte and Doolittle (1982) were performed using the MacVector 3.5 (IBI-A Kodak, New Haven, USA) program.

1-3. Results and Discussion

Identification and genetic analysis of the *argos* locus

We performed P-element insertion mutagenesis to detect as yet unidentified genes that are important in eye development. In such mutagenesis, a P-transposable element is randomly integrated into the genome and often disrupts or reduces gene activity (Cooley et al., 1988; O'Kane and Gehring, 1987). P-element insertion mutagenesis was performed by the method of Cooley et al. (Cooley et al., 1988). The *3639* mutations (3639^{sty1} and 3639^{sty2}) were identified by P-element (Bier et al., 1989; Mlodzik and Hiromi, 1992) mutagenesis screening as mutations that produced a severe rough eye phenotype. In addition to inducing the rough eye phenotype, these mutations greatly reduced viability. However, surviving adult flies were fertile. The 3639^{sty1} and 3639^{sty2} genomes each had a single P-element insert, as shown by Southern blot analysis (data not shown). The transposon in 3639^{sty1} was mobilized by mating to flies carrying a stable source of transposase activity (Robertson et al., 1988). We established 24 lines that had lost the ry^+ marker gene carried in the PZ element. In 75 % of these lines, the mutant eye phenotype had reverted to the wild type, indicating that the phenotype is due solely to the insertion of the P-element. Of the excision lines, 8% still showed recessive eye phenotypes. The $3639^{sty1e20}$ is a line displaying a slightly rough eye phenotype. All these excision lines with the rough eye phenotype were semilethal and 16 % showed a completely lethal phenotype (Table 1). The P-lacW+ in 3639^{sty2} was also excised similarly and 27 excision lines were established. In 52 % of these lines, the mutant phenotype had reverted to the wild type and 30 % of the excision lines showed eye phenotypes raging in severity from "slightly rough" to "very rough". The 3639^{2e1} is a line displaying a slightly rough eye phenotype. Of the excision lines, 18% showed a completely lethal phenotype (Table 1).

The cytogenetic position of the *3639* locus was determined to be 73A1-2 on the third chromosome by the polytene chromosome in situ hybridization technique using P-element DNA as a probe (Fig. 1a). There is a known visual system mutation at this locus, *argos* (Freeman et al., 1992; synonim: *giant lens*, Kretzschmar et al., 1992), suggesting that *3639* is allelic to *argos*. Sequence of the cloned *3639* cDNA clearly showed that *3639* is identical to *argos* (see below). Therefore, *3639* is called *argos* in the rest of this article. To define the *argos* locus genetically, flies bearing two *argos* alleles [*argos*^{sty1} and *argos*^{sty2} (see Materials and methods)] were mated to two lines (*l(3)73Aa* and *l(3)73Ab*) and a series of lines with deficiencies surrounding the 73A locus (*Df(3l)st-e4, Df(3L)st-f13, Df(3L)st-j7, Df(3L)st-k10, Df(3L)st4, Df(3L)g24* and *Df(3L)TRDS*) (Fig. 1b). Two of the lethal mutations included in *Df(3L)st-f13* [*l(3)73Aa* and *l(3)73Ab*] complemented *argos*^{sty2}. The *argos*^{sty2} resembled *argos*^{sty2} in trans to a deficiency [*Df(3l)st-e4, Df(3L)st-f13, Df(3L)st-j7, Df(3L)st-k10 , Df(3L)st4* or *Df(3L)g24* ; Fig. 1b] with respect to the eye phenotype and lethality, suggesting that these phenotypes reflect a loss of function. *Df(3L)TRDS*, however, did complement the *argos* mutation. These deficiency mapping data placed *argos* to the right of the centromere distal breakpoint of the *Df(3L)st-j7* at 73A1-2 , and left of the centromere proximal breakpoint of *Df(3L)st-f13* at 73A3-4. This position is consistent with the results obtained by polytene chromosome in situ hybridization. The rough eye phenotype of *argos*^{sty2} was enhanced by a deficiency placed in trans, suggesting that the phenotype is the result of reduced *argos* function.

argos embryonic mutant phenotype

The *argos*^{sty1} and *argos*^{sty2} homozygotes exhibited severely reduced viability and most of them died during embryogenesis, suggesting that *argos* has another role besides that in the visual system. We characterized the *LacZ* expression pattern of the *argos* enhancer trap line (Fig. 2) and its mutant phenotype (Fig. 3). To characterize the expression of the *argos* gene, I took advantage of the fact that *argos*^{sty1} and *argos*^{sty2} mutations were induced by insertion of a P-element vector containing the *LacZ* gene (PZ- and P-lacW-elements, respectively). If these P-element vectors are inserted near a genomic transcriptional enhancer, the pattern of β–galactosidase expression from the weak P-element promoter is known in most cases, to reflect the pattern of expression of the genes normally regulated by the enhancer (Bellen et al., 1989; Bier et al., 1989; O'Kane and Gehring, 1987). Both the PZ- and P-lacW-elements encode P-transposase-b-galactosidase fusion proteins which are localized in the nuclei of cells where the gene is expressed.

Here I describe b-galactosidase expression in *argos*^{sty2} embryos only, because I found that *argos*^{sty1} embryos also showed an essentially similar pattern of expression. Fig.2 shows β-galactosidase expression in *argos*^{sty2} heterozygous embryos at the end of germ band retraction. The expression of β-galactosidase in the gnathal segment was detected in prominent structures in mandibular and maxillary segments which probably would give rise to the antenno-maxillary complex. The expression of β-galactosidase was also detected in abdominal segments, especially at segment boundaries, and it was much lower in thoracic segments.

We next examined cuticle preparations of wild type and *argos* mutant embryos (Fig. 3). Several alleles and combinations of them were studied, among which, *argos*^{2e1}/*Df(3L)st4* embryos showed the most severe phenotype and are described here. The most prominent defect was failure of head involution. In addition, the majority of severely affected embryos failed to retract a germ band (Fig. 3e,f). We also noticed that ventral denticle belts were expanded laterally, however, their patterns were similar to those of wild type larvae. Close examination of the antenno-maxillary complex, a prominent sense organ in the head, revealed that mutant embryos had an increased number of sensilla. The antenno-maxillary complex is composed of several sensilla. The dome shaped antennal sense organ (aso) is derived from the procephalon. The maxillary part is composed of two large sensilla (dorso-lateral and dorso-medial papilla; dlp and dmp) and seven small sensilla. Jürgen et al. (1986). showed that these regions have separate origins, aso and dmp from the procephalic lobe, dlp from the mandibular segment and the rest of them from the maxillary segment. In the *argos* mutant embryo, there were one or two additional large and small sensilla. In some cases, aso was duplicated. But in spite of these abnormalities, the arrangement of sensilla was essentially normal, suggesting that the process of head segment fusion of this part took place relatively normally. These results suggests that one function of *argos* is to maintain the correct number of larval sense organs.

The mutant phenotype and *LacZ* expression in adult visual systems

Analysis of adult eyes showed that mutations in the *argos* gene affected eye development, leading to irregular spacing of ommatidia, an increase in the number of photoreceptor cells within each ommatidium, lens fusion and axonal guidance misrouting in the optic lobes (Fig. 5).

The fine structure of adult compound eyes were analyzed in detail by electron microscopy. Transmission electronmicroscopic analysis of a section through the eye of a young *argos*^{sty2} fly revealed that the extra neural cells observed in the eye disc developed into supernumerary photoreceptors (Fig. 7a,b). The organization of rhabdomeres was severely disrupted in *argos* mutant eyes. The diameter of all the rhabdomeres seemed to be expanded and the extraretinula space was narrower than in wild-type flies. Although the rhabdomeres in each ommatidium were arranged in a trapezoid manner in *argos* mutants, the axis was not fixed and often oriented abnormally. The arrangement of R1 to R6 cells was not fixed, their order being clockwise in some and anti-clockwise in other cases. Additional outer rhabdomeres were sometimes seen.

The scanning electron microscopic analysis revealed a roughening of the external surface of the eye in *argos*^{sty2} flies. Several lenses fused with each other and the number and spacing of bristles were also affected (Fig. 6 b,c). The sockets and mechanosensory bristles on the compound eye were occasionally duplicated. In the compound eye of *Drosophila*, each bristle group is formed by four cells, which are known to be derived from a single precursor cell (Cagan and Ready, 1989). Two rounds of cell divisions result in four cells: the tormogen which secretes the socket; the trichogen which secretes the bristle; and a sensory neuron and its supporting glial cell, the thecogen. The trichogen and tormogen appear first, followed by the neuron and thecogen. Our present observations indicated that extra precursor cells may be formed in the mutants in which *argos* has lost its function. Alternatively, an additional trichogen may be recruited from an uncommitted precursor cell.

Interestingly, I also found that the projection pattern of photoreceptor cell axons and laminar structures of the optic lobe were severely disorganized in the adult head of the *argos*^{sty2} mutant judging from the staining pattern with monoclonal antibody 22C10 (Fujita et al., 1982), which recognizes ubiquitous *Drosophila* neural antigen (Fig. 6g,h). Despite the severe defect in morphology of the photoreceptor cells, mutant flies showed a normal profile of response in an electroretinogram to light stimuli (data not shown). The on and off transient component did not differ from that of wild-type flies. This result indicates that the machinery for visual excitation in the retinula cells was not impaired in the mutants.

Next, I characterized the *LacZ* expression pattern in adult visual systems of the *argos* heterozygotes (*argos*^{sty1}/+ or *argos*^{sty2}/+). The *argos*^{sty1} and *argos*^{sty2} mutations were recessive for the mutant phenotypes described above and heterozygotes were nearly wild type (data not shown). In the adult, X-gal stainings were observed in the nuclei of cell clusters near the surface of compound eyes and lamina (Fig. 5e). For determination of the positions of photoreceptor nuclei, sections of adult head, that had been stained by the X-gal were stained again with monoclonal antibodies against a ubiquitous neuronal antigen 44C11 (Bier et al., 1988). The 44C11 epitope is encoded by the *embryonic lethal abnormal visual system* (*elav*) gene and is present in the nuclei of all neurons (Bier et al., 1988; Bier et al., 1989). As the nuclei that stained "blue" were located more apically than the nuclei of photoreceptor cells marked by 44C11, the cells expressing the *argos* in the adult retina are not photoreceptor cells (data not shown).

The mutant phenotype and *LacZ* expression in developing visual systems

To obtain information on the *argos* adult phenotypes, I studied the development of imaginal tissues in third instar larvae. The wave of differentiation to form ommatidia is associated with the progression of the morphogenetic furrow, a dorso-ventral groove, anteriorly across the eye disc (Ready et al., 1976). A monoclonal antibody, 22C10 (Fujita et al., 1982), has been used to study the sequence of photoreceptor differentiation in developing ommatidia (Tomlinson and Ready, 1987). The study revealed that R8 is the first to differentiate, followed by the pairs R2/R5, R3/R4 and R1/R6, and finally by R7. Here I analyzed the eye phenotype of the *argos* mutant by immunolocalization of the 22C10 antigen (Fujita et al., 1982). Our analysis indicated that the initial stages of *argos*^{sty2} ommatidial development are indistinguishable from those of the wild type (Fig. 4). R8 showed neuronal differentiation first in both *argos*^{sty2} and wild type eye imaginal discs. However, the developmental sequence following this point did not occur correctly. We detected extra neural cells in the ommatidia posterior to the third or fourth rows from the morphogenetic furrow of the *argos* eye disc (Fig. 4b). The *argos*^{sty1} homozygotes showed a more severely abnormal phenotype. In addition to the presence of extra neural cells, the *argos*^{sty1} ommatidia were spaced irregularly.

We also characterized the *LacZ* expression pattern in developing eye discs of *argos* heterozygotes. The β-galactosidase protein was first detectable in some photoreceptor cells located 2-3 rows behind the morphogenetic furrow (Fig. 5a,b,c). In the larval brain, the *argos* gene expression was detected in the developing optic lobes (Fig. 5g), implying that *argos* gene expression within the optic lobe may be necessary for the normal laminar formation in addition to the axonal innervation from the photoreceptor cells.

The mutant phenotype and *LacZ* expression outside of the visual systems

In addition to the visual system, I noticed that the mutations in the *argos* gene caused abnormal developments of the labial pulp and wings (Fig. 6 d, e,f), although these penetrances are varied among *argos* alleles. In nearly all *argos*^{sty1e20} flies, the pattern of the wing vein network was abnormal. We found that sensilla formation as well as the gross morphology of the labial pulps were abnormal, as shown in Fig. 6e. We also analyzed the *LacZ* expression pattern outside of the visual system. In the larval central nervous system, X-gal staining was detected in the midline cells of the ventral ganglion. In the wing discs (Fig. 5c), b-galactosidase protein was detected in four spots near the marginal zone, which may account for the wing phenotype in the mutant to some extent. We also found that X-gal staining in the third instar antenna disc (Fig. 5a) and the putative John-stone body, where the sensory neurons of mechano-sensory systems are localized, in the antenna-region of the adult flies (Fig. 5f). The effects of *argos* mutation on olfactory and mechano-sensory systems have still to be examined.

Cloning of the *argos* locus

DNA sequences flanking the P-element insertion site in the *argos*^{sty1} and *argos*^{sty2} lines were recovered by the plasmid rescue technique and subsequent screenings of the *Drosophila* genomic library (Fig. 8). The genomic DNA fragment surrounding the P-element insertion site in *argos*^{sty2} was used as a probe to screen embryonic cDNA libraries (See Methods). We isolated and characterized two cDNA clones (Stb b3-3 and cStb-1) belonging to a transcription unit close to the P-element insertion site. These cDNAs were found to hybridize to genomic DNA spanning the insertion site in *argos*^{sty2} line, indicating that the P-element was inserted within the transcription unit (Fig. 8a,b). To determine the site of insertion relative to the open reading frame (ORF), I sequenced the genomic region surrounding the P-insertion site.

I determined the complete nucleotide sequence of the 2.0 kb cDNA and found a long ORF of 1332 nucleotides capable of translating to a 444 amino acid residue protein with a molecular weight of 50 kd (Fig. 8b).

The sequence had no significant homology to any known genes except the *argos* gene recently reported (Freeman et al., 1992; Kretzschmar et al., 1992). Thus, it has been shown that these three genes encode identical protein. This protein has a possible NH_2-linked glycosylation site at residue 333. The hydrophobicity profile (Fig. 8c) of the protein sequence showed the presence of only one long stretch of hydrophobic amino acids extending from amino acid 1 to 23, which could represent signal peptides. Therefore, it is likely that *argos* encodes a secreted protein. I next examined the *argos* mRNA profile by Northern blot analysis. A sample of 4mg of poly(A)$^+$ RNA prepared from 8-22-hour embryos and was fractionated on gel, transferred to a nylon filter [Hybond-N$^+$ (Amersham, Buckinghamshire, England)] and probed with the 0.7 kb *Eco*RI fragment from the *argos* (stb b3-3) cDNA clone. One major RNA species of 2.8kb was detected (data not shown).

Potential roles of *argos* gene products in the nervous system

In the present study, I found that the numbers of sensilla in the antenno-maxillary complex, neural cells within each ommatidium in the developing eye discs, and mechanosensory bristles on the adult compound eyes were increased in mutants in which *argos* had lost its function (Figs. 2, 4, 6). One interpretation of this phenotype is that a factor required to suppress the recruitment of additional neuronal cells is reduced in *argos* mutants. The nucleotide sequence data indicated that the *argos* gene encodes a secreted protein (Freeman et al., 1992; Kretzschmar et al., 1992; Okano et al., 1992). This protein could function as a diffusible inhibitory factor that prevents neighboring cells from adopting the neuronal developmental pathway. In fact, the mosaic analyses (Freeman et al., 1992; Kretzschmar et al., 1992) and the later study with a cell culture system (Freeman, 1994) revealed that the *argos* protein is secreted by cells and acts in a nonautonomous fashion. The *scabrous* gene also encodes a putatively secreted protein, that is partly related to the β and γ chains of fibrinogen (Baker et al., 1990; Mlodzik et al., 1990). It is proposed that the *scabrous* (*sca*) gene product functions as a lateral inhibitor of R8 differentiation through interaction with the *Notch* gene product and *Drosophila* EGF-receptor homologue. Interestingly, as it was suggested that the *argos* gene product has an EGF-like motif (Freeman et al., 1992; Kretzschmar et al., 1992), the interaction of the *argos* gene product with its putative receptor to exert the inhibitory function might be mediated through the EGF motifs.

In addition to acting as a lateral inhibitor involved in cell fate decisions, the *argos* gene product has additional functions. We found that the arrangement of photoreceptor cells within the ommatidia were abnormal in *argos* mutants (Fig. 6k). Therefore, the *argos* gene product may be necessary for the normal spacing of photoreceptor cells within the ommatidia. The mechanism of this action is still to be determined. The *argos* gene product is also likely to be required in guidance of photoreceptor cell axons and optic lobe development judging from the mutant phenotype (Fig. 5). Two possible explanations for the impaired optic lobe development in the *argos* mutants may be considered. First, mutations of the *argos* may primarily affect the projection patterns of photoreceptor axons, which finally result in impaired laminar formation of the optic lobe (the innervation hypothesis). Photoreceptor cell innervation on lamina ganglion cells is reported to have an inductive effect in lamina development (Meyerowitz and Kankel, 1978). Second, during normal development, the *argos* protein may act directly on neurons in the optic lobe as an "inductive" diffusible factor (the autocrine and/or paracrine hypothesis). It is still to be determined by using a well-established cell marking system of *Drosophila* such as mosaic analysis and gyandromorphs (Lawrence et al., 1986) whether the *argos* gene activity is required in a cell-autonomous fashion for the development of the optic lobe.

In order to clarify the mechanisms of pleiotropic function of the *argos* gene product, I am planning to characterize the molecular nature of its putative receptor(s) by a combination of genetic and biochemical method.

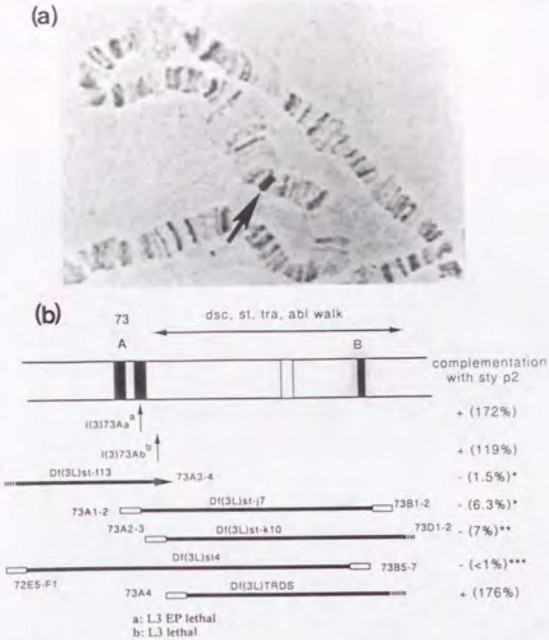

Fig. 1. The *argos* locus. (A) The cytological mapping of the *argos* locus determined by polytene chromosome in situ hybridization. A digoxygenin-dUTP-labeled P-element was used as a hybridization probe to determine the chromosomal location. A hybridization signal is indicated by the arrow at the 73A 1-2 site of the chromosome 3L; no other hybridization site was detected. (B) Genetics of the *argos* locus. The *argos*^{sty2} (I previously called this allele *sty*^{P2} in Okano et al., 1992) mutant was mated to two lethal stocks (*l(3)73Aa and l(3)73Ab*) and a series of lines with deficiencies surrounding the 73A locus (*Df(3L)st-f13, Df(3L)st-j7, Df(3L)st-k10, Df(3L)st4 and Df(3L)TRDS*). Relative positions of lethal mutations and deficiency breakpoints are indicated. Results of complementation tests with *argos*^{sty2} (*sty*^{P2}) are also shown. The viability of each heterozygote relative to that of each lethal or deficiency stock balanced with TM3 is indicated as a percentage. The presence (+) or absence (-) of complementation is shown for each line. Some deficiencies (*Df(3L)st-f13, Df(3L)st-j7, Df(3L)st-k10* or *Df(3L)st4*) failed to complement the *argos*^{sty2} mutation. All the viable heterozygotes from these lines showed rough eye phenotypes. From these data, the cytological position of the *argos* gene was assigned to 73A1-4.

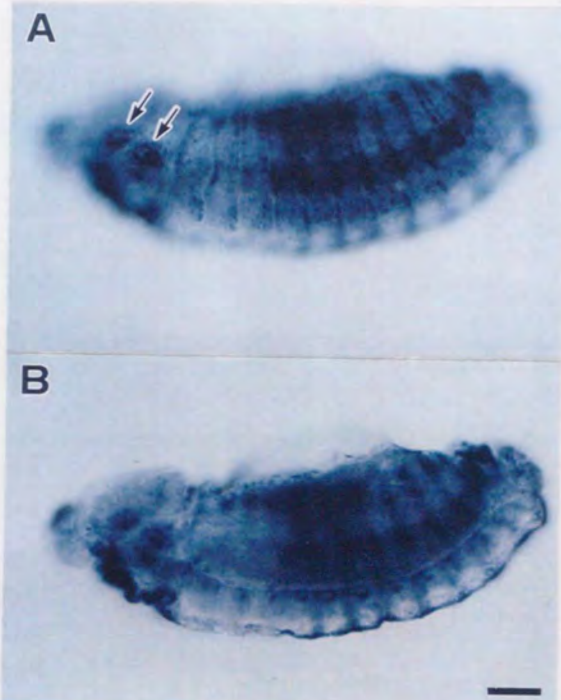

Fig. 2. Spatial expression of ß-galactosidase in the *argos* heterozygous embryos. The ß-galactosidase protein immunolocalized in *argos*^{sty2} heterozygote embryos at stage 14 is shown. (A). A surface view. Strong ß-galactosidase expression was detected in the putative antenno-maxillary complex precursor (arrows) and in the segmental boundary in the abdomen. (B). A sagittal section. ß-galactosidase expression in the ventral ectoderm was detected. Bar 50μm

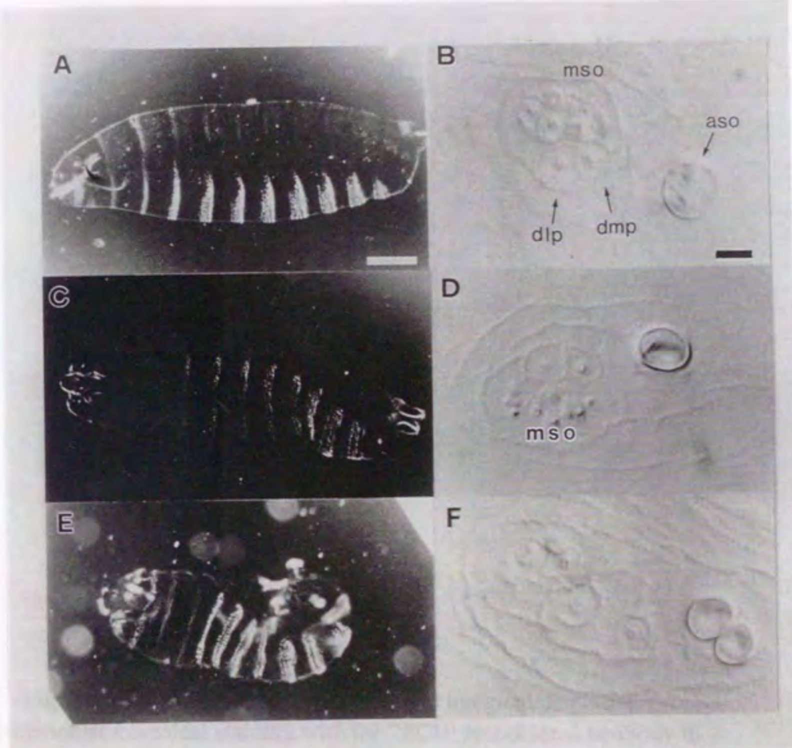

Fig. 3. Mutant phenotype in embryos. (A,C,E) Cuticle patterns of wild-type (A) and *argos*^{2e1}/*Df(3L)st4* (C, E) embryos. Various degrees of abnormal head involution were observed in the mutant embryos. (B, D, F) Nomarski views of the anntenno-maxillary complexes of wild type (B) and *argos*^{2e1}/*Df(3L)st4* (D,F) embryos are shown. The antennal sense organ (aso), dorso-lateral and dorsomedial papilla (dop, dmp) are indicated. Note the increased number of maxillary sense organs in (D) and aso in (F). Bar is 50μm in (A,C,E) and 5μm in (B,D,F).

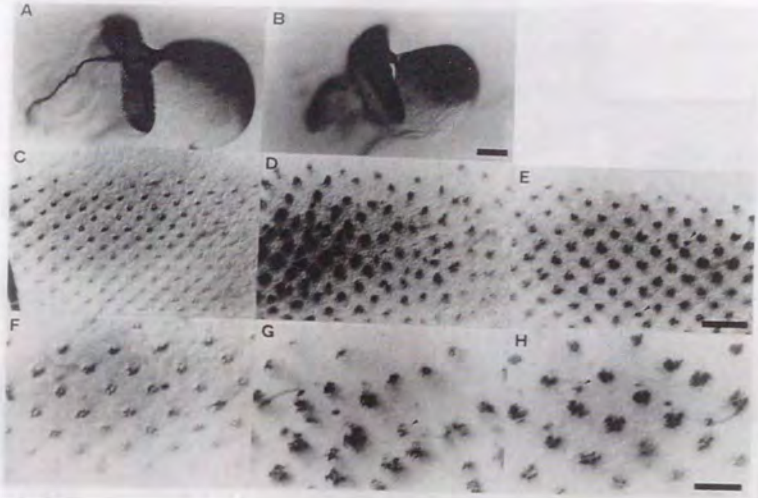

Fig. 4. Mutant phenotype in a larval eye imaginal disc. Immunohistochemical staining with the 22C10 monoclonal antibody in eye discs from third instar larvae of the wild-type (A,C,F), *argos*^{sty1} (B,D,G) and *argos*^{sty2} (E,H) homozygotes at lower (A,B), middle (C,D,E) and higher (F,G,H) magnifications. The eye discs are oriented with the posterior to the right (A,B) and on the bottom (C-H). In the *argos* eye disc, presence of extra neural cells were observed in ommatidia preclusters (D,E,G,H). Note the presence of ectopic ommatidial preclusters composed of a few neuronal cells (arrowheads; D,E,G,H) The spacing of the ommatidia was also impaired in *argos*^{sty1} (D,G). Note that the half moon shaped 22C10 staining pattern obseved in the wild-type optic lobe (A) was altered in *argos*^{sty1} (B). Bar: 100mm in (A,B), 30mm in (C,D,E) and 15mm in (F,G,H).

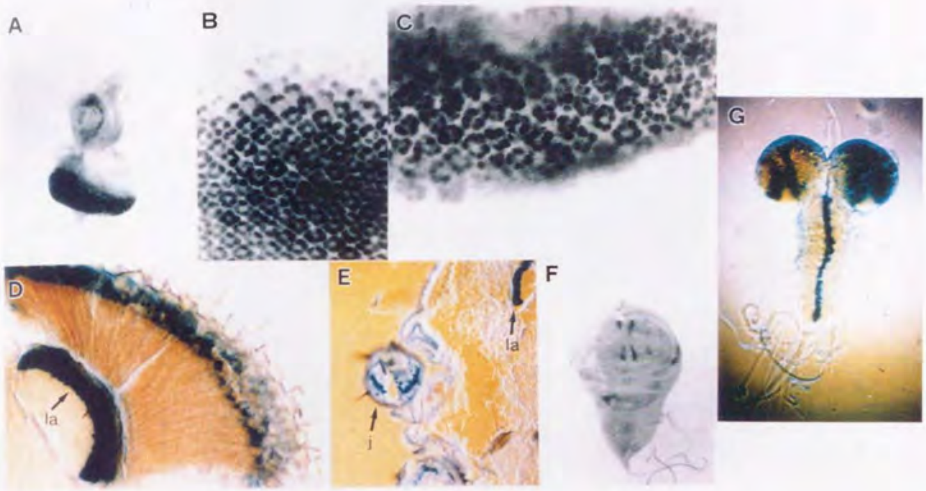

Fig. 5. Expression pattern of *argos-LacZ* reporter. The *argos* gene expression was monitored by localizing ß-galactosidase protein in *argos*^{sty1} heterozygotes. (A,B,C) ß-galactosidase expression in eye discs from third instar larvae of (A,B) and homozygotes (C) at lower (A) and higher magnifications. The eye discs were oriented with the posterior on the bottom. Note the number of ß-galactosidase positive cells were increased in *argos*^{sty1} homozygotes. (D) adult eye. ß-galactosidase expression was detected in the lamina (la) and retina. (E) Horizontal section of the antennae region in the adult head. ß-galactosidase expression was detected in Johnston's organ (j). (F) Wing disc from third instar larvae. (G) Optic lobe and ventral nerve cord from the third instar larva. The localization of ß-galactosidase protein was determined immunohistochemically (A,B,C,F) or by X-gal staining (D,E,G).

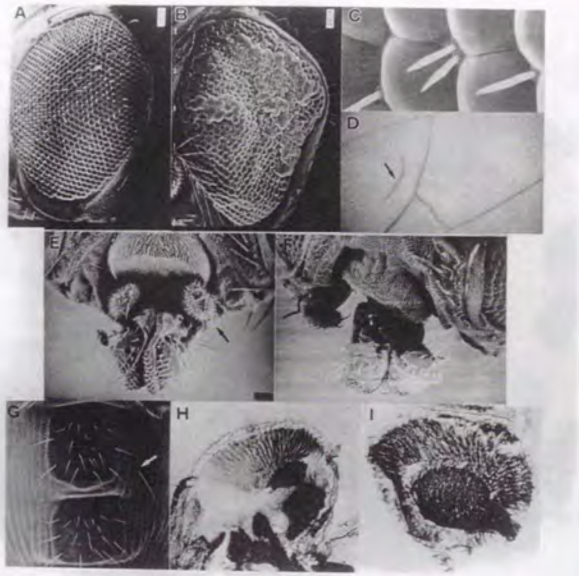

Fig. 6. Histological phenotype in the adult. (A) Scanning electron micrograph of a wild-type compound eye. (B,C) Scanning electron micrographs of a *argos* compound eye. A low magnification view of *argos*^{2e1}/Df(3L)st4 eye (B). A high magnification view of *argos*^{sty2} eye (C). Note the duplication of the mechanosensory bristles. (D) Wing phenotype of a *argos*^{sty1e20} fly. The arrow indicates an ectopic vein. (E,F) Scanning electron micrographs of mouth parts from wild-type (E) and *argos*^{2e1}/*Df(3L)st4* (F) flies. The maxillally palp, normally located on the rostrum (E, arrow) was missing, or mislocated to prefrons in the *argos* mutant (F). (G) Ventral abdomen from a *argos*^{sty1e20} fly. Note the extra rudimentary bristles on the sternite and at an ectopic position (arrow). (H,I) Immunohistochemical localization of a neuronal antigen (22C10) in wild-type (H) and *argos*^{sty2} (I) flies. The regular laminar structure of neurons in the optic lobe of wild type flies is observed by 22C10 staining (H). Note the disrupted laminar structure of the optic lobe in *argos*^{sty2} homozygotes (I).

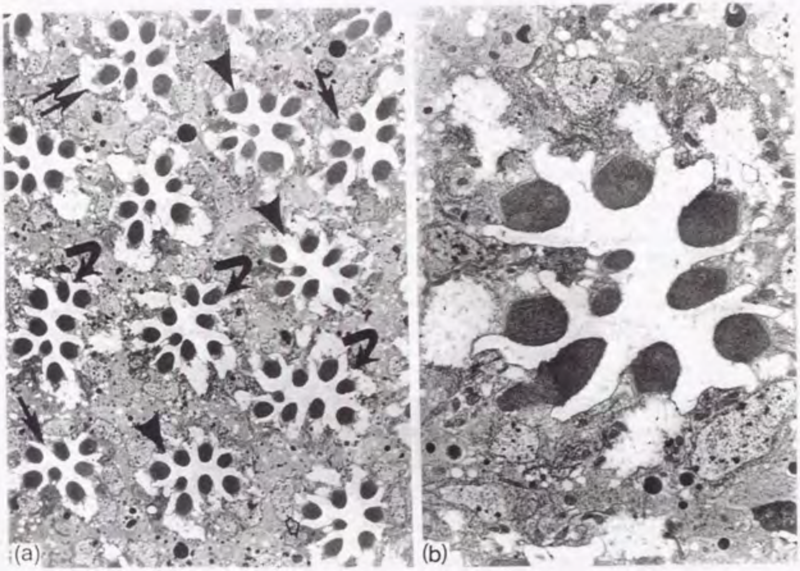

Fig. 7. Transmission electron micrograph of a *argos* compound eye. Low (A) and high (B) power electron micrographs of a tangential section through the dorsal hemisphere of a *argos*^{sty2} eye at the R7 level. The upper side of the figure is dorsal, and the right is frontal. (A) Two ommatidia (arrows) containing seven rhabdomeres form asymmetric trapezoids in which R1-3 are arranged in a vertical direction. In the indicated ommatidium (double arrow), the trapezoid pattern was rotated 90 degrees. In another ommatidium (open arrow), the trapezoid pattern is rotated and mirror-imaged. Three ommatidia (arrowheads) had one extra rhabdomere and three ommatidia (curved arrows) have two extra rhabdomeres. (B) High magnification of an ommatidium with eight outer photoreceptor cells and a split or fused R7 cell.

```
   2 ATTACAAAATTCATTGAGTATCAATTACAAACCGCGAAGAAAACAACACGCACGGAGATT    61

  62 CGGAAAGATTCCCAAGATCCAAATACAAGATCCAGATTCTCGAACATCCAGAGATCCCAG   121
                                      ▼
 122 CCAGAGTCAGAGTCATAAATCATGCCTACGACATTGATGTTGCTGCCGTGCATGCTGCTG   181
   1                       M  P  T  T  L  M  L  L  P  C  M  L  L    13
 182 TTGCTGCTGACCGCCGCTGCCGTTGCTGTCGGCGGCACGCGACTGCCGCTCGAGGTGTTC   241
  13  L  L  L  T  A  A  A  V  A  V  G  G  T  R  L  P  L  E  V  F    33
 242 GAGATTACGCCGACCACATCCACAGCGGACAAGCACAAGAGTCTGCAGTACACCGTCGTC   301
  33  E  I  T  P  T  T  S  T  A  D  K  H  K  S  L  Q  Y  T  V  V    53
 302 TACGATGCCAAAGATATTTCAGGAGCAGCGGCAGCAACTGGAGTGGCGAGCAGTACAGTG   361
  53  Y  D  A  K  D  I  S  G  A  A  A  A  T  G  V  A  S  S  T  V    73
 362 AAGCCCGCCACCGAGCAACTGACCGTTGTGAGCATTTCCTCCACAGCGGCTGCGGAGAAG   421
  73  K  P  A  T  E  Q  L  T  V  V  S  I  S  S  T  A  A  A  E  K    93
 422 GATCTCGCCGAGTCGCGGCGACATGCGCGACAAATGTTGCAGAAACAACAGCAGCATCGC   481
  93  D  L  A  E  S  R  R  H  A  R  Q  M  L  Q  K  Q  Q  Q  H  R   113
 482 AGCATCATCGGCGGCAAGCACGGCGATCGGGATGTGCGCATCCTCTACCAAGTGGGGGAC   541
 113  S  I  I  G  G  K  H  G  D  R  D  V  R  I  L  Y  Q  V  G  D   133
 542 TCTGAAGAGGATTTGCCCGTCTGTGCACCGAATGCAGTTTGCTCCAAGATCGATCTATAC   601
 133  S  E  E  D  L  P  V  C  A  P  N  A  V  C  S  K  I  D  L  Y   153
 602 GAAACCCCGTGGATCGAGCGACAATGTCGTTGTCCTGAATCGAATCGCATGCCCAACAAT   661
 153  E  T  P  W  I  E  R  Q  C  R  C  P  E  S  N  R  M  P  N  N   173
 662 GTGATCATCCATCATCACAGTCATTCCTCGGGATCGGTGGATTCCCTGAAGTACAGGAAC   721
 173  V  I  I  H  H  H  S  H  S  S  G  S  V  D  S  L  K  Y  R  N   193
 722 TACTACGAAAGGGAGAAGATGATGCAGCACAAGCGAATGCTGTTGGGTGAATTTCAGGAT   781
 193  Y  Y  E  R  E  K  M  M  Q  H  K  R  M  L  L  G  E  F  Q  D   213
 782 AAGAAATTCGAAAGTCTGCATATGAAGAAGCTGATGCAGAAACTGGGCGCCGTCTACGAG   841
 213  K  K  F  E  S  L  H  M  K  K  L  M  Q  K  L  G  A  V  Y  E   233
 842 GATGATTTGGATCATCTGGACCAGTCGCCGGACTATAATGACGCCCTGCCCTATGCGGAG   901
 233  D  D  L  D  H  L  D  Q  S  P  D  Y  N  D  A  L  P  Y  A  E   253
 902 GTGCAGGACAATGAGTTTCCCAGGGGATCGGCGCACATGAGGCATTCCGGGCACCGAGGA   961
 253  V  Q  D  N  E  F  P  R  G  S  A  H  M  R  H  S  G  H  R  G   273
 962 TCCAAAGAGCCTGCAACCACATTCATTGGCGGCTGTCCCAGCAGTTTGGGCGTGGAAGAT  1021
 273  S  K  E  P  A  T  T  F  I  G  G  C  P  S  S  L  G  V  E  D   293
1022 GGCCACACCATTGCCGATAAGACTAGGCATTACAAAATGTGCCAGCCGGTGCATAAGTTG  1081
 293  G  H  T  I  A  D  K  T  R  H  Y  K  M  C  Q  P  V  H  K  L   313
1082 CCAGTTTGCAAACACTTCCGTGACTACACTTGGACTTTGACAACAGCAGCCGAGTTGAAT  1141
 313  P  V  C  K  H  F  R  D  Y  T  W  T  L  T  T  A  A  E  L  N   333
1142 GTGACGGAGCAGATAGTCCATTGTCGGTGTCCCCGGAATTCGGTGACATACTTGACCAAG  1201
 333  V  T  E  Q  I  V  H  C  R  C  P  R  N  S  V  T  Y  L  T  K   353
1202 AGGGAACCCATTGGCAATGACAGTCCGGGCTACAGATATCTGTTCGCCTGCTCTCCCCTG  1261
 353  R  E  P  I  G  N  D  S  P  G  Y  R  Y  L  F  A  C  S  P  L   373
1262 ACGCGTCTTCGCTGTCAGCGAAAGCAACCGTGCAAATTGTTCACGGTGCGAAAGCGCCAG  1321
 373  T  R  L  R  C  Q  R  K  Q  P  C  K  L  F  T  V  R  K  R  Q   393
1322 GAGTTCCTGGACGAGGTCAACATTAACTCGTTGTGCCAGTGCCCCAAAGGGCACCGCTGT  1381
 393  E  F  L  D  E  V  N  I  N  S  L  C  Q  C  P  K  G  H  R  C   413
1382 CCCAGTCATCACACGCAATCCGGCGTGATAGCCGGCGAGAGTTTTCTGGAGGACAACATA  1441
 413  P  S  H  H  T  Q  S  G  V  I  A  G  E  S  F  L  E  D  N  I   433
1442 CAGACATATTCCGGTTACTGCATGGCCAACGATTGAGTGCATCGCCCAGGGGATCATTCC  1501
 433  Q  T  Y  S  G  Y  C  M  A  N  D                              444
1502 ACACATAATATATATAGAATACACTTTGTAAAGGAAGATAGAGTTGAGCGGAGGAGCAAC  1561
1562 AGCTACTATATAGATATCGACTGAGCCAATTGAGTCTCGCCAAGTTACCAACTAATGAAC  1621
1622 TAATGAGAAGGGAAAAACGAACAAATACAAGCTAGGAACTTAAAATGCACTTCCACACAG  1681
1682 ATCATTTTGAAGTTTTTCACGAAAAAGAGAGAGAGAGCTTGTTTCTTTTGCTACCAAATT  1741
1742 TTGGTCATAAAACGTATGATATAAATATTTAATTAGTTTTAAGCATCGATATGTGCGCAG  1801
1802 TTTGTTATACAAATAATTTGTAATGAATATTTATGAAAACAAGAGGCAAAACCTGCAACG  1861
1862 AAGGAGGGCACTCCACTATGTAATATAGCAACAAACTATACTCGTAAACTAACCCGCATA  1921
1922 AATGTAT                                                       1928
```

Fig. 8 Sequence of the *argos* cDNA clone, cSty-2, together with the deduced amino acid sequence. The putative signal sequence (1-23 a.a.) is underlined. There is a possible NH2-linked glycosylation site at residues 333 aa. The epidermal growth factor (EGF)-like motif is indicated by a broken underline. The P-element insertion sites in the *argos* gene were determined by sequencing the rescued plasmids using sequences at the 5' ($argos^{sty1}$) or 3' ($argos^{sty2}$) ends of the P-elements as primers. The position of the P[$lacW^{+}$] element in the $argos^{sty2}$ line is indicated by the arrow.

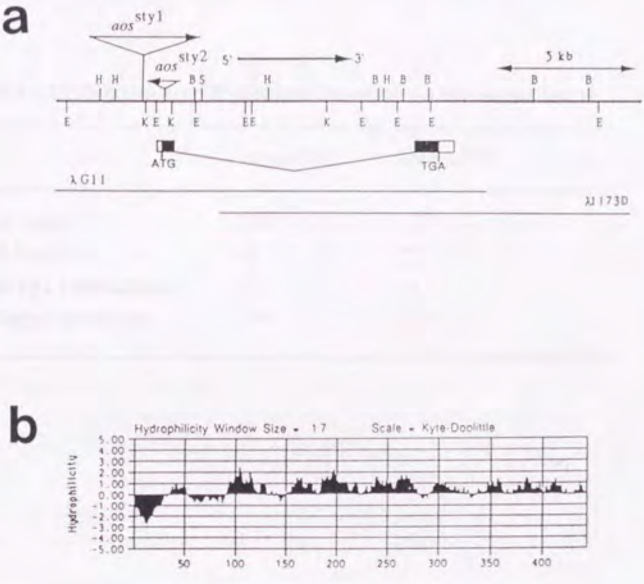

Fig. 9. Molecular analysis of the *argos* locus. (a) Genomic organization at the *argos* locus. A restriction map of ~20 kb of cloned DNA is shown. Two genomic phage clones (λG11 and λ1173D) that encopass the *argos* locus. Restriction sites are shown for *Bam*HI (B), *Eco*RI (E), *Hind*III (H), *Kpn*I (K) and *Sac*I (S). The positions of the P-element insertions are indicated by the vertical lines. The two alleles *argos*^{sty1} and *argos*^{sty2} were previously called as *sty*^{P1} and *sty*^{P2}, respectively (Okano et al., 1992). The P-element are represented by triangles and the arrows indicate the orientations of the P-elements (5'-3'). The longest cDNA clone, cSty-2 (2.0 kb), is indicated by the boxes. The open reading frame is shown by the filled boxes. The orientation of the transcription is indicated by the horizontal arrow above the restriction map. (b) Hydrophilicity plot of the *argos* coding region. The plot was computed according to Kyte and Doolittle (19); the window size is 17.

Table 1. Mobilization of P-element inserted on the *argos* locus

	$argos^{sty1}$	$argos^{sty2}$
no. of lines	24	27
lethal lines	4	5
rough eye (semilethal)	2	8
wild-type revertant	18	14

Chapter 2

Ectopic overexpression of *argos* inhibits cell differentiation during *Drosophila* eye and wing vein development

Abstract

The *Drosophila argos* gene, which encodes a secreted protein with an EGF motif, is involved in several developmental processes regulating cell-cell interactions such as eye morphogenesis. Loss-of-function mutations in the *argos* gene causes the increase of the number of photoreceptor cells and cone cells, impaired retinal projections to the optic lobe, and the formation of extra veins. I show here that ubiquitously expressed *argos* product restored all these loss-of-function phenotypes. Overexpression of *argos* in the wild-type background resulted in the reduced number of photoreceptor cells, cone cells and pigment cells, which are opposite phenotypes to those of the loss-of-function mutants. The *argos* gene is expressed in developing wing veins. Ubiquitous *argos* expression caused loss of veins in a dosage-dependent manner. This phenotype was enhanced by the loss-of-function rhomboid mutation, implying the possibility that *argos* and rhomboid play key roles in a common pathway for the normal wing vein formation. I propose that the *argos* acts as an inhibitory signal for cellular differentiation in the developing eye and wing.

2-1. Introduction

Communication among cells is important for the generation of different cell types during development of multicellular organisms. Many problems remain unsolved about the molecular mechanism by which signals from neighboring cells regulate cell fates. *Drosophila* eye development is an excellent model for studying the molecular mechanisms underlying cell-cell interactions. The structure of the compound eye of *Drosophila* is stereotypically organized, providing a convenient system for studying the mechanism of cell assembly (Ready, 1989). The compound eye is composed of about 800 ommatidia, each containing eight photoreceptor cells (R1-8), cone cells and pigment cells. Determination of cell fates in the *Drosophila* retina is known to be a consequence of cell-cell interactions rather than cell lineage (Lawrence and Green, 1979; Ready et al., 1976). Neuronal differentiation in the compound eyes starts during the third instar larval stage in a specialized retinal epithelium, the eye imaginal disc. The morphogenetic furrow, a dorso-ventral indentation, sweeps from the posterior part of the disc anteriorly. In the posterior part of the furrow, cells begin to differentiate and assemble into pre-ommatidial clusters and express neuron-specific antigens (Tomlinson and Ready, 1987). Intensive analyses have been carried out by taking advantage of this system and many genes have been identified that are involved in regulating the specification of cell fates. An example of well-characterized inductive events mediated by an interaction between adjacent cells is the differentiation of the photoreceptor cell R7. The R7 precursor requires a signal from the adjacent R8 cell for neuronal differentiation. This event is mediated by a receptor kinase, sevenless, expressed in R7 (Hafen et al., 1987; Bowtell et al., 1988; Basler and Hafen, 1988; Simon et al., 1989) and the ligand, bride of sevenless, expressed in R8 (Hart et al.,1990; Kramer et al., 1991).

Communication between cells can also be mediated by inhibitory signals from the neighboring cells. *scabrous* (*sca*) encodes a diffusible protein regulating the cell-cell interactions over a long distance during eye development (Mlodzik et al., 1990; Baker et al., 1990). *sca* encodes a secreted protein with homology to fibrinogen whose function is essential for regulating the evenly spaced ommatidia. The *sca* product is a signal molecule secreted by R8 that laterally inhibits neighbors from becoming R8. The *argos* gene encodes a new type of diffusible molecule that regulates cell differentiation and gross assembly of ommatidia (Kretzschmar et al., 1992; Okano et al, 1992; Freeman et al., 1992a). Loss-of-function *argos* mutations cause a severe rough-eye phenotype, characterized by the production of supernumerary photoreceptor cells, cone cells, pigment cells and mechanosensory bristles and irregular development of the ommatidial array (Freeman et al., 1992a; Kretzschmar et al., 1992; Okano et al., 1992). *argos* is also required for axonal guidance in the optic lobe (Kretzschmar et al., 1992; Okano et al., 1992). Clonal analyses indicate that the gene product acts nonautonomously to regulate cell fate decisions in the *Drosophila* eye (Freeman et al., 1992a; Kretzschmar et al., 1992). Sequence analyses of *argos* have shown that it encodes a putative secreted protein with an EGF motif (Freeman et al., 1992a; Kretzschmar et al., 1992; Okano et al., 1992). The EGF motif has been found in many proteins that interact with other proteins localized in the interface of contacting cells (Wharton et al., 1985; Davis et al., 1990). Furthermore, Freeman (1994) obtained a direct evidence showing that argos is secreted from the cells. These findings suggest that *argos* encodes an lateral inhibitor that regulates the cell fate decisions in ommatidia. "Lateral inhibition" is known as a mechanism cells that become neural cells appear to inhibit their neighbors from also adopting a neural fate during the course of neural development (Wigglesworth, 1940; Doe and Goodman, 1985). Genes required for eye development are sometimes known to function in the development of other organs. These include *Notch* (*N*), *Epidermal growth factor receptor homologue* (*Egfr*), and *rhomboid* (*rho*), which play essential roles in pattern formation of wing veins (Diaz-Benjumera and García-Bellido, 1990; Rebay et al., 1993; Sturtevant et al., 1993). Previously I have shown that *argos* is expressed in the wing imaginal disc and noted extra veins in the mutant (Okano et al., 1992).

To investigate the role of *argos* in the eye and wing development, ectopic expression of *argos* under the control of the *hsp70* promoter was performed in wild-type and loss-of-function *argos* genetic backgrounds (Freeman, 1994; Sawamoto et al., 1994). If *argos* functions as a lateral inhibitor, excess *argos* protein is then expected to cause a loss of differentiated cells, provided the receptor for *argos* is expressed in these cells. The results clearly support the view that *argos* functions to regulate cell fate decisions as a negative signal in the developing eye and wing discs. I will also describe the genetic interaction of *argos* with *rho*.

2-2. Materials and Methods

Fly strains and culture

Drosophila melanogaster stocks were maintained and crossed on standard yeast-cornmeal-agar-glucose medium at 25°C unless otherwise noted. The wild-type stock was Canton-Special. All genes and allele designations are as described in Lindsley and Zimm (1992). *Dr*/*TMS, Sb* P[ry^+, Δ2-3] was obtained from the Indiana Stock Center. rho^{ve} was from the Bowling Green Stock Center. For heat shock experiments, second instar larvae were collected in a glass vial with medium and repeatedly heat-shocked at 36°C for 1 hr with an interval of 25°C for 5 hr using a temperature-programmable incubator. A single heat pulse was applied using a standard water bath at 37°C for 1 hr.

Plasmid construction and P-element-mediated germline transformation

The 2 kb EcoRI fragment of the *argos* cDNA including the entire coding region (Okano et al., 1992) was inserted into an appropriate site of pCaSpeRhs (Thummel and Pirrotta, 1991), pHT4 (Schneuwly et al., 1987) or pKB255 (K. Basler and E. Hafen, unpublished). These vectors contained a hsp70 promoter. Since pKB255 also contains the sev enhancer element, preferential expression of the transgene in the sev-expressing cells is expected. The constructs were injected into embryos at 1 mg/ml and a helper plasmid pπ25.7wc at 0.1 mg/ml as described (Karess and Rubin, 1984). For rescue experiments of loss-of-function *argos* phenotypes, I used *argos*^{sty1e20}/*TM3* as a host strain. For overexpression experiments in the wild-type genetic background, *Dr*/*TMS*, *Sb* P[*ry*$^+$, Δ2-3] embryos were injected without the helper plasmid. *Dr* was removed by free recombination when the insertion occurred onto the *Dr* third chromosome.

Histology

Antibody stainings of eye imaginal discs were performed essentially as described (Tomlinson and Ready, 1987), except that discs were fixed in 4% paraformaldehyde in PBS. Monoclonal antibody Mab22C10 was kind gift from Dr. Shinobu C. Fujita (Fujita et al., 1982). Cobalt sulfide staining of pupal eyes at 50 hr after puparium formation (APF) was carried out using the method of Wolff and Ready (1991). Acridine orange staining was carried out as described by Wolff and Ready (1991). X-gal staining of wing discs and adult wings were performed as described previously (Okano et al, 1992).

For plastic sections, adult heads were fixed in 2% glutaraldehyde/2% paraformaldehyde in 0.1 M sodium cacodylate buffer (pH 7.2) at 4°C overnight. After washing in 0.1 M sodium cacodylate buffer (pH 7.2) at 4°C overnight, heads were post-fixed in 1% OsO_4 in the buffer for 1.5 hr at 4°C and then dehydrated in a graded ethanol series. After clearing in propylene oxide, heads were embedded in Araldite and sectioned with an ultramicrotome. One μm horizontal sections were stained with AzurII. Adult wings were dissected out in 1-butanol, cleared in xylene and mounted with Permount (Fisher). Photographs were taken with a Zeiss Axio-Photo microscope.

datacomp electron microscopy

Adult flies were dehydrated in a graded acetone series and dried at 60°C for 1 hr. Mounted flies were sputter coated with platinum and observed with a Hitachi S-100 scanning electron microscope.

2-3. Results

Rescue of *argos* phenotypes with wild-type cDNA

In order to verify the biological activity of the *argos* gene product expressed from the transgene, the *hs-argos* construct using pHT4 vector was introduced into the $argos^{sty1e20}$/TM3 mutant, which was called sty^{P1e20} previously (Okano et al., 1992). Three independent transformant lines were obtained showing similar rescuing phenotypes. All data presented in this paper are from a single strain.

The $argos^{sty1e20}$ mutation is a semilethal allele which was generated by imprecise excision of the enhancer trap P-element vector from the $argos^{sty1}$ line (Okano et al., 1992). The homozygous $argos^{sty1e20}$ mutant flies show a roughened eye appearance (Fig. 1B), contrasting with the regular array of ommatidia in the wild-type eye (Fig. 1A). Transformants carrying two copies of *hs-argos* were repeatedly heat-shocked from the second instar to the pupal stage and phenotypes of the eclosed flies were examined. Heat pulses delivered at these stages to $argos^{sty1e20}$ homozygotes with no transgene had no phenotypic consequence in the adult eye. $argos^{sty1e20}$ homozygotes with two copies of *hs-argos* revealed typical mutant phenotypes if they were not heat shocked (data not shown). In contrast, heat pulses delivered in the $argos^{sty1e20}$ homozygotes with two copies of *hs-argos* resulted in almost normal external morphology (Fig. 1C). Interestingly, when heat pulses were delivered after the wandering larval stage, only the anterior half of the compound eye showed normal morphology (data not shown). Tangential sections through the eyes of the $argos^{sty1e20}$ homozygous adult flies revealed supernumerary photoreceptor cells and abnormal spacing pattern of ommatidia (Fig. 1E). However, the sections of heat shocked *hs-argos* ; $argos^{sty1e20}$ flies were morphologically indistinguishable from those of the wild-type (Fig. 1D,F).

Fig.2 represents cobalt sulfide staining of pupal retinae at 50 hr APF. In the wild-type, four cone cells are surrounded by two primary pigment cells (Fig. 2A). In $argos^{sty1e20}$ flies, supernumerary cone cells (average number: 7) and primary pigment cells (average number: 4) were observed (Fig. 2B). *hs-argos/hs-argos* ; $argos^{sty1e20}/argos^{sty1e20}$ flies showed the similar phenotype to $argos^{sty1e20}$ flies without heat shock. However, a single heat pulse (for 1 hr at 38°C) to *hs-argos/hs-argos* ; $argos^{sty1e20}/argos^{sty1e20}$ third instar larva generated a rescued region where most of the ommatidia contained four cone cells (Fig. 2C) unlike typical *argos*^{sty1e20} ommatidia with extra cone cells. In this region, some ommatidia contained even fewer cone cells than wild-type, probably due to the over-dosage of *argos*. The number of extra cone cells gradually increased as the distance from the rescued region increased (Fig. 2D). A single heat pulse induced an elevation of the amount of the *argos* product in a entire disc. Then cells only at a particular developmental stage are thought to be capable to respond to the *argos* product. Since the induced *argos* product would degrade, the gradual change of the cone cells also indicate *argos* may regulate the recruitment of cone cells in a dosage-dependent manner.

Expression of *hs-argos* produced various effects outside the visual system. The *argos*^{sty1e20} homozygotes have very low viability due to the embryonic lethality. Transformant flies with two copies of *hs-argos* had almost normal viability even without heat-shock. Other phenotypes of the *argos*^{sty1e20} mutant flies, such as abnormal morphogenesis of the maxillary palp (data not shown) and wing veins (Fig.5B,C), were also rescued by heat pulses to *argos*^{sty1e20} homozygotes with two copies of *hs-argos*.

An excess of *argos* activity inhibits the differentiation of retinular cells

To test the hypothesis that *argos* negatively regulates cell differentiation in the developing eye disc as a diffusible factor, I examined the effect of ectopic overexpression of the *argos* gene product in the wild-type background. I placed a full-length *argos* cDNA under the control of a heat-inducible promoter using two kinds of transformation vectors. The sev enhancer element contained in pKB255 induces gene expression in all ommatidial cells including non-neuronal cells except for R8, R2 and R5. By applying heat pulses to the transformants, especially high level of *argos* expression in these cells and a lower level in all other cells is expected. Ten independent *sev-hs-argos* transformants carrying the pKB255 construct and 9 *hs-argos* lines carrying pCaSpeRhs construct were obtained. Upon heat shock, all these lines showed a range of the rough eye phenotypes and wing phenotypes. The gain-of-function phenotypes in the eye and wing were enhanced by increasing the copy number of inserts or the number of heat pulses. The eyes of *sev-hs-argos* flies were often slightly roughened even without heat shock, probably reflecting constitutive expression of the *argos* cDNA due to the sev enhancer (Fig.3A). Administration of heat shock to *sev-hs-argos* flies resulted in the similar eye and wing phenotypes as heat-shocked *hs-argos* flies described below (data not shown). One of the *hs-argos* lines (*hs-argos*#4) showed a rough eye phenotype when raised at 25°C, and others had almost normal eyes (data not shown). The *hs-argos*#4 fly had *hs-argos* inserts on both the second and the third chromosomes. Later studies revealed that the inserts on the second chromosome were sufficient to cause the rough eye phenotype even without heat shock, suggesting that *hs-argos* was inserted close enough to an enhancer element on the second chromosomes that constitutively promotes transcription of the *argos*. *hs-argos*#1 and *hs-argos*#4 were used for further studies. Raising at 30°C throughout larval and pupal stages, almost all flies died at the pupal stage. Unless otherwise noted, I applied 1 hr heat pulses at 36°C with intervals of 5 hr at 25°C from second instar to the end of the pupal stage. Higher temperature pulses or pulses with shorter intervals caused reduced viability, which is ascribable to pupal lethality. I examined the amount of the *argos* protein in the *hs-argos* larva after heat shock. Immuno blot analysis showed that level of *argos* is dramatically elevated within one hour after heat shock and decrease to the normal level five hour after heat pulse.

The *hs-argos*#4 transformants heat-shocked at the second instar larvae and later stages showed severe roughening of the eye surface (Fig.3B). They often had eyes reduced in size (Fig.3C), indicating that ommatidial development was suppressed by overexpression of the *argos* gene. Disruption in bristle pattern was also observed and lenses were occasionally fused with each other (Fig.3D).

Fig. 3E represents a tangential section of an eye of a heat shocked *hs-argos*#1 fly, which expressed the moderate gain-of-function phenotype of *argos*. The primary defect found in the *hs-argos*#1 eye is a reduction in the number of photoreceptor cells. The ommatidia containing only 4-6 photoreceptor cells were occasionally observed (Fig.3E arrows). Any cell types are affected by ectopic overexpression of *argos*. Some ommatidia lacked outer-photoreceptor cells (R1-6), some lacked inner-photoreceptor cells (R7,R8), and others lost both of them, judging from the size and position in ommatidia. This is in contrast to the phenotype of loss-of-function *argos* mutants, in which most ommatidia have extra outer-photoreceptor cells (Freeman et al., 1992a; Kretzschmar et al., 1992; Okano et al., 1992).

The irregular spacing of ommatidia, the fusion of ommatidia due to the loss of secondary or tertiary pigment cells and the rotation of trapezoidal pattern of rhabdomeres were also observed in *hs-argos*#1 flies. In the eye section of the heat-shocked *hs-argos*#4, there were many ommatidia containing two small inner-rhabdomeres (Fig.3F). Since the two rhabdomeres project to a same direction and always smaller than the wild type cells in all the cases I observed, these are judged to be split rhabdomeres rather than two distinct cells. A similar defect was also found in the loss-of-function *argos* and *tramtrack* mutants (Okano et. al., 1992; Xiong and Montell, 1993). Although I have no explanation for the defect, the proper dosage of *argos* may be required for the development of the rhabdomere of the central cells.

The arrangement of cone cells and primary pigment cells of pupal retina was examined by cobalt sulfide staining (Fig.3G). Administration of a single heat pulse to wandering larvae of *hs-argos*#4 fly occasionally caused a reduction in the number of cone cells (indicated by arrows in Fig. 3G). The number of primary pigment cells surrounding the cone cells were not affected, due to the fact that the differentiation of the primary pigment cells occurs at a later stage.

In the developing eye imaginal disc of *hs-argos*#4 larvae, I have no evidence that the number of 22C10-positive cells is decreased by applying heat-shock at the larval stage. The level of cell death appeared not to be accelerated in the eye imaginal discs at the wandering larval stage as estimated by acridine orange staining (data not shown).

argos **is expressed in developing wing veins**

To analyze *argos* functions in wing development, I determined expression pattern of *argos* by X-gal staining of $argos^{sty1}$/*TM6* wing discs. *argos* expression in the wing pouch region of the larval disc begins at the late third instar. At this stage, a perpendicularly crossing double array of stained cells is observed in the position where the margin of the wing and longitudinal wing veins L3 and L4 will be formed (Campuzano and Modolell,1992) (Fig.4A). At 30 hr APF, *argos* is expressed in the wing margin and putative L3, 4, and 5 wing veins (Fig.4B). At 72 hr APF, *argos* is strongly expressed in the wing margin and all wing veins; L2-L5, the anterior cross vein, and the posterior cross vein can be unequivocally identified (Fig.4C). In the adult wing, stained cells were located on all veins and the wing margin (Fig.4D).

Proper dosage of *argos* is required for the pattern formation of wing veins

In the *argos*^{sty1e20} wing, small deltas and extra veins were observed (Fig.5B). Administration of heat pulses to *hs-argos/hs-argos* ; *argos*^{sty1e20}/*argos*^{sty1e20} flies from the second instar to pupal stages perfectly rescued the extra vein phenotype (Fig.5C). Heat pulsing during the larval stages only resulted in an incomplete rescue (data not shown). The *hs-argos*#4 flies heat pulsed from the second instar to pupal stages have wings in which L2, L4 and L5 veins were strikingly shortened and cross veins were absent (Fig.5D). L3 was not affected in most cases.

argos* interacts with *rhomboid

rhomboid (*rho*), encoding a transmembrane protein, is known to mediate the pattern formation of wing veins (Sturtevant et al., 1993). Flies homozygous for the loss-of-function allele *rho*^{ve} have wings with shortened longitudinal veins. The L2 - L5 veins do not reach the wing margin, but the cross veins are normal (Fig.6A). The third chromosomes of the *hs-argos*#4 line were replaced with the chromosomes carrying the *rho*^{ve} mutation. Even without heat shock, the wings of *hs-argos/hs-argos* ; *rho*^{ve}/*rho*^{ve} flies had stronger phenotypes than *rho*^{ve}/*rho*^{ve} (data not shown). When heat pulses were applied to these flies from the second-third instar to pupal stages, most of the L2-L4 veins and the entire L5 vein were eliminated (Fig.6C). Campaniform sensila on L3 were usually remained intact. Such a striking defect was not observed in either *hs-argos/hs-argos* (Fig. 6B) or *rho*^{ve}/*rho*^{ve}. Therefore, *argos* and *rho* may function in a common pathway during wing vein development.

2-4. Discussion

Lateral inhibition is thought to play key roles in regulating the spacing pattern and differentiation of the proper number of cells during development. In the *Drosophila* eye, sca and *argos* have been identified as candidates for genes encoding diffusible factors that negatively regulate cellular differentiation during ommatidial assembly (Baker et al., 1990; Mlodzik et al., 1990; Freeman et al., 1992a; Kretzschmar et al., 1992; Okano et al., 1992). I utilized gain-of-function mutants, in which ectopic overexpression of *argos* could be induced under the control of hsp70 promoter, and presented evidence that the *argos* product has inhibitory effects on cellular differentiation in eye and wing development (Fig. 7)

(Sawamoto et al., 1994). Similar results were published by Freeman (1994) and Brunner et al (1994) later.

Rescue of *argos* mutation by ubiquitous *argos*$^+$ expression

I showed that both the rough eye and extra wing vein phenotypes of *argos* mutants were rescued by heat-induced *argos* protein in the transformants with the *argos* wild-type cDNA. This fact indicates that the *argos* mutant phenotypes are indeed due to the loss-of-function of the *argos* product as expected by the molecular analyses of the *argos* mutation. The lethality of the *argos*^{sty1e20} homozygote was also considerably rescued, probably due to the rescue of embryonic phenotypes such as abnormal head involution (Freeman et al., 1992a; Okano et al., 1992). Since the rescue occurred without heat shock, lower dosage of *argos* seems to be required for the embryonic development than for the post-embryonic morphogenesis. Alternatively, it is possible that the hsp70 promoter fragment is leakier in the embryo than later.

In the eye imaginal disc, *argos* is expressed in photoreceptor cells, primary pigment cells and cone cells during the ommatidial development (Freeman et al., 1992a). Mystery cells are thought to be recruited as extra photoreceptor cells in the eye disc of the *argos* mutant (Freeman et al., 1992a). It is also proposed that additional cells including primary pigment cells and cone cells are recruited from uncommitted cells that exist in the developing eye discs of loss-of-function *argos* mutants (Freeman et al., 1992a). Therefore, *argos* is thought to play a key role in the regulation of the recruitment of these cells. The *argos* eye phenotypes are characterized by abnormally spaced ommatidia, improper rotation of ommatidia, and existence of supernumerary photoreceptor cells, cone cells and pigment cells. All of these defects were completely rescued by ubiquitous *argos* expression. Therefore, the spatiotemporally restricted localization of *argos* is not necessary for normal eye development, suggesting that the availability of the potential receptor for the *argos* is restricted spatially and/or temporally. Alternatively, it is also possible that some other component(s) of the signal, which might include sca, are spatially limiting, thus providing spatial specificity. Therefore, the signal transduction through argos can be spatially limited even if both the *argos* and its potential receptor are generally distributed. However, I can not completely rule out the possibility that the *argos* activity is still significantly higher in the cells in which *argos* is expressed, even after the heat shock, since *argos*^{sty1e20} is not a complete null allele.

Role of *argos* in ommatidial development

To examine *argos* function in more detail, I overexpressed the *hs-argos* gene in the wild-type genetic background. The comparative study of gain-of-function phenotypes with loss-of-function phenotypes provided further evidence that *argos* functions as a lateral inhibitor. Ectopic overexpression of *argos* decreased photoreceptor cells and cone cells in ommatidia. Although I have not identified positively the subtypes of photoreceptor cells lost in the *hs-argos* flies, it is likely that any of the photoreceptor cells can be eliminated by *argos* overexpression, judging from the gain-of-function phenotype (see Fig.3E). Furthermore, some of the secondary pigment cells, tertiary pigment cells and mechanosensory bristles are also lost in *hs-argos* adult eyes. These are opposite to the loss-of-function phenotypes (Okano et al., 1992), supporting the notion that *argos* functions as a negative signal of cell differentiation of almost all the cell types indicated above. It is possible that the receptor molecule for *argos* is expressed in these cells during the development.

Overexpression of *argos* also affected the trapezoidal pattern of photoreceptor cells in ommatidia and normal spacing of ommatidia. Because the loss-of-function *argos* mutants display practically the same phenotypes, it is suggested that the proper dosage of *argos* is essential for achieving normal pattern formation in the eye. I suppose that *argos* plays a role in the cell fate decisions and assembly of all cell types in the ommatidium.

The eye imaginal discs from the *hs-argos*#4 larva had no discernible defect sufficient to explain the adult phenotypes when stained with Mab22C10 or acridine orange. Some of the Mab22C10 positive cells appeared in the *hs-argos*#4 larval eye discs may not complete differentiation as photoreceptor cells and result in cell death in the pupal stage. The cell death induced by an insufficient cellular differentiation is also true in the glass mutant, where developing photoreceptor cells in the eye imaginal discs express the early neuron specific antigen recognized by Mab22C10, however, they can not express the photoreceptor cell specific antigen and die at ~60 hr APF (Ready et al., 1986; Moses et al., 1989).

Roles of *argos* in wing vein development

The *argos* mutation has been shown to cause morphological defects not only in the compound eye, but also in other organs such as wings and maxillary palps (Okano et al., 1992). However, the function of *argos* outside the eye was not clear. The *argos* gene is expressed exclusively in wing vein primordia during wing development, suggesting that *argos* plays an important role in wing vein formation. Forced expression of *hs-argos* in the *argos* loss-of-function mutant inhibited the formation of the extra veins. The fact that localized expression of *argos* is not needed for the normal pattern formation of wing veins implies that any other molecules including the potential receptor for *argos* or other components of the signal are expressed in a localized pattern. Overexpression of *hs-argos* in the wild-type background resulted in the partial loss of wing veins, depending on the dosage of the *argos* product. These results suggest that *argos* also plays a key role as an inhibitory signal in the differentiation of the cells forming wing veins. The *rho* gene is expressed in a localized pattern corresponding to wing vein primordia and mutations in this gene impair wing vein development (Sturtevant et al., 1993). rhove, a loss-of-function allele of rho, eliminates some veins, as in the case of heat-shocked *hs-argos* flies. Conversely, ubiquitous expression of rho leads to the formation of extra veins, the phenotype similar to that of loss-of-function alleles of *argos* (Sturtevant et al., 1993). Moreover, ectopic expression of rho causes formation of extra photoreceptor cells (Freeman et al., 1992b), as loss-of-function alleles of *argos* do. I showed that overexpression of *argos* enhanced the wing vein phenotype of rho^{ve}. Therefore, it seems that *argos* and *rho* have an opposing function in a common pathway during both eye and wing vein development. *rho* is a member of the *spitz* group (Mayer and Nüsslein-Volhard 1988) and interacts genetically with components of the *Egfr* signaling pathway (Sturtevant et al., 1993). Further experiments are required to clarify the relationships between *argos* and members of the *spitz* group and the *Egfr* signaling pathway. In addition, genetic screening for modifiers of the gain-of-function *argos* phenotypes should lead to the identification of novel genes involved in a signal transduction pathway mediated by *argos*.

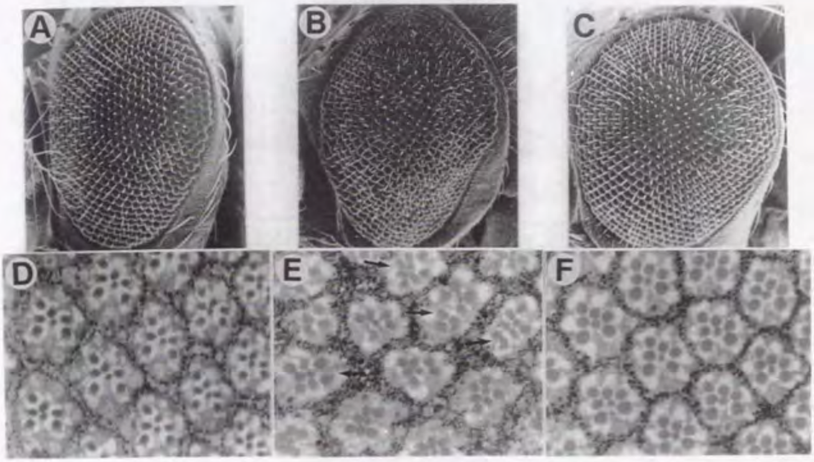

Fig. 1. Heat induced expression of the *hs-argos* gene restores defects in the visual system of *argos*^{sty1e20}. (A-C) Scanning electron micrographs of the compound eyes. (A) The wild-type eye shows regular arrays of ommatidia. (B) In the *argos*^{sty1e20}/*argos*^{sty1e20} eye, the regular arrays of ommatidia are disrupted. (C) The normal external morphology was restored in the of *hs-argos/hs-argos* ; *argos*^{sty1e20}/*argos*^{sty1e20} eye by heat-shock induction of *argos*. (D-F) Tangential sections of adult eyes. Photoreceptor cells are recognized by their rhabdomeres seen as dark spots. (D) In the wild-type, each ommatidium has eight photoreceptor cells, seven of which can be observed in one tangential section. (E) In the *argos*^{sty1e20}/*argos*^{sty1e20} eye, ommatidia often contain extra outer-photoreceptor cells (arrows). The orientation of ommatidia is not uniform. (F) The *hs-argos/hs-argos* ; *argos*^{sty1e20}/*argos*^{sty1e20} eye shows a wild-type ommatidial pattern.

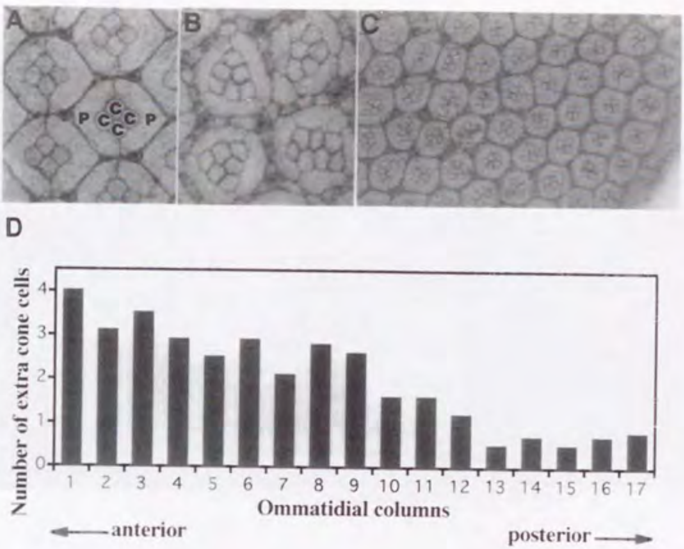

Fig. 2. Heat induced expression of *hs-argos* restores the number of cone cells in the *argos* mutant. (A-C) Cobalt sulfide staining of pupal eyes (at 40-50 hr APF). (A) Wild-type ommatidia have four cone cells (c) surrounded by two primary pigment cells (p). (B) $argos^{sty1e20}/argos^{sty1e20}$ ommatidia have many extra cone cells and pigment cells. (C) The posterior edge of a pupal eye of *hs-argos /hs-argos* ; $argos^{sty1e20}/argos^{sty1e20}$ fly that were heat pulsed at third instar larval stage. In the posterior region, most of the ommatidia contain four cone cells. In anterior region, most of the ommatidia show the *argos* phenotype and have extra cone cells. Anterior to the left. (D) The mean number of extra cone cells in ommatidial columns of flies at 50 hr APF. The transformants were heat-pulsed once (37°C 1hr) in the wandering larval stage. The analysis for a single eye is shown here. I examined ten different flies and obtained similar results.

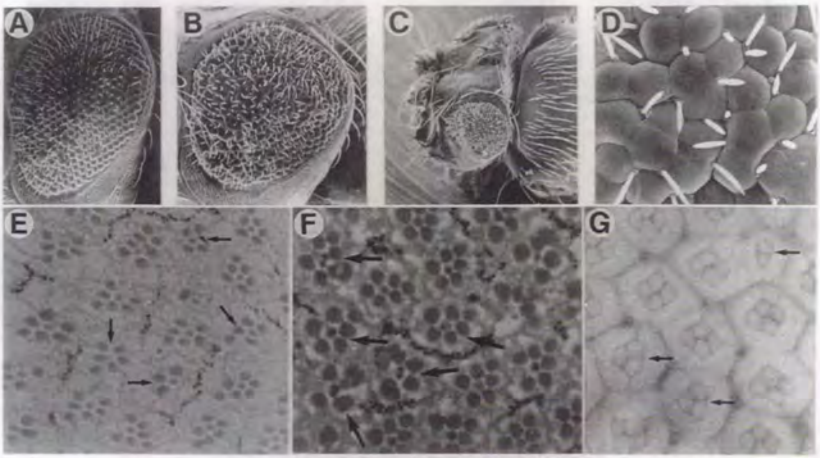

Fig. 3. Phenotypes in the visual system of heat-shocked *hs-argos* flies. (A) A scanning electron micrograph of a compound eye of sev-*hs-argos* raised at 25°C. Note the slightly roughened array of ommatidia. (B-F) Scanning electron micrographs of compound eyes of heat-shocked *hs-argos*#4 flies. When heat pulses are delivered from second instar larval stage, the entire region of the eye becomes very rough (B) and sometimes smaller than wild-type (C). In addition, fusion of lenses and disturbed bristle pattern are observed (D). (E) A tangential section of the compound eye of a heat-shocked *hs-argos*#1 fly. Note the ommatidia with the decreased number of photoreceptor cells (arrows) and loss of pigmented lattices which are composed of secondary pigment cells and tertiary pigment cells. (F) A tangential section of the compound eye of a heat-shocked *hs-argos*#4 fly. Note extra small rhabdomeres (arrows). Otherwise it is similar to *hs-argos*#1 shown in (E). (G) Cobalt sulfide staining of a retina from 50 hr APF pupa of *hs-argos*#4. Note the ommatidia containing only two or three cone cells (arrows).

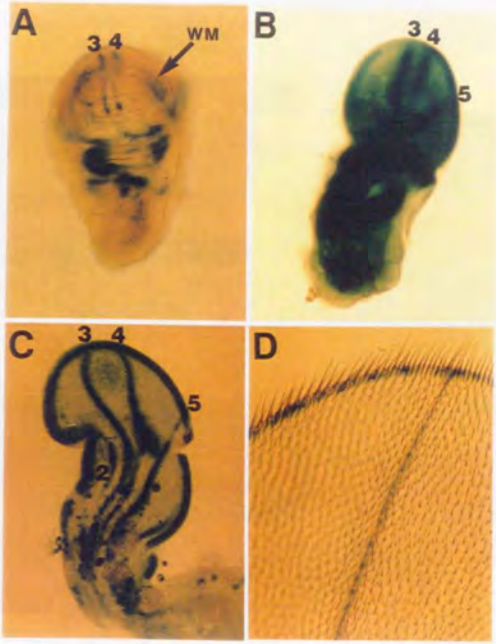

Fig. 4. Expression pattern of *argos* in the developing wing vein. *argos* expression pattern monitored by X-gal staining of the $argos^{sty1}$ heterozygotes. (A) In the late third instar larval stage, two perpendicularly crossing double arrays of cells are stained. The staining is observed along the future wing margin (WM), L3 (3) and L4 (4). (B) At 30 hr APF, stained cells are seen in the wing margin and developing presumptive longitudinal veins L3, L4 and L5. (C) At 72 hr APF, ß-galactosidase expression is detected in the wing margin, all longitudinal veins (L2-L5), the anterior cross vein and the posterior cross vein. (D) A high power view of an adult wing. ß-galactosidase expression is detected in the wing margin and in the wing vein.

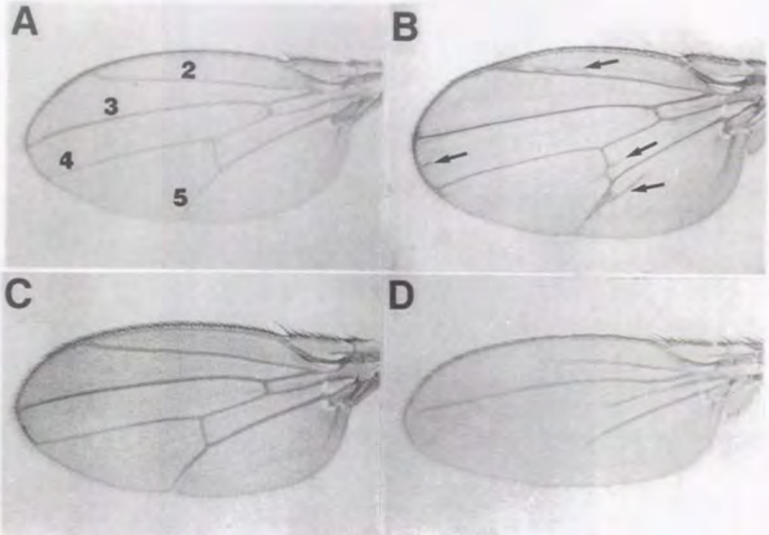

Fig. 5. Wing phenotypes of the *argos* loss-of-function and gain-of-function mutants. Light microscope photographs of adult wings. (A) Wild-type. The marginal vein (L1), the longitudinal veins (L2-L5), the anterior cross vein and the posterior cross vein are shown. (B) A wing of a *argos*$^{\mathrm{sty1e20}}$/*argos*$^{\mathrm{sty1e20}}$ fly. L2 and L3 end in prominent deltas. Extra vein materials are often seen between L3 and L4, between L4 and L5 crossing posterior cross vein, and outside the L2 and L5 (arrows). (C) A wing of *hs-argos/hs-argos* ; *argos*$^{\mathrm{sty1e20}}$/*argos*$^{\mathrm{sty1e20}}$. *hs-argos* completely suppresses the extra vein phenotype of *argos*. (D) A wing of *hs-argos*#4. All longitudinal veins are shortened. Cross veins are lost. L3 is relatively intact in most cases.

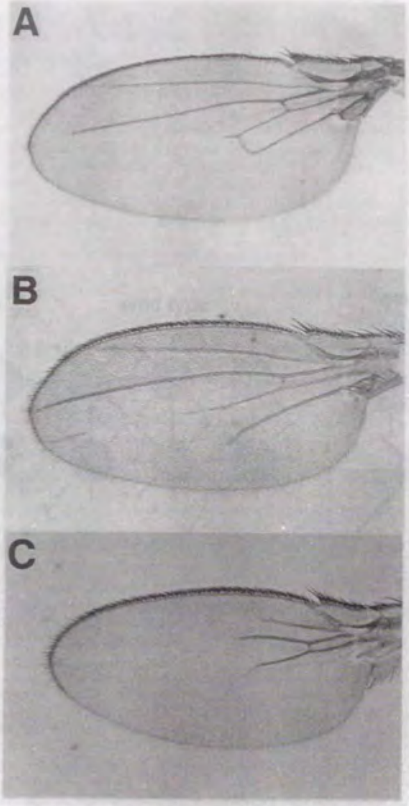

Fig. 6. *argos* genetically interacts with *rho* in developing wing veins. (A) A wing of rho^{ve}/rho^{ve}. Longitudinal veins are shortened. L4 and L5 are most affected, but are not drawn back behind the posterior crossvein. L2 and cross veins are not affected. (B) A wing of heat shocked *hs-argos/hs-argos*. L4 and L5 are shortened. L3 is not affected. (C) A wing of a heat-shocked *hs-argos/hs-argos* ; rho^{ve}/rho^{ve} fly. L2-L4 are strikingly shortened and L5 and the posterior cross vein disappeared completely. Neither *hs-argos/hs-argos* nor rho^{ve}/rho^{ve} alone cause the severe elimination of veins like this.

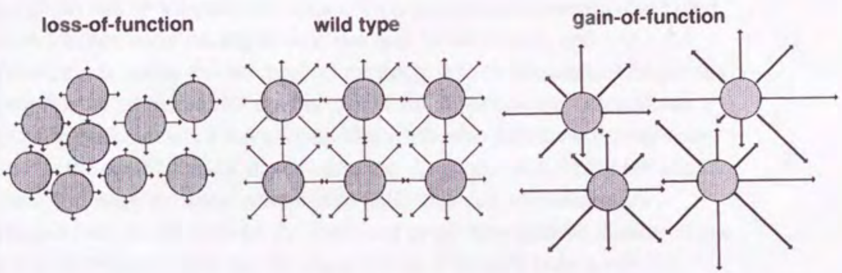

Fig. 7. The *argos* gene product acts as a lateral inhibitor. The gain-of-function and loss-of-function phenotypes of *argos* indicate that the *argos* protein acts on neighboring, undifferentiated cells by inhibiting their cellular differentiation. Such function is reffered as lateral inhibition. Upon the loss-of-function mutation, such an inhibitory signal is removed. Consequently, the number of photoreceptor cells increases. When this inhibitory signal is too strong, the number of photoreceptor cells increases.

Chapter 3

The function of *argos* in projection of photoreceptor axons during optic lobe development in *Drosophila*

Abstract

The *Drosophila argos* gene encodes a secreted protein with an EGF motif, which acts as an inhibitor of cell recruitment in the developing eye and wing. Here, I have analyzed the role of *argos* during optic lobe development. *argos* expression was observed in the optic lobes throughout the developmental stages. In *argos* mutants, neuropiles failed to develop normally during embryonic and larval stages, and photoreceptor axons did not project properly into the lamina. Ubiquitous expression of *argos*, under control of the *hsp70* promoter, rescued the defects in optic lobes. I have found that glial cells failed to differentiate in the larval optic lobes of *argos* mutants. Correspondingly, in the loss-of-function *repo* mutants, whose glial cells also fail to differentiate, photoreceptor axons showed the impaired projection pattern similar to the *argos* phenotype. These results suggest that glial cells play a role for guidance of photoreceptor axons. The loss-of-function *Star* mutation ($Star^{X155}$) dominantly suppressed the defects in the *argos* optic lobes, suggesting that these two genes act in an antagonistic fashion during optic lobe development.

3-1. Introduction

The *Drosophila* visual system, consisting of the compound eyes and the optic ganglia, offers an excellent opportunity to study the molecular and cellular mechanisms regulating the various processes of the neural development such as pattern formation, cell differentiation and axon guidance. The compound eye is comprised of approximately 800 repeat units called ommatidia. Each ommatidium has eight photoreceptor cells (R1-R8) and several accessory cells. Photoreceptor axons (R-axons) must extend a long distance and make a large number of specific choices for precise targeting during the third instar larval period. R-axons project through an epithelial tube, the optic stalk, into the developing optic lobes (Meinertzhagen, 1973). The R1-R6 axons enter into the developing lamina. The R7 and R8 axons penetrate these layers and terminate in a medulla neuropile.

There are several studies carried out to elucidate the mechanism of retinal axon guidance (reviewed by Kunes and Steller, 1993; Meinertzhagen, 1993). Bolwig's nerve, composed of axons of the larval photoreceptor organ, extends into the optic lobe before the innervation of R-axons (Meinertzhagen, 1973). R-axons fail to project into the proper target cells in the mutants which have defects in the development of Bolwig's nerve (Bolwig, 1946; Steller et al., 1987). These observations suggest a role of Bolwig's nerve as a pioneer in retinal axon guidance. However, it has been shown that R-axons do not need the Bolwig's nerve as a pioneer axon for their precise pattern of projection (Kunes and Steller, 1991; Kunes et al., 1993). Given the highly ordered spatio-temporal innervation of R-axons, it was possible that interactions between the neighboring R-axons play an important role in retinal axon guidance (Trujio-Cenoz and Melamed, 1973; Ready et al., 1978). However, the R-axons in *sine oculis* (*so*) and *Ellipse* (*Elp*) mutant project to proper dorsoventral positions in spite of the absence of the usual neighboring R-axons (Kunes et al., 1993), indicating that an R-axon can make pathfinding independently of other R-axons. Thus, there are likely other cues in developing optic lobe which regulate the R-axon projection pattern.

The optic lobes of the adult brain originate from a population of cells located in the embryonic brain (Green et al., 1993). These cells then invaginate from the ectoderm and attach to the surface of the developing brain hemispheres during stages 12 and 13. During the larval stage, the optic lobe primordia are organized into two parts, the inner optic anlagen and outer optic anlagen (White and Kankel, 1978; Hofbauer and Campos-Ortega, 1990). The outer optic anlage gives rise to the target neuropiles for the R-axons, lamina and medulla. The inner optic anlagen generates the remaining neuropiles, lobula and lobula plates. Several genes have been reported to be expressed in the developing optic lobes and some of them are essential for the normal development. These include *neuralized* (*neu*) (Boulianne et al., 1991), *Notch* (*N*) (Markopoulou and Artavanis-Tsakonas, 1989; Green et al., 1993), *asense* (González et al, 1989), *l(1)ogre* (Watanabe and Kankel, 1992), *l(1)optomoter blind* (Pflugfelder et al, 1992), *argos* (Freeman et al., 1992; synonyms: *strawberry*, Okano et al., 1992, and *giant lens* (*gil*), Kretzschmar et al., 1992), *anachronism* (*ana*) (Ebens et al., 1993), *Star* (*S*) (Heberlein et al., 1993; Kolodkin et al., 1994) and *sine oculis* (*so*) (Cheyette et al., 1994; Serikaku et al., 1994).

argos, which encodes a putative secreted protein with an EGF motif, is one of the locus regulating optic lobe development (Kretzschmar et al., 1992; Okano et al., 1992; Brunner et al., 1994). One of the functions of *argos* is to negatively regulate cell differentiation during the development of eye (Freeman et al., 1992; Kretzschmar et al., 1992; Okano et al., 1992; Brunner et al., 1994; Freeman, 1994; Sawamoto et al., 1994) and wing vein (Okano et al., 1992; Sawamoto et al., 1994). *argos* was also suggested to regulate R-axon guidance and optic lobe development. Previous studies have shown that the *argos* mutations result in the impaired projection of R-axons in third instar larvae and the disorganization of optic lobe neuropiles in adult brains (Kretzschmar et al., 1992; Okano et al., 1992). *argos* was shown to be expressed in the optic lobes as well as in photoreceptor cells, and *argos* loss-of-function mutations cause an aberrant projection pattern of R-axons (Kretzschmar et al., 1992; Okano et al., 1992; Brunner et al., 1994). Recent mosaic analysis has shown that *argos* expression is not required in photoreceptor cells for proper axon guidance (Brunner et al., 1994). This result suggests *argos* may be required in the developing optic lobes for guidance of R-axons.

In the present study, I describe the expression and the mutant phenotype of *argos* in the developing optic lobes during the embryonic and larval stages (Sawamoto et al., 1996). I analyzed the role of glia in R-axon guidance using mutants of *repo*, which encodes a glial specific homeodomain protein required for glial differentiation (Campbell et al., 1994; Xiong et al., 1994; Halter et al., 1995). These results of *argos* and *repo* suggest that the glial cells in lamina are required for proper R-axon guidance. I will also describe the genetic interaction of *argos* with *S* in optic lobes.

3-2. Materials and Methods

Fly strains and culture

Canton-S or $white^{1118}$ were used as the wild-type strains. Flies were grown on standard cornmeal medium at 25°C unless otherwise specified. $argos^{sty1}$, $argos^{257}$, *hs-argos#4*, $repo^1$ and $repo^2$ were previously described (Okano et al.,1992; Sawamoto et al., 1994; Xiong et al., 1994). S^{X155} was obtained from G.M. Rubin. S^1 was obtained from U. Banerjee. *3-109* was a gift of C.S. Goodman. $argos^{257}$ is a null-type allele generated by imprecise excision of the P-element from the original $argos^{sty2}$ stock. For heat shock experiment, first instar larvae collected in a glass vial with medium were repeatedly heat-shocked at 36°C for 1 hour with an interval of 25°C for 5 hours by the appropriate stages for examinations using a temperature-programmable incubator.

In situ hybridization

Whole mount in situ hybridization was done by use of RNA digoxigenin-labeled probes as described by Tautz and Pfeifle (1989). The RNA probe was prepared from the longest *argos* cDNA clone, cSty-2 (Okano et al., 1992). Strand-specific RNA digoxygenin probe was generated by in vitro transcription using a standard procedure for a digoxygenin RNA-labeling (Boehringer Mannheim).

Immunohistochemistry

mAb24B10 was a kind gift of S.C.Fujita (Fujita et al., 1982). rk2-5' was obtained from A. Tomlimson (Campbell et. al., 1994). Anti crumbs (crb) antibody was gifted by E. Knust (Tepass et al., 1990).

Embryos were collected, dechorionated, and fixed for 10 min in a mixture of 3.7% formaldehyde in PEMS (0.1M PIPES, 2mM $MgSO_4$, 1mM EGTA, pH7.0) with heptane. Subsequently, they were devitellinized in methanol. After several washes in PBS containing 0.1% Triton X-100 and 0.2% BSA (PBT), embryos were incubated for 30 minutes in PBS containing 5% goat serum and 0.1% Triton X-100 (PBT+N). Embryos were then incubated with anti-crb antibody overnight at 4°C. After several washes in PBT, embryos were incubated at room temperature for 2 hours in a HRP conjugated goat anti-mouse IgG (Jackson Immunoresearch) used at 1:500 dilution in PBT+N. Preparations were washed several times in PBT, then incubated in 0.2 mg/ml diaminobenzidine (Sigma) solution and 0.0003% H_2O_2 in PBT. The reaction was stopped after 15-20 minutes by diluting the substrate with PBT.

Antibody staining of larval brains were essentially performed as described previously (Tomlinson and Ready, 1987), except that brains were fixed in 4% paraformaldehyde (PFA) in PBS instead of PLP.

X-gal Staining

X-gal staining was carried out as described by Okano et al.(1992). For double staining with antibodies and X-gal, brains were fixed with 2%

paraformaldehyde at 4°C for 10 minutes, stained according to the method of Okano et al. (1992) and then incubated with antibodies.

Adult head sections

Adult fly heads were dissected out and fixed in Carnoy's fixative for 30 minutes, washed in PBS, dehydrated in an ethanol series, and embedded in paraffin. Horizontal sections of 8 μm were stained with hematoxylin and eosin. Silver staining of the sections were carried out as previously described (Meyerowitz and Kankel, 1978).

BrdU labeling of larval brains in vitro

Larval nervous systems with imaginal discs were dissected out in cold PBS and cultured in *Drosophila* Ringer solution containing 500 μM BrdU (Sigma) for 1 hour at 25°C. Brains were fixed in 4% PFA in PBS for 1 hour at 25°C, washed in PBS, treated with 2N-HCl in PBT, washed in PBT, and then incubated in anti-BrdU antibody (Becton Dickinson) at 1 : 1000 dilution. The primary antibody was detected using a ABC kit (Vector Lab.).

3-3. Results

***argos* is expressed in the developing optic lobes**

To investigate the role of *argos* in optic lobe development before retinal innervation, I characterized the expression pattern of *argos* in embryos and larvae. Adult optic lobes originate from the optic lobe primordia in the developing brain of embryo. Therefore, I examined the expression of *argos* transcripts in embryos by in situ hybridization. *argos* mRNA was detected in several cells of presumptive optic lobe primordia in the brain hemisphere of stage 12 embryos (data not shown). The *argos*-expressing cells increased in number as the embryos developed (Fig. 1). A similar expression pattern was observed by anti ß-galactosidase antibody staining of embryos heterozygous for the $argos^{sty1}$ or $argos^{sty2}$ P[*LacZ*] enhancer trap element (data not shown).

In the early first-instar larva, the *argos-LacZ* reporter was expressed in a small number of cells in the optic lobe of $argos^{sty1}$ heterozygote (Fig. 2A). The *LacZ* expression continued in the developing optic lobes through the first and second instar of larval development (Fig. 2B).

In the early third-instar larva, the *LacZ* began to be expressed at the area of lamina where the axons of photoreceptor cells innervate (Fig. 2C). The *argos-LacZ* expressing cells, consisting of both neurons and glia (Brunner et. al., 1994), were strikingly decreased in number in the lamina of late-third-instar larvae homozygous for *argos*^{sty2} (Fig.2E). These *argos*-positive cells were observed only in the area innervated by R-axons stained with mAb24B10 (Fig. 2E).

argos is essential for the development of optic lobes before the innervation of R-axons

To examine the effects of the loss of *argos* function on the development of optic lobes, the target region of retinal axons, developing optic lobes of the *argos* embryo and larva, were compared to the wild-type using several cell-type specific markers expressed in the optic lobes. The optic lobe primordia invaginates during stages 12 and 13 from the head ectoderm of the embryo. The invagination forms a flattened vesicle, that are attached to the ventrolateral surface of the brain (Green et al., 1993; Cheyette et al., 1994). The lining of its lumen can be visualized with anti-crb antibody (Tepass et al., 1990). The anti-crb antibody stained circles located at the ventrolateral surface of the wild-type stage 16 brain (Fig. 3A, C). Various defects were observed in optic lobe primordia of *argos* homozygous embryos. In *argos*^{257} embryos, the optic lobe primordia often failed to form the complete circles and/or were mis-located at the dorsal surface of the brains (Fig. 3B,D), suggesting that *argos* is required for the early developmental processes of optic lobes.

To explore defects in the optic anlagen in *argos* larvae, I stained whole mounts with the anti-FasII antibody. FasII was expressed in a subset of cells in the outer optic anlagen in an arc-shape during the second instar (Kaphingst and Kunes, 1994; Fig. 4A). In *argos*, the morphology of outer optic anlagen was disorganized (Fig. 4B). The *argos* brain-hemispheres were sometimes larger than that of the wild-type (Fig. 4G) and fused together (Fig. 4C), suggesting that *argos* regulates the brain morphogenesis. The pair of optic lobes was also fused at the dorsal surface of the brains in individuals with severe defects in the brain morphogenesis (Fig. 4C). To determine whether cell proliferation is affected in the *argos* larval brain, I analyzed the pattern of BrdU incorporation. Fig. 4D shows the pattern of BrdU incorporation for a wild-type third instar larva. There are three domains of mitotic active cells: outer proliferation center (OPC), inner proliferation center (IPC) and lamina precursor cells (LPCs). It has been shown that OPC produces the neurons of medulla, whereas neurons of lobla complex and inner medulla derives from IPC (White and Kankel, 1978; Hofbauer and Campos-Ortega, 1990). LPCs, which generate the neurons of lamina, show a narrow stripe between OPC and IPC (Selleck and Steller, 1991). In *argos* third instar larvae, the mitotic LPCs remarkably decreased in number, while the pattern of mitosis in the OPC appears normal. Interestingly, proliferating cells in the IPC also decreased in number in the *argos* mutant. Thus, *argos* is likely to be essential for the development of target neuropiles of retinal axons during embryonic and larval stages.

Transformation rescue of the aberrant axon projection

To demonstrate that the loss of *argos* function is responsible for the aberrant projection of R-axons and the disorganized adult optic lobes, I introduced the *hs-argos* transgene (Sawamoto et al., 1994) into the *argos*^{sty2} mutant fly (Okano et al., 1992). The projection pattern of R-axons were labeled with mAb24B10 which recognizes the photoreceptor cell specific antigen, Chaoptin (Fujita et al., 1982; Zipursky et al., 1984). The projection pattern in the wild-type brain at the third instar is shown in Fig. 5A. The R-axons extend through the optic stalk and grow into the brain, and spread in a half-moon shaped fashion, outlining the area of the developing lamina (Meinertzhagen, 1973; Trujillo-Cenoz and Melamed, 1973). Although the axons of the flies homozygous for *argos*^{sty2} reached the surface of the brain, they failed to spread in a half-moon shape (Fig. 5B). However, administration of heat-pulses to *hs-argos*; *argos*^{sty2} through the larval stages restored the projection pattern of R-axons (Fig. 5C). Such a rescue of the mutant phenotype was not observed by the application of heat pulses only during the embryonic, first instar or late-third instar larval stage (data not shown). This suggest that *argos* is required to be expressed at multiple stages for normal development.

A section of a wild-type adult head is shown in Fig. 5E. The optic lobe contains four neuropiles with a columnar structure: lamina, medulla, lobula and lobula plate (Strausfeld, 1976; Fischbach and Dittrich, 1989; Fig. 5E). *argos*^{sty2} flies show an impaired optic lobe structure (Okano et al., 1992; Fig. 5F) similar to other *argos* alleles previously described (Kretzschmar et al., 1992; Brunner et al., 1994). The *hs-argos*; *argos*^{sty2} flies which received heat-pulses during the larval and pupal stages showed optic lobes with normal structure (Fig. 5G). These results indicated that the optic lobe phenotype described above is a result of the loss of *argos* function.

Ubiquitous overexpression of *argos*

To test the possibility that *argos* directly functions as a positional signaling molecule in retinal axon navigation, the innervation pattern of R-axons was characterized in the *hs-argos*; *argos*$^{+}$ transgenic flies (Sawamoto et al., 1994). If *argos* has any attractive or repulsive activity regulating the interaction between axons and target neurons, ubiquitous overexpression of *argos* would be expected to result in a disturbed projection pattern of R-axons. However, R-axons of heat-shocked *hs-argos*#4 larva innervated normally in a half-moon shape (Fig. 5D), implying that the ectopic overexpressed *argos* did not impair the retinal innervation. The adults also showed normally organized neuropiles (Fig. 5H), which confirms that ectopically expressed *argos* does not affect the development of the optic lobe. Silver staining of the *hs-argos*#4 adult head sections revealed that projection pattern of axons in the optic lobes was also normal (data not shown).

Glial development in the optic lobes

In the previous studies, *argos* was shown to be involved in cell determinations during eye and wing development (Freeman et al., 1992; Kretzschmar et al., 1992; Okano et al., 1992; Brunner et al., 1994; Freeman, 1994; Sawamoto et al., 1994). Therefore, *argos* may be required for development of certain types of cells which play roles in the axon guidance in the optic lobes. Glial cells are good candidates for a guidance cue for R-axons, because lamina glia (L-glia) are generated before the retinal innervation (Winberg et al., 1992). To investigate the role of *argos* in the development of glial cells in the lamina, the developing L-glia were labeled with a monoclonal antibody rk2-5', recognizing a glial-specific homeodomain protein repo (Xiong et al., 1994; Campbell et al., 1994; Halter et al., 1995). The expression of the repo protein was detected in a group of glial cells in the optic lobes of third instar larva (Fig. 6C). In the *argos* mutant, the number of L-glial cells stained with this glial marker decreased and neuropiles in optic lobes showed a very irregular morphology (Fig.6D), although the penetrance of this phenotype was variable. This result indicate that *argos* is required for the optic lobe development and glial differentiation. The pattern of repo-positive glial cells elsewhere in the brain and eye discs was indistinguishable from the wild-type (Fig. 6A,B).

To investigate the possibility that the loss of L-glia in *argos* is responsible for the aberrant R-axon projection, I examined the pattern of retinal innervation in repo mutants, where glial cells fail to differentiate properly (Xiong et al., 1994; Campbell et al., 1994; Halter et al., 1995). In the developing brain of larvae homozygous for *repo*^{1}, a viable allele, the projection pattern of R-axons is strikingly disordered in a similar way as *argos* in ~20% of mutants examined . The morphology of the lamina neuropile, however, appeared normal in *repo*^{1} (Fig. 7B). In addition, fasciculation of R-axons in the optic stalk was disordered in ~10% of the *repo*^{1} mutants examined (Fig. 7A). Similar defects were observed in the *repo*^{1}/*repo*^{2} (a lethal allele) larvae (data not shown).

Interaction of *Star* and *argos* in the developing optic lobes

I have shown that *argos* interacts with *rhomboid* (*rho*) in wing vein development (Sawamoto et al., 1994). I analyzed the role of members of the *spitz* group including *rho* in the optic lobe development. *Star* (*S*), a member of the *spitz* group, encodes a putative transmembrane protein based on hydropathy profile which is required for embryogenesis and differentiation of photoreceptor cells, R8, R2 and R5 (Heberlein and Rubin, 1991; Heberlein et al., 1993; Kolodkin et al., 1994). Previous studies showed that *S* is expressed in the optic lobe primordia of the embryonic brain at stages 12-15 and developing optic lobes at third instar (Heberlein et al., 1993; Kolodkin et al., 1994), in a similar pattern to that of *argos* at these stages (Figs. 1, 2).

The projection pattern of R-axons in the larva heterozygous for the loss-of-function *S* mutations, S^{X155} (Heberlein and Rubin, 1991) and S^1 (Kolodkin et al., 1994), were indistinguishable from the wild-type (data not shown). To analyze effect of *S* loss-of-function mutations on the optic lobe phenotype of *argos*, I crossed S^{X155} flies to $argos^{257}$ flies. In $argos^{257}$ homozygous larva, the R-axons failed to innervate the lamina properly (Fig. 8A). Their phenotype was similar to but considerably severer than the $argos^{sty2}$ allele (Fig. 5B). However, nearly normal projection of axons was observed in S^{X155}/CyO; $argos^{257}/argos^{257}$ larva (Fig.8B). Expression pattern of repo in L-glia and morphology of lamina neuropiles also appeared normal in S^{X155}/CyO; $argos^{257}/argos^{257}$ larva (data not shown). Thus, it is likely that *S* acts in optic lobe development in a common pathway with *argos*.

3-4. Discussion

Projection pattern of R-axons is highly disorganized in the adult visual system of *argos* (Kretzschmar et al., 1992; Okano et al., 1992). Since *argos* is expressed in both photoreceptor cells and optic lobes, three possibilities can be proposed as the mechanism of *argos* function in retinal axon guidance. First, argos secreted from R-axons could serve as a signal for optic lobe development and proper targeting of R-axons to lamina neurons. However, mosaic analysis recently showed that *argos* expression is not required in photoreceptor cells for proper axon guidance (Brunner et al., 1994). The second possibility is that the *argos* expressed in optic lobe could be an attractive molecule for incoming retinal axons and directly regulate axonal pathfinding like vertebrate netrin-1 which attracts commissure neurons (Serafini et al., 1994). However, ubiquitous expression of *argos* did not affect the axonal guidance and optic lobe development (Fig. 5). Therefore, argos is not an affinity molecule for R-axons in the lamina or its expression is not sufficient to act as an affinity cue. The third possibility is that argos plays a role in the development of optic lobes, which is the target region of R-axons and is expected to be important for axonal guidance. Here, I focused on the expression pattern and mutant phenotype of *argos* in the developing optic lobes during the embryonic and larval stages to examine the role of *argos* required for retinal innervation (Sawamoto et al., 1996).

In the embryo, *argos* transcripts were detected in the cells forming optic lobe primordia at stages 12 and 13, when the optic lobes primordia invaginate from the head ectoderm, form the closed vesicles and then attach to the ventro-lateral surface of brain hemispheres (Green et al., 1993). I found that the *argos* mutation caused failure in the morphogenesis of optic lobes at this stages (Fig. 3). On the basis of the expression pattern and mutant phenotype, it is likely that *argos* plays a role early in the process of optic lobe development. Mutations in the neurogenic genes cause similar defects in optic lobe development at the embryonic stages (Hartenstein et al., 1992; Green et al., 1993). Notch is strongly expressed in the optic lobes during the invagination and is necessary for the cells of optic lobe to remain as epithelium (Green et al., 1993). Although the mechanism of regulating optic lobe development in the embryo by *argos* remains unclear, it is possible that *argos* is also involved in the cell fate decisions during the invagination. so, which encodes a homeodomain protein, is known to play a role in the process of optic lobe invagination at the embryonic stages. so is expressed in the optic lobe invagination and loss of function mutation cause a failure of the optic lobe invagination similar to *argos* (Cheyette et al., 1994; Serikaku et al., 1994). Therefore, *so* may control the expression of genes required for the cellular morphogenesis in the optic lobes such as neurogenic genes and *argos*.

After hatching, neuroblasts in the optic lobes segregate into two separate populations, the outer and inner anlagen. The outer optic anlagen gives rise to the target neuropils for retinal axons, lamina and medulla. The *argos LacZ* reporter was expressed in the optic anlagen throughout the larval development. The *argos* mutation resulted in disorganized morphogenesis of optic lobes at this stage, as shown by the anti-FasII immunostaining. I found that proliferation pattern in the brains were disordered in *argos*. Decrease of LPCs in *argos* could be due to the impaired R-axon projection, because the cell division to produce lamina neurons is known to depend on the innervation of R-axons (Selleck and Steller, 1991; Selleck et al., 1992). On the other hand, defective mitosis in the IPC explains the disorganization of lobula complex in the *argos* adults. Thus, *argos* is required during the larval stages for normal optic lobe proliferation and development.

At larval stages, *argos* may be essential for the differentiation of cells in the optic lobes which are required for the guidance of R-axons. Candidates for the cells acting as a guidance cue are glial cells, because they are generated before the retinal innervation to be located in the route of the subsequent R-axonal projection (Winberg et al., 1992). In several systems of both vertebrate and invertebrate, glial cells are present before neuronal differentiation and act as a substrate required for axonal guidance and neuronal migration (Hutchins and Casagrande, 1988; Jacobs and Goodman, 1989). This view is supported by the present result that expression of repo in the lamina are impaired in the *argos* mutant. The expression of another glial marker, *3-109*, in L-glia is known to depend on the R-axon innervation (Winberg et al., 1992). On the other hand, medulla glia and subretinal cells express *3-109* independently of retinal innervation (Winberg et al., 1992). Therefore, one possible interpretation of these observations is that the altered expression of the markers in the *argos* L-glia could result from the impaired projection of R-axons. However, this possibility could not fully explain the following observation. The expression of repo and *3-109* were also weakened even in the medulla glia and the innervated area of lamina in *argos* mutants (repo, Fig. 6D; *3-109*, data not shown). Therefore, glial development was likely to be disturbed prior to the retinal innervation in the *argos* mutant.

Importance of glial function in the retinal axon guidance was also indicated by the phenotype of the *repo* mutant, where glial cells fail to differentiate normally (Xiong et al., 1994; Campbell et al., 1994; Halter et al., 1995). Hypomorphic *repo* mutations resulted in aberrant projections of R-axons, a phenotype similar to *argos*. This result is consistent with the proposal that the misrouting of R-axons in the *argos* mutant is a consequence of failure in the glial development (Fig. 9). Strictly, I can not exclude the possibility that impaired development of cells other than glial cells are responsible for altered R-axon guidance in *argos*.

I have described previously that *rho*, a member of the *spitz* group, interact genetically with *argos* in the wing development (Sawamoto et al., 1994). The *rho* gene did not appear to function in the optic lobes because the *rho LacZ* reporter was not detected there (data not shown). Expression of *S* was observed in the developing optic lobes (Heberlein et al., 1993; Kolodkin et al., 1994) as is *argos*. Furthermore the genetic interaction between *argos* and *S* indicates that *S* plays a role in retinal axon guidance and/or optic lobe development. The present observation that the loss-of-function *S* mutation acted as a dominant suppressor of the *argos* optic lobe phenotype suggests that *argos* and *S* have opposing functions in a common pathway. It is unlikely that *S* negatively regulates the expression of *argos*, because the S^{X155} mutation could suppress the phenotype in the null type allele of *argos*. It is possible that *S* is required in the cells receiving the signal by the *argos*. *S* and *rho* activate the signal transduction interacting with components of the Ras signaling cascade (Heberlein et al., 1993; Sturtevant et al., 1993; Kolodkin et al., 1993). Our genetic data reveal that *argos* acts as an inhibitor of the signal transduction in the MAP kinase cascade (See Chapter 4). Therefore, *argos* and *S* may act on the Ras/MAP kinase cascade in an antagonistic fashion. Mosaic analysis would further clarify the function of *S* in the optic lobe development.

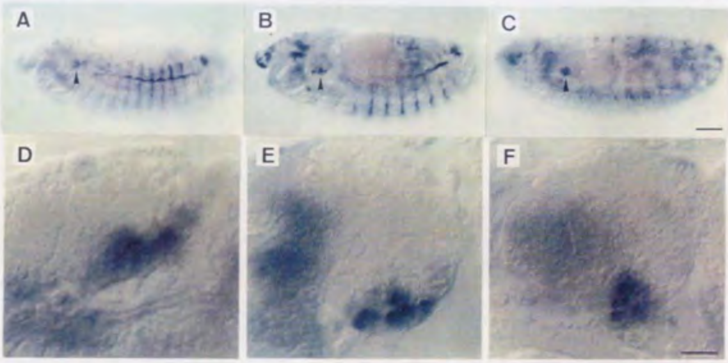

Fig.1. Expression pattern of *argos* in the optic lobe primordia in the embryo. *argos* expression was detected by whole-mount in situ hybridization. Each photograph shows a lateral view of stages 13 (A, D), 14 (B, E) and 16 (C, F). D, E and F correspond to the higher magnification of the brain of embryos shown in A, B and C, respectively. Optic lobe primordia are marked with arrow heads in A, B and C. Anterior is to the left. Bar: 50μm in (A,B,C) and 15 μm in (D,E,F).

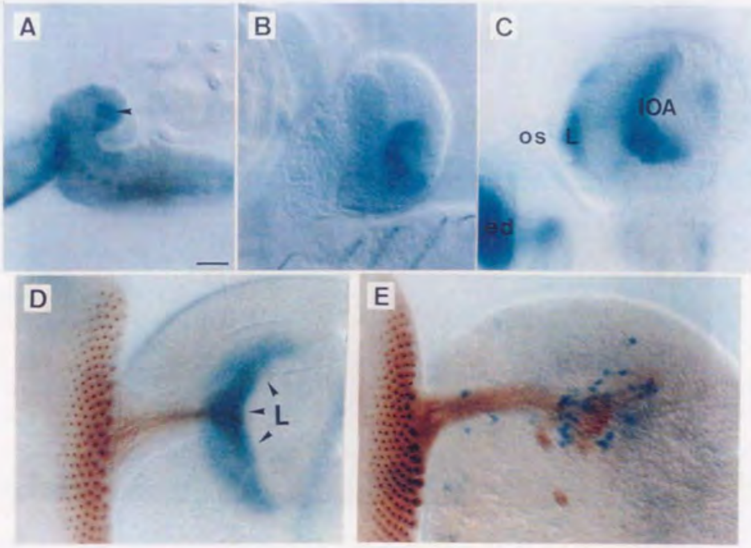

Fig. 2. Expression of *argos-LacZ* in the larval optic lobes in the *argos* enhancer trap lines. Each photograph shows a lateral view of brain in the first instar (A), second instar (B) and early-third instar (C) larva. In the panel A, optic anlage is marked with an arrow head. (D, E) Brains of the third-instar larvae stained with both mAb24B10 (brown) and X-gal (blue). (D) Wild-type. (E) In $argos^{sty2}$ homozygotes, there are small number of cells expressing *argos* (blue) in the area where R-axons (brown) innervate. Anterior is to the left. Abbreviations are as follows: IOA, inner optic anlage; L, lamina; os, optic stalk. Bar: 50μm in (A-C) and 15μm in (D,E).

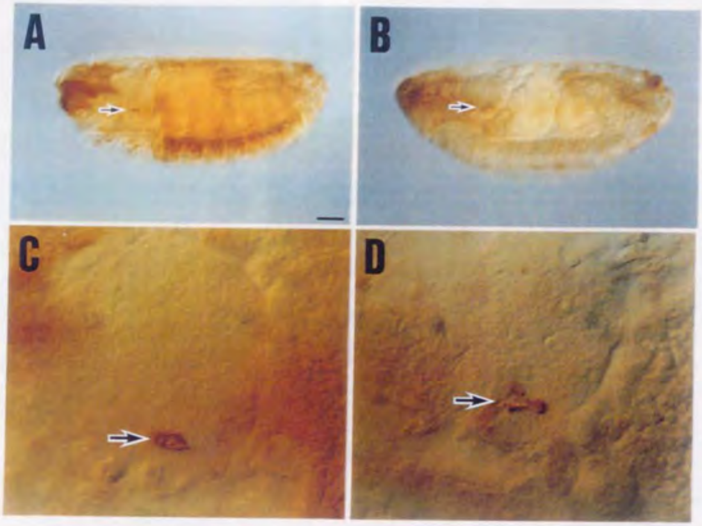

Fig. 3. Impaired optic lobe development in the *argos* mutant embryo. Brains of stage 15 embryos were stained with anti-crb antibody. To distinguish homozygotes from heterozygotes, the expression of *Ubx-LacZ* on the *TM6* chromosome was examined by anti-ß-galactosidase staining. C and D correspond to the higher magnification of the brain of embryos shown in A and B, respectively. (A, C) Closed vesicle of optic lobe primordium is visualized at the ventro-lateral surface of the brain of $argos^{257}$/TM6, P[*Ubx-LacZ*]. (B, D) Brains of embryo homozygous for $argos^{257}$ stained with anti-crb. The optic lobe primordia fail to form the complete circle (marked with arrows). Anterior is to the left. Bar: 50μm in (A,B) and 10μm in (C,D).

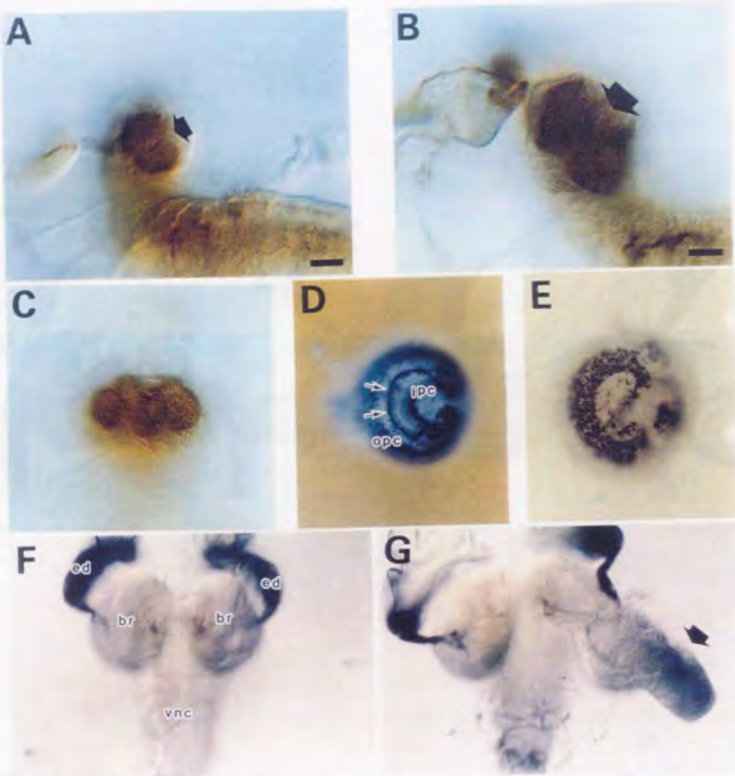

Fig. 4. Impaired optic lobe development in the *argos* mutant larva. (A-C) Brains from the second-instar larva were stained with anti-FasII antibody. (A) The optic lobe stained with anti-FasII antibody at this stage shows a horseshoe-like shape in the wild-type (marked with arrow). Bar, 10μm. (B) In the $argos^{sty2}$ larva, the morphology of optic lobes is disorganized (marked with arrow). Bar, 10μm. (C) Dorsal view of optic lobes of $argos^{sty2}$ larva with a severe phenotype. Note that the two optic lobes are fused at the dorsal surface of the fused brain. (D, E) Patterns of cell division in the brains of wild-type and *argos* third instar larvae. Mitotically active cells are labeled with BrdU and detected by immunohistochemistry. (D) In the wild-type, there are three domains of BrdU incorporated cells: OPC, IPC and LPCs (marked with arrows). (E) In the *argos*, proliferating cells in the IPC and LPCs decrease in number, while OPC is normal. (F,G) Low magnification views of eye-anntenal discs and central nervous systems. Photoreceptor cells are stained with mAb24B10. (F) Wild-type. (G) In the $argos^{sty2}$ larva, brain hemisphere expands abnormally (arrow). In panels A, B, D, and E,anterior is to the left and dorsal is up. In panel C, F and G, anterior is up. Abbreviations are as follows: br, brain; ed, eye disc; ipc, inner proliferation center; opc, outer proliferation center; vnc, ventral nerve cord.

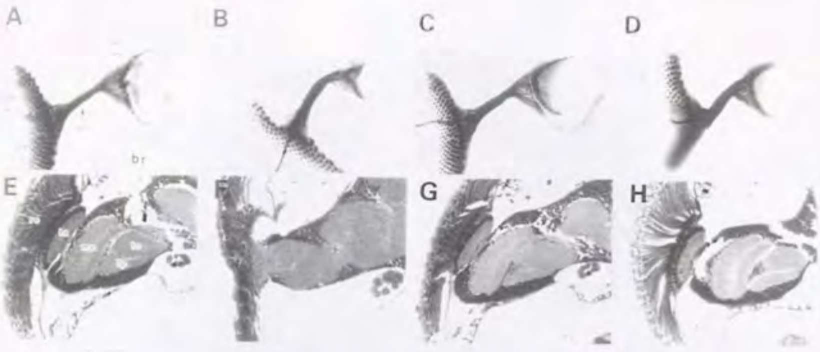

Fig. 5. Rescue of *argos* phenotype and ectopic expression with the *hs-argos* transgene. (A-D) Projection pattern of R-axons from the eye disc into the optic lobe labeled with mAb24B10. The halfmoon-shaped projection pattern of R-axons seen in wild-type (A) is disrupted in *argos*^{sty2} (B). (C) Projection pattern of axons is restored by applying heat pulses to *hs-argos*; *argos*^{sty2} larva. (D) The projection pattern of R-axons is normal in the heat shocked *hs-argos*#4 larva. (E-H) Horizontal sections of adult optic lobes. (E) The wild-type optic lobe consists of a lamina, medulla, lobula and lobula plate. Note the columnar organization of neuropiles. (F) In the *argos*^{sty2} brain, the regular organization of the neuropiles is disrupted. (G) The disorganization of the optic lobes is significantly improved in the *hs-argos* ; *argos*^{sty2} fly. (H) A section of optic lobe from a heat-shocked *hs-argos*#4 fly. The organization of neuropiles appears to be normal. Anterior is to the left. Abbreviations are as follows: bn, Bolwig's nerve; br, brain; ed, eye disc; la, lamina; lo, lobula; lp, lobula plate; me, medulla; os, optic stalk; re, retina.

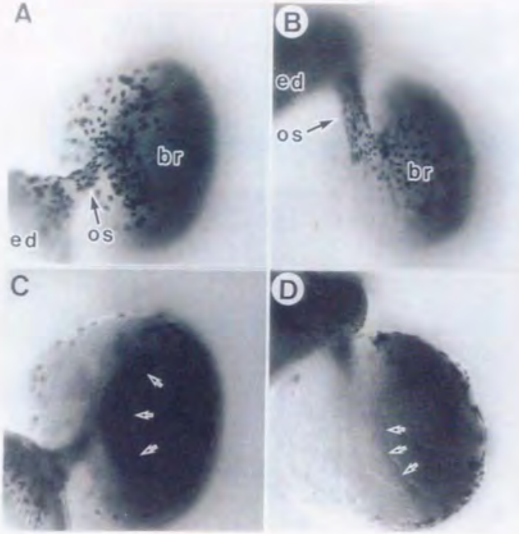

Fig. 6. Expression of repo in the lamina of the wild-type (A, C) and *argos*^{sty2} mutant (B, D) third instar larvae. (A, B) Surface views of brains. Pattern of repo-positive cells stained with rk2-5' antibody (Campbell et al., 1994) in the optic stalk and on the brain surface of *argos* (B) is indistinguishable from the wild-type (A). (C, D) Sagittal optical planes at the level of lamina. Lamina are marked with arrows. (C) There are large number of glial cells in the wild-type lamina. (D) In the *argos*^{sty2} lamina, glial cells stained with the rk2-5' dramatically decreased in number. Note that the morphology of lamina, which is normally crescent shaped, appears to be irregular in the *argos* mutants. Anterior is to the left. Abbreviations are as in Fig. 5.

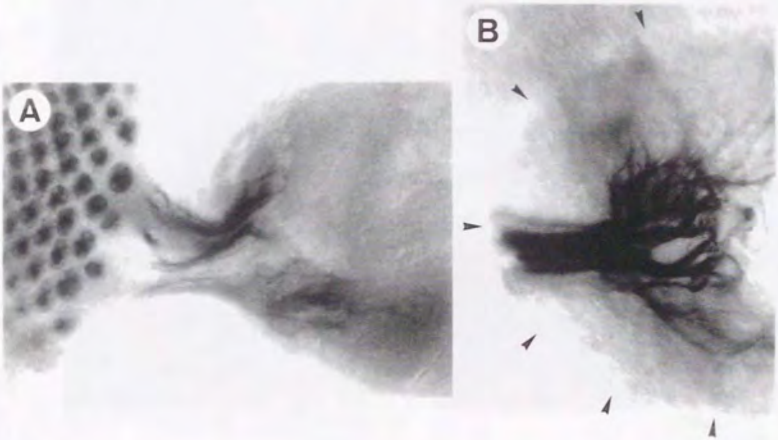

Fig. 7. Projection pattern of R-axons in the *repo* mutant. Brains attached to eye imaginal discs were dissected from the *repo*[1] third instar larva and stained with mAb24B10. (A) In the optic stalk, the fasciculation of R-axons is disordered. (B) Projection pattern of R-axons in the *repo* lamina is impaired, whereas morphology of the lamina neuropile appears normal (arrows). Anterior is to the left.

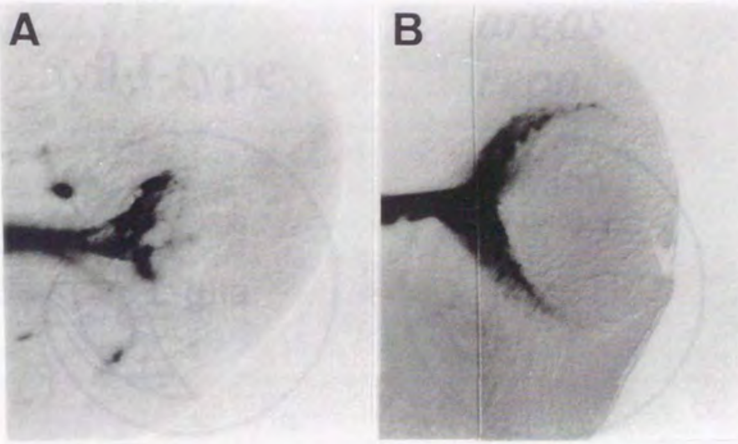

Fig. 8. *Star* acts as a dominant suppressor of *argos* in the developing optic lobes. R-axons were stained with mAb24B10. (A) R-axons reached the brain surface but did not project into the deep layer of optic lobes in $argos^{257}$. (B) In S^{X155}; $argos^{257}$ brain, R-axons show a normal projection pattern. Anterior is to the left.

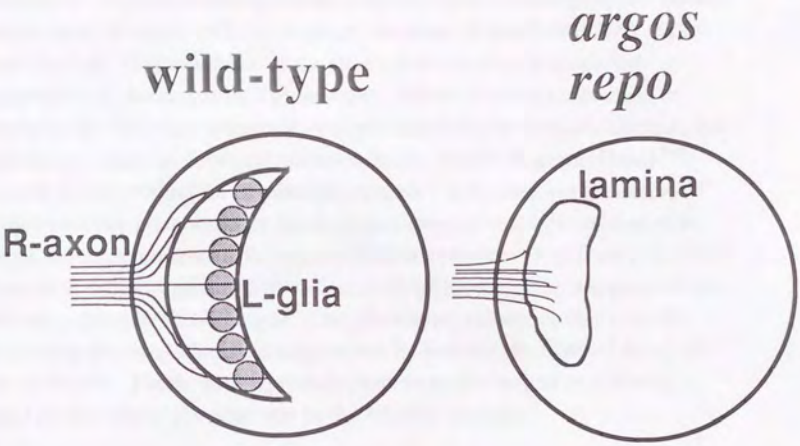

Fig. 9. Relationship between L-glia and R-axon innervation in the wild-type and mutants. In the wild-type, L-glia is generated before the R-axon ingrowth. In the lamina of *argos* and *repo* mutants, R-axons fail to project properly. Failure of glial development in the lamina is possibly responsible for the aberrant projection pattern of R-axons in these mutants. Anterior is to the left.

Chapter 4. *argos* inhibits signal transduction in the MAP kinase cascade

Abstract

The *Drosophila argos* gene encodes a secreted protein which acts as an inhibitor for cellular differentiation in the multiple developmental processes. To better understand the role of *argos*, I have analyzed genetic interactions of *argos* with other genes involved in the Ras/MAPK signal transduction. Hypomorphic mutation in *Star* acted as a dominant suppressor of the *argos* null phenotype. Effect of over expression of *argos* by the *hs-argos* transgene was enhanced by the loss-of-function *Star* mutations. Gain-of-function mutation in the MAPKK gene (*Dsor1*^{Su1}) caused a overproduction of photoreceptor R7 and wing veins. *Dsor1*^{Su1} suppressed the phenotype by the *hs-argos* expression. Loss-of-function *argos* mutation enhanced the gain-of-funtion phenotype of *Dsor1* and *Sos*. Gain-of-function mutations of *rolled*, a MAP kinase gene, suppressed the defects caused by the *hs-argos*. The phenotype caused by the loss-of-function *argos* mutation was suppressed by halving the dose of *Ras1*, *D-raf* or *Dsor1*. These results provide evidences that *argos* negatively regulate the signal transduction in the MAPK cascade.

4-1. Introduction

Cell-to-cell signalings are important for normal cellular proliferation and differentiation during development of muticellular organisms. Elucidating both inductive and suppressive mechanisms required for control of these signals is one of the central goal of developmental biologists. Cell specifications in the several developmental processes are known to be induced by the signal transduction activated by a family of receptor tyrosine kinases which respond to extracellular signals. In *Drosophila*, the receptor tyrosine kinase encoded by *torso* controls the development of terminal structures in the embryo (Klingler et al., 1988; Sprenger er al., 1989) and the receptor tyrosine kinase encoded by *sevenless* (*sev*) is required for the specification of the R7 photoreceptor cell fate in the developing eye (Tomlinson and Ready, 1986; Hafen et al., 1987; Bastler et al., 1988; Bowtell et al., 1988). Compared to these receptor tyrosine kinases involved in the specific phenomena, the *Drosophila* homologue of the EGF receptor (*DER*) is required for multiple developmental processes such as eye (Baker and Rubin, 1989, 1992; Xu and Rubin, 1993), wing vein (Diaz-Benjumea and Garcia-Bellido, 1990; Diaz-Benjumea and Hafen, 1994) and dorsoventral patterning of the follicular cells in the embryo (Schüpbach, 1987). Genetic screening for dominant modifiers of the *sev* mutations have identified the components in the signal transduction cascade (Simon et al., 1991). They include Drk (Simon et al., 1993; Olivier et al., 1993), an SH3-SH2-SH3 adapter protein, Sos (Rogge et al., 1991), a putative guanine-nucleotide releasing factor and Ras1 (Simon et al., 1991). Drk, Sos and Ras1 also functions downstream of torso and DER (Simon et al., 1992; Doyle and Bishop, 1993). Gap1 acts as a negative regulator of signaling by receptor tyrosine kinases by down-regulating the activity of the Ras1 protein (Gaul et al., 1992). Activated Ras1 causes the activation of D-raf (Ambrosio et al., 1989; Dickson et al., 1992), which result in phosphorylation of MAP kinase kinase (MAPKK) encoded by *Dsor1* (Tsuda et al., 1993) and MAP kinase (MAPK) encoded by *rolled* (*rl*) (Biggs et al., 1994; Brunner et al., 1994). In addition, *spitz* (*spi*), *rhomboid* (*rho*) and *Star* (*S*), members of the *spitz* group gene, interact with components of the Ras signaling cascades in the developing eye and wing vein (Sturtevant et al., 1993; Heberlein et al., 1993; Freeman, 1994; Kolodkin et al., 1994). Thus, a number of components in the cascades have been identified, however, the extracellular mechanism to regulate negatively the signal transduction for normal development is still unknown.

argos, a secreted protein with an EGF motif, acts as an inhibitor of cell recruitment in the developing eye and wing (Freeman et al., 1992; Kretzschmar et al., 1992; Okano et al., 1992; Freeman, 1994; Brunner et al., 1994; Sawamoto et al., 1994; reviewed by Okano, 1995). *argos* is also required for projection of photoreceptor axons during optic lobe development (Brunner et al., 1994; Sawamoto et al., 1995). Our previous study suggested that *argos* plays an opposite function in the common pathway with *rho* (Sawamoto et al., 1994) and *S* (Sawamoto et al., 1995). Recently, it has been suggested that *argos* inhibits activation of the EGF receptor by spitz, a *Drosophila* TGF-α homologue (Schweitzer et al., 1995). In this work, I have analyzed genetic interactions of *argos* with components of the signal transduction cascade in detail. We also describe the dominant phenotype of $Dsor1^{Su1}$ in the eye and wing vein development. The present results indicates that *argos* functions as a diffusible antagonist in the MAPK pathway to regulate the signal transduction required for cellular differentiation.

4-2. Materials and Methods

Fly stocks

Canton-Special was used as the wild-type strain. *argos*^{95}, *argos*^{152}, *argos*^{162} and *argos*^{257} were generated by imprecise excision of the P[lac-W] element of the enhancer trap line, *argos*^{sty2}. *hs-argos* (Sawamoto et al., 1994) and *Dsor1*^{Su1} (Tsuda et al., 1993) were previously described. *S*^{X155} (Heberlein et al., 1993) was obtained from G.M. Rubin. *S*^{218} was from Yasushi Hiromi. *rl*^{Su14} and *rl*^{Su23} are the gain-of-function alleles generated by Lim, Y.-M. et al. (manuscript in preparation). Molecular analysis of the genomic DNA from the mutant flies have revealed that *rl*^{Su23} is the same mutation as *rl*^{SEM} (Brunner et al., 1994).

Genetics

Fly culture and crosses were performed according to standard procedures. For heat-shock experiment, second instar larva were repeatedly heat-shocked at 36°C for 1 hour with an interval of 25°C for 5 hour using a temperature-programmable incubator.

Immunohistochemistry

anti-Elav antibody was obtained from Developmental Studies Hybridoma Bank. Cy3-conjugated anti mouse IgG antibody was purchased from Chemicon. Eye imaginal discs were fixed in 4% paraformaldehyde in PBS for 30 min. After rinsing in PBNT (10% normal goat serum, 0.3% TritonX-100 in PBS), discs were incubated in anti-Elav antibody (1:100 dilution in PBNT) at 4°C overnight. After rinsing in PBNT, discs were incubated in Cy3-conjugated anti mouse IgG (1:500 dilution in PBNT) for 1 hr at room temperature. After washing in PBS, discs were cleared in 80 % glycerol in PBS and analyzed with a Zeiss Axio-Scope microscope.

Scaning electron microscopy

Adult flies were dehydrated in a grated acetone series and dried at 60°C for 1 hr. Mounted flies were sputter coated with platinum and observed with a Hitachi S-100 scanning electron microscope.

Wing preparation

Adult wings were dissected out in 1-butanol. The wings were cleared in Xylene and mounted with Permount (Fisher). Photographs were taken with a Zeiss Axio-Scope microscope.

Plastic sections of adult heads

Adult heads were fixed in 2% glutaraldehyde/2% paraformaldehyde in 0.1M phosphate buffer (pH 7.2) at 4°C overnight. After washing in 0.1M phosphate buffer (pH 7.2), heads were postfixed in 1% OsO_4 in the buffer for 2 hr at 4°C and then dehydrated in a graded ethanol series. After clearing in propylene oxide, heads were embedded in PolyBed 218 sectioned with an ultramicrotome. One micrometer sections were stained with Toluisine Blue.

Cuticle preparation

Preparation and analysis of embryonic cuticle were performed as described previously (Tsuda et al., 1993).

Acridine orange staining

Staining eye discs with acridine orange was performed as described (Spreij, 1971). Briefly, eye discs from third instar larva were dissected out in $1.6X10^{-6}$M acridine orange (Sigma) in Ringer's and examined immediately using fluorescein.

4-3. Results

argos* interacts with *Star

In order to identify modifiers of *argos* phenotypes, various mutants showing eye or wing phenotype were examined whether they show genetic interaction between loss-of-function or gain-of-function of *argos*. For example, there are no obvious interactions between *argos* and mutants of the genes involved in the Notch pathway such as Notch, Delta and Serrate (data not shown).

The *hs-argos* transgenic flies have a severe rough eye phenotype (Sawamoto et al., 1994; Fig. 1B) contrasting with the regular array of ommatidia in the wild-type eye (Fig. 1A) caused by decrease of the photoreceptor cells (Fig. 1A). This gain-of-function phenotype of *argos* was enhanced by *S* mutations: weakly by S^{X155} (a weak allele, Heberlein et al., 1993), and more strongly by S^{218} (a null allele, Kolodkin et al., 1994). The S^{218} ; *hs-argos* flies had rough and narrower eyes (Fig. 1C) compared to the *hs-argos* (Fig.1B). Examing tangential sections of the S^{218} ; *hs-argos* eyes showed that photoreceptor cells were decreased in number in most of the ommatidia. To analyze this severe phenotype more in detail, I stained eye imaginal discs from S^{218}/+; *argos*^{257}/*argos*^{257} with anti Elav antibody (staining neuronal nuclei) and acrydine orange (staining nuclei of the apoptotic cells). The Elav positive neuronal nuclei were decreased in number in the S^{218}/+; *argos*^{257}/*argos*^{257} discs (Fig. 1L), indicating that photoreceptor cells could not differentiate normally. The level of cell death did not appear to be accelerated in the S^{218}/+; *argos*^{257}/*argos*^{257} eye imaginal discs at the wandering larval stage as estimated by acridine orange staining (data not shown). In addition, the effect of ectopic overexpression of *argos* was suppressed by one copy of sE-hs-S transgene (data not shown).

Flies homozygous for the *argos*^{257} mutation (a null-type allele) had severely roughened eyes. Fusion of the lenses were often observed at the posterior region of the compound eyes (Fig. 1D). Examing tangential sections showed that photoreceptor cells increased in number and spacing pattern among the ommatidia were remarkably disorganized in *argos*^{257} eyes (Fig. 1I). Eyes of the flies heterozygous for the S^{X155} mutation (a weak loss-of-function allele) show almost normal external morphology and internal structure (data not shown). In the S^{X155}/+; *argos*^{257}/*argos*^{257} flies, the rough eye phenotype of *argos* was restored (Fig. 1E). Number and organization of photoreceptor cells in the ommatidia also appeared normal in the S^{X155}/+; *argos*^{257}/*argos*^{257} retina (Fig. 1J).

Similar interactions between *argos* and S as in the eye were observed in the wing development (Fig. 1M-O). Adult flies heterozygous for S^{X155} and S^{1}have normal wings. Heat-shocked *hs-argos* adults have wings where wing veins are partially lost (Sawamoto et al., 1994; Fig. 1N). This phenotype was enhanced by S^{X155} (data not shown) and S^{218} (Fig. 1O). In addition, the effect of ectopic overexpression of *argos* was suppressed by one copy of *sE-hs-S* transgene (data not shown). Thus, *S* interacts with not only the loss-of-function allele of *argos* but also its gain-of-function allele. These results indicate that *argos* functions in the common pathway with *S* in an antagonistic fashion. The interaction of *argos* with the *spitz* group genes such as *rho* (Sawamoto et al., 1994) and *S* (Sawamoto et al., 1995; this work) suggests that *argos* functions on the Ras/MAPK cascade as the *spitz* group genes do. Therefore, I have analyzed the interaction among *argos* and the components in the cascade including *Sos, Ras1, D-raf, Dsor1* and *rl* (see blow).

Gain-of-function mutation in *Dsor1* causes formation of multiple R7 cells and extra wing veins

The previous work by Tsuda et al. (1993) showed that *Dsor1*, also known as *D-mek* (Hsu and Perrimon, 1994), is required for development of terminal structure in the embryonic development and acts downstream of *D-raf* in the *torso* pathway. A temperature sensitive mutation, *D-mek*^{ts}, causes phenotypes similar to those of loss-of-function mutations in *sev* and *DER* (Hsu and Perrimon, 1994), suggesting that *Dsor1/MEK* functions downstream of *sev* and *DER* as well as *Torso*. To analyze the effect of hyperactivation of MAPKK on the other developmental processes, the eyes and wings of *Dsor1*^{Su1} mutants were examined. The external morphology of the *Dsor1*^{Su1} eye is indistinguishable from the wild-type (data not shown). Analyses of sections through the compound eye of *Dsor1*^{Su1} adults revealed that supernumerary R7 cells were developed in about 2% (N=566) ommatidia (Fig. 2A), while other cell types were not affected. This indicates that hyperactivation of MAPKK causes an over-induction of R7 cell fate. Furthermore, the *Dsor1*^{Su1} mutation caused R7 induction in the *sev*^{E4} mutatnt eyes (Fig. 2B), suggesting that activation of MAPKK can compensate for a partial loss of sev function. Moreover, a gain-of-function mutation of *Sos*, *Sos*^{JC2}, remarkably enhanced the R7 formation in the sevE4 *Dsor1*^{Su1} genetic background (Fig. 2D). These results indicates that *Dsor1* acts for determination of the R7 cell fate in the sev cascade.

Dsor1^{Su1} also affected wing vein development. Extra veins were observed in the 5% (N=106) of *Dsor1*^{Su1} wings (Fig. 2E), indicating the requirement of MAPKK in wing vein formation. This phenotype was similar to those of mutants in which the DER signaling was hyperactivated, e.g., *Ellipse*, the gain-of-function *DER* mutation (Baker and Rubin, 1989), loss-of-function *Gap1* mutations (Gaul et al., 1992) and gain-of-function mutations of *rl* (Brunner et al., 1994; Lim, Y.-M. et al., paper in preparation). The similarity of the phenotypes imply *Dsor1* functions downstream of DER as demonstrated by Hsu and Perrimon (1994).

argos enhances the R7 formation in _Dsor1_^{Su1}and _Sos_^{Jc2} mutants

To examine the effect of *argos* on the *Dsor1*^{Su1} eye phenotype, a weak *argos* allele was crossed to the *Dsor1*^{Su1} mutant. If *argos* acts as negative regulator in the common cascade, *argos* is then expected to enhance the phenotype caused by *Dsor1*^{Su1}. Compound eyes of *argos*^{152} homozygotes showed slightly rough morphology (data not shown). Analyses of section through the *argos*^{152} eyes revealed that about 15% (N=476) of ommatidia contain extra outer (R1-6) photoreceptor cells (marked with arrows), while R7 was not affected (Fig. 3A). *Dsor1*^{Su1}; *argos*^{152} flies have eyes with a little more severe roughness than that of either *Dsor1*^{Su1} or *argos*^{152} (data not shown). Sections of the eyes showed 25% (N=286) of ommatidia contained extra R7 like cells (arrow heads) in the *Dsor1*^{Su1}; *argos*^{152} (Fig. 3B). In addition, *argos*^{152} had the enhancing effect on the eye phenotype of *Sos*^{JC2} similar to on *Dsor1*^{Su1}. *Sos*^{Jc2} does not cause any visible abnormality on the eye development (Rogge et al., 1991). However, some of ommatidia contain extra R7 like cells (arrows) in the *Sos*^{JC2} ; *argos*^{152} flies (Fig. 3C). These results suggest *argos* acts as negative regulator for R7 formation in the common cascade with *Sos* and *Dsor1*.

Gain-of-function mutations of _Dsor1_ and _rolled_ suppress _hs-argos_ phenotype

To determine if *argos* functions through the MAPK cascade, the *hs-argos* transgenic flies were crossed to gain-of-function alleles of *Dsor1* and *rolled*. *Dsor1*^{Su1} is known to suppress the phenotypes of the mutants of several genes acting upstream of *D-raf*. The *hs-argos* phenotype in eye and wing were suppressed by *Dsor1*^{Su1}. Overexpression of *argos* from the *hs-argos* transgene (Sawamoto et al., 1994) causes a severe rough eye phenotype (Fig. 4A) due to the reduction of retinular cells (Fig. 4E, marked with arrow heads) and a partial loss of wing veins (Fig. 4I). The *hs-argos* phenotype was remarkably suppressed by *Dsor1*^{Su1}in a dosage dependent manner. The rough eye phenotype of *hs-argos* was almost completely suppressed in the males carrying the *Dsor1*^{Su1} X chromosome (Fig. 4C), whereas the females carrying one copy of the *Dsor1*^{Su1} mutations showed a weak rough eye phenotype (Fig. 4B). Number and organization of the photoreceptor cells in the *Dsor1*^{Su1}/Y ; *hs-argos* was also indistinguishable form the wild-type (Fig. 4F). The wing phenotype of *hs-argos* was completely suppressed by one copy of the $Dsor1^{Su1}$ mutations (Fig. 4J).

The phenotype caused by overexpression of *argos* was also suppressed by hyperactive MAPK activity. rl^{Su14} and rl^{Su23} are novel gain-of-function mutations in the *Drosophila* MAPK gene, *rl* (Lim, Y.-M. et al., paper in preparation). These mutants show similar phenotypes on eye and wing development. Supernumerary R7 cells and extra wing veins are observed in rl^{Su14} and rl^{Su23} flies, although the phenotype of rl^{Su23} is more severe than that of rl^{Su14} (Lim, Y.-M. et al., paper in preparation). Molecular analysis of the genomic DNA revealed that rl^{SEM} (Brunner et al., 1994) is the same mutation as rl^{Su23} (Lim, Y.-M. et al., paper in preparation). The *hs-argos* phenotype was suppressed by these gain-of-function mutations of *rl*. The rl^{Su23} ; *hs-argos* flies had eyes with a less severe roughness than those of *hs-argos* or rl^{Su23}(Fig. 4D). Formation of the extra R7 cells generated by rl^{Su23} (Fig. 4G) was suppressed by *hs-argos* (Fig. 4H), suggesting that overexpressed *argos* could inhibit the MAPK hyperactivation by rl^{Su23}. The wing phenotype of *hs-argos* was also suppressed by rl^{Su23} (Fig. 4K). rl^{Su14} had suppressed the *hs-argos* phenotype in a similar as to rl^{Su23} (data not shown).

Interaction between $Dsor1^{Su1}$ and *argos* mutants on the embryonic phenotype

Strong *argos* alleles exhibit severely reduced viability. The lethality is likely to be due to the defective head involution during embryogenesis (Freeman et al., 1992; Okano et al., 1992). On the other hand, the weaker alleles such as $argos^{162}$ and $argos^{95}$ did not affect the viability of larva (Table 1). To examine the effect of $Dsor1^{Su1}$ on the embryonic phenotype of *argos*, a reciprocal crossing between $Dsor1^{Su1}$ and weak *argos* mutants ($argos^{162}$ or $argos^{95}$) was performed (Table 1). $Dsor1^{Su1}$ did not affect the embryonic development (data not shown). When $Dsor1^{Su1}$; *argos* females were crossed to $Dsor1^{+}$; *argos* males, the ratio of embryos hatched was dramatically decreased. To investigate the embryonic phenotype enhanced by $Dsor1^{Su1}$, cuticle preparation of the embryos was examined. The dead embryos from $Dsor1^{Su1}$; *argos* females showed abnormal head involution (data not shown). This is a similar phenotype to those of more severe alleles of *argos* (Freeman et al., 1992; Okano et al., 1992). Embryos homozygous for *argos* from crossing between *Dsor1*+ ; *argos* females and *Dsor1*^{Su1} ; *argos* males showed normal development.

The lethality of the *argos*^{257} mutant flies was also rescued by decreasing the doses of Star and Ras1. *argos*^{257} is a null type allele showing severely reduced viability. On the other hand, *S*^{X155}/CyO ; *argos*^{257}/*argos*^{257} and *Ras1*^{e2F} ;*argos*^{257}/*argos*^{257} flies showed viability similar to the *argos*^{257} heterozygotes (data not shown).

Decreases in *Ras1*, *D-raf* and *Dsor1* activities suppress the *argos* eye phenotype

To determine the epistasis between *argos* and components in the MAPK cascade, I crossed null type alleles of *Ras1, D-raf* and *Dsor1* to *argos*. If *argos* functions upstream of *Ras1, D-raf* and *Dsor1*, halving the dose of these genes is expected to suppress the *argos* phenotype. The eyes of the flies heterozygous for *Ras1*^{e2F}, *D-raf*^{1} and *Dsor1*^{GAP158} were indistinguishable from the wild-type eye (data not shown). In the *argos*^{257} mutant eye, the regular array of ommatidia is disrupted and the posterior region shows characteristic blistering (Fig. 6A). However, halving the dose of *Ras1*^{e2F}, *D-raf*^{1} and *Dsor1*^{GAP158} resulted in the considerable recover of this phenotype. That is, the fusion of lenses were seldom observed on the eyes of *Ras1*^{e2F} *argos*^{257}/*argos*^{257} (Fig. 6B), D-*raf*^{1}/FM7 ; *argos*^{257}/*argos*^{257} (Fig. 6C) and *Dsor1*^{GAP158}/FM7 ; *argos*^{257}/*argos*^{257} (Fig. 6D). To analyze the interaction between *argos* and *Ras1, D-raf* or *Dsor1* more in detail, tangential sections of the compound eyes were examined. Formation of the extra outer photoreceptor-cells by the *argos*^{257} mutation (Fig. 6E) was considerably suppressed by halving the dose of *Ras1*^{e2F} (Fig. 6F), *D-raf*^{1} (Fig. 6G) and *Dsor1*^{GAP158} (Fig. 6H). In the *argos*^{257} mutant ommatidia, the mean number of the extra outer photoreceptor-cells is 1.3 (SD=0.9, N=403) (Fig. 7). On the other hand, the mean number of the extra photoreceptor cells decreased to 0.3 in *Ras1*^{e2F} *argos*^{257}/*argos*^{257} (SD=0.5, N=698), 0.3 in *D-raf*^{1}/FM7 ; *argos*^{257}/*argos*^{257} (SD=0.5, N=690) and *Dsor1*^{GAP158}/FM7 ; *argos*^{257}/*argos*^{257} (SD=0.6, N=965) (Fig. 7). The differences in the mean number of the extra outer photoreceptor-cells are statistically significant between control and each of others in Fig. 7 (t-test, $P<0.001$). These results mean that *argos* acts as negative regulator for signal transduction upstream of *Ras1*.

4-4. Discussion

Loss-of-function mutations in the *argos* gene cause an excessed cellular recruitment (Freeman et al., 1992; Kretzschmar et al., 1992; Okano et al., 1992), whereas ectopic overexpression of *argos* inhibits differentiation (Freeman, 1994; Brunner et al., 1994; Sawamoto et al., 1994). These observations had suggested that *argos* regulates signal transduction for cellular differentiation as an antagonist. As *argos* is a secreted protein (Freeman, 1994) and its function is non-cell autonomous (Freeman et al., 1992; Kretzschmar et al., 1992), *argos* can be referred as a lateral inhibitor. In order to elucidate the signal cascade of *argos*, genetic interaction between *argos* and mutants affecting eye and wing vein development were examined. As *argos* is a lateral inhibitor with an EGF motif, I have analyzed genetic interactions between *argos* and components involved in the Notch signaling pathway, e.g., *Notch* and *Delta*, which are also involved in lateral inhibition and contain EGF like repeats (Fehon et al., 1990; Heitzler and Simpson, 1991; Rebay et al., 1991). However, I have not detected any significant interactions between them. Another candidate for the cascade in which *argos* functions is the MAPK cascade. It is known that determination of the photoreceptor cell fates and wing vein formation are induced by the signal transductions through the MAPK cascade. In this work, I analyzed genetic interactions of *argos* with components of the MAPK cascade and obtained results confirming this idea. Therefore, *argos* is a lateral inhibitor which acts on the MAPK cascade rather than the Notch signaling pathway.

We have described previously that *argos* interact with *rho* (Sawamoto et al., 1994) and *S* (Sawamoto et al., 1995). *rho* and *S* are members of the *spitz* group and interact with components of the EGF receptor signaling pathway (Sturtevant et al., 1993; Kolodkin et al., 1994). The present study showed that S suppressed the *argos* null-type mutation and enhanced the phenotype caused by ectopic overexpression of *argos*. Such strong interactions mean that *argos* and *S* have opposing functions in a common pathway. It is known that *rho* and *S* participate in both the sevenless and DER pathways (Sturtevant et al., 1993; Kolodkin et al., 1994). Schweitzer et al. (1995a) demonstrated that *rho* and *S* may facilitate processing of spitz, which is the TGF-a like ligand for DER. Since *argos* interacts with both rho (Sawamoto et al., 1994) and *S* (Sawamoto et al., 1995; this work), *argos* is likely to act on the DER pathway.

In this work, *argos* was clearly shown to interact with major components of the signal pathway acting downstream of the receptor tyrosine kinases such as sev, DER and torso. The *argos* overexpression phenotype was suppressed by increased MAPKK (*Dsor1*) and MAPK (*rl*) function (Fig. 4). On the other hand, the phenotype by gain-of-function of Sos and *Dsor1* was enhanced by the loss-of-function of *argos* (Fig. 3). Furthermore, the phenotype caused by loss of *argos* function was suppressed by decreased function of *Ras1*, *D-raf* and *Dsor1* (Fig. 6,7). These results strongly support the idea that *argos* is a negative regulator for signal transduction in the MAPK cascade.

I showed that *argos* enhanced the extra R7 formation by $Dsor1^{Su1}$ and Sos^{Jc2}. In addition, the overexpressed *argos* suppressed the extra R7 formation by hyperactivated MAPK. These results suggest *argos* also functions as a negative factor for the R7 differentiation. However, it is still unclear whether *argos* functions in the Sev cascade, because R7 cells normally differentiate in the *argos* null mutant eyes.

Schweitzer et al. (1995b) have clearly revealed that *argos* inhibits activation of the EGF receptor by spi by using a cell culture system. They also presented the genetic interaction between *argos* and *DER*. The results indicate *argos* inhibits EGF receptor signaling in vivo. We have also analyzed genetic interaction between *argos* and *spi* or *DER*, but failed to obtain any clear results showing significant interactions (data not shown). That may be due to the difference in the temperature used for the heat-shock experiment and/or the mutant alleles tested. However, *argos* is likely to be a diffusible antagonist for the DER cascade judging from results from biochemistry (Schweitzer et al., 1995b) and genetics (Schweitzer et al., 1995b; this work). There can be two distinct mechanisms for the *argos* function in the inhibition of the signal transduction (Fig. 8). Since *argos* encodes an EGF-like ligand, it is possible that *argos* directly binds to the EGF receptor competing with spi and inhibits the activation of the receptor. Alternatively, *argos* can bind to another unknown receptor which blocks signal transduction in the MAPK cascade. In the latter case, the unknown receptor may activate factors negatively regulating the signal transduction such as protein phosphatases or GTPase activating proteins (GAPs). It is possible that *argos* activates protein kinase C, as PKC is known to block the signal transduction by the EGF receptor in mammals. Recent study by Cullen et al. (1995) revealed that an Ins(1,2,4,5)P4-binding protein has Ras GAP activity and its activity is specifically stimulated by Ins(1,2,4,5)P4.

Consequently, *argos* may activate the inositol phosphate synthesis and then activated the Gap1, which blocks the Ras signaling. Genetic screening for modifiers of *argos* phenotype should identify unknown genes involved in the cascade required for the negative regulation of the inductive signals. *balge* and *soba* have been recently isolated as candidates for mutations of genes encoding the molecules involved in the signaling cascade for *argos* in a screening for modifiers of *argos* (Wemmer and Klämbt, 1995).

argos is the first example of the extracellular protein which inhibits signal transduction in the MAPK cascade. For the proper regulation of cellular differentiation, extracellular inhibitor proteins such as *argos* may be required for keeping the inductive signals from receptor tyrosine kinases in a proper level. Components of the EGF receptor signaling cascades are highly conserved evolutionally (Dickson and Hafen, 1994). Therefore, it is possible that there are mammalian homologues of *argos*. Potential *argos* homologues may play key roles in regulation of cellular differentiation and proliferation during mammalian development. Furthermore, if human homologue of *argos* exists, the inhibitory effect of *argos* on the Ras/MAPK cascade can be applied for the gene therapy of cancer.

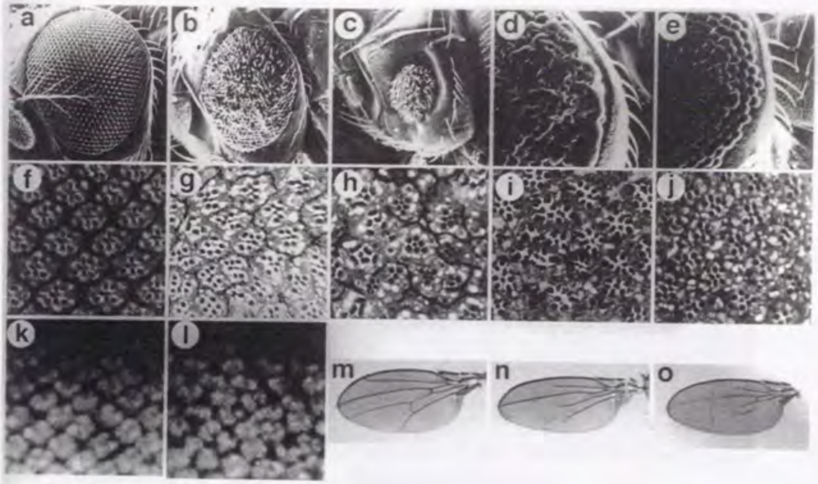

Fig. 1 Genetic interaction between *argos* and Star. (A-E) Scanning electron micrographs of adult compound eyes. (A) wild-type. The facets are in a uniform hexagonal array. (B) *hs-argos*. overexpression of *argos* causes a rough eye phenotype. (C) *hs-argos* ; S^{218}. Removal of one copy of the S gene remarkably enhances the *hs-argos* phenotype. Overproduction of bristles are observed at the surface of the compound eye. (D) $argos^{257}$. The regular hexagonal array of facets are disrupted. Occasionally, fusion of lenses are observed at the posterior region of the eye. (E) S^{218} ;$argos^{257}$.The fusion of lenses is not observed. (F-J) Sections of adult eyes. (F) In the wild-type, each ommatidium has eight photoreceptor cells, seven of which can be observed in one tangential section. (G) *hs-argos*. There are many ommatidia with decreased number of photoreceptor cells (arrows). (H) *hs-argos* ; S^{218}. The *hs-argos* phenotype is enhanced by halving the dose of the *S* gene. (I) In the $argos^{257}$ /$argos^{257}$ eye, almost all the ommatidia contain extra outer photoreceptor cells. (J) Removal of one copy of the *S* gene suppresses the *argos* phenotype. (K,L) Anti Elav immuno-staining of eye imaginal discs from third instar larva. (K) In the *hs-argos*, neuronal differentiation and ommatidial assembly appears normal. (L) *hs-argos* ; S^{218}. Many ommatidia lack one or more photoreceeptor cells. (M-O) adult wings. (M) wild-type. (N) *hs-argos*. Overexpression of *argos* causes a partial loss of the longitudinal wing veins. (O) *hs-argos* ; S^{218}. Decrease in the dose of the *S* gene enhances the wing phenotype of *hs-argos*.

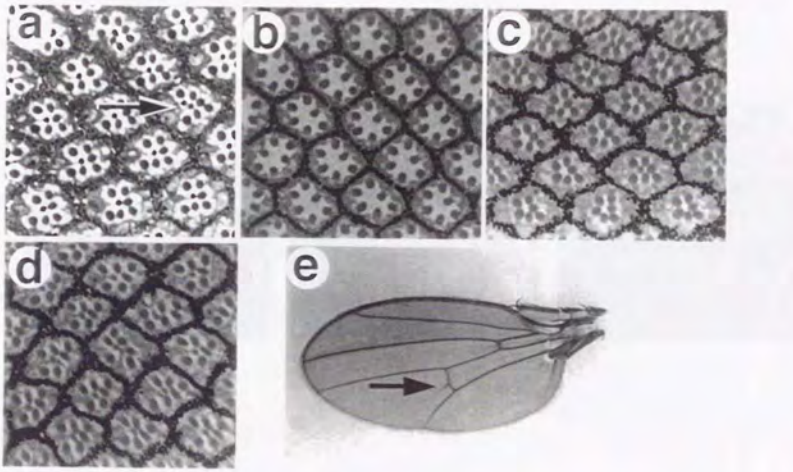

Fig. 2

Gain-of-function phenotype of *Dsor1*^{Su1} in the eye and wing. (A-D) Sections of adult eyes. (A) *Dsor1*^{Su1}. An ommatidium with two R7 cells are marked with an arrow. (B) In the *sev*^{E4} eye, all the ommatidia lack the R7 photoreceptor. (C) In the *sev*^{E4} *Dsor1*^{Su1}, there are some ommatidia with R7. (D) In the *sev*^{E4} *Dsor1*^{Su1}; *Sos*^{JC2}, increased number of omatidia contain R7. (E) An adult wing of *Dsor1*^{Su1}. Note the extra vein material between L4 and L5 crossing the posterior cross vein.

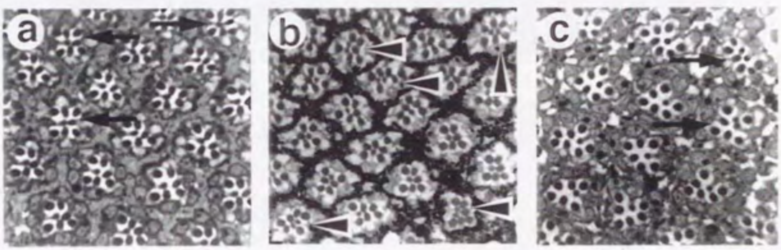

Fig. 3

argos enhances the R7 formation in *Dsor1*$^{\text{Su1}}$and *Sos*$^{\text{Jc2}}$ mutants. (A-C) Sections of adult eyes. (A) *argos*^{152}/*argos*^{152}. The ommatidia with supernumerary outer photoreceptors are marked with arrows. R7 is not affected in this mutant. (B) *Dsor1*$^{\text{Su1}}$; *argos*^{152}/*argos*^{152}. About 25% of the ommatidia contain more than two R7 (arrows). (C) *Sos*$^{\text{JC2}}$; *argos*^{152}/*argos*^{152}. The ommatidia with extra R7 are marked with arrows. The R7 formation is never affected by the *Sos*$^{\text{JC2}}$ mutaion alone.

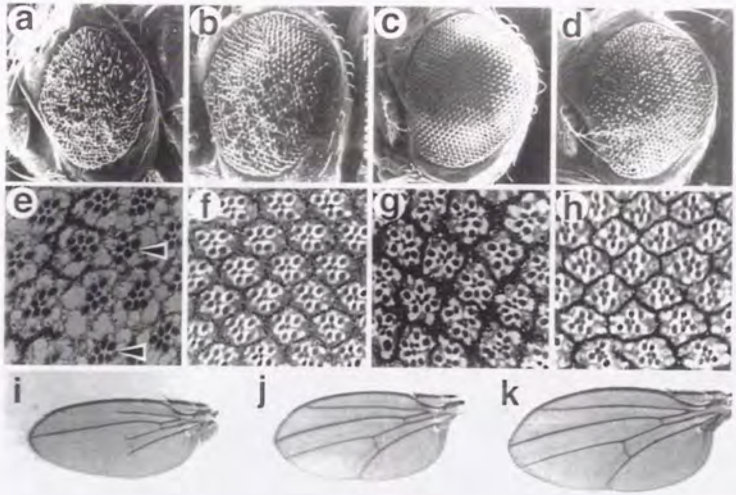

Fig. 4 The *hs-argos* phenotype is suppressed by gain-of-function mutations of *Dsor1* and *rl*. (A-D) SEMs of adult eyes. (A) *hs-argos*. Ovrexpression of *argos* causes a severe rough eye phenotype. (B) $Dsor1^{Su1}$/X ; *hs-argos*. One copy of the gain-of-function *Dsor1* mutation considerably rescues the rough eye phenotype by *hs-argos*. (C) $Dsor1^{Su1}$/Y ; *hs-argos*. The external morphology of the eye is indistinguishable form the wild-type. (D) rl^{Su23}/*hs-argos*. One copy of the gain-of-function *rl* mutation also rescues the rough eye phenotype by *hs-argos*. (E-H) Sections of adult eyes. (E) *hs-argos*. The ommatidia lacking photoreceptor cells are marked with arrows. (F) In the $Dsor1^{Su1}$/Y ;*hs-argos*, cellular organization in ommatidia appears normal. I observed lack of outer photoreceptors in $Dsor1^{Su1}$/+ ;*hs-argos*, although the phenotype was less severe than the *hs-argos* alone (data not shown). (G) rl^{Su23}. Almost all the ommatidia contain extra R7 cells. (H) Over expression of *argos* from the *hs-argos* transgene eliminates most of the extra R7 cells formed by the rl^{Su23} mutation. (I-K) Adult wings. (I) *hs-argos*. (J) $Dsor1^{Su1}$;*hs-argos*. (K) rl^{Su23}/*hs-argos*. Longitudinal wing veins are shortened by *argos* overexpression (I). This phenotype is completely suppressed by the gain-of-function mutations of *Dsor1* (J) and *rl* (K).

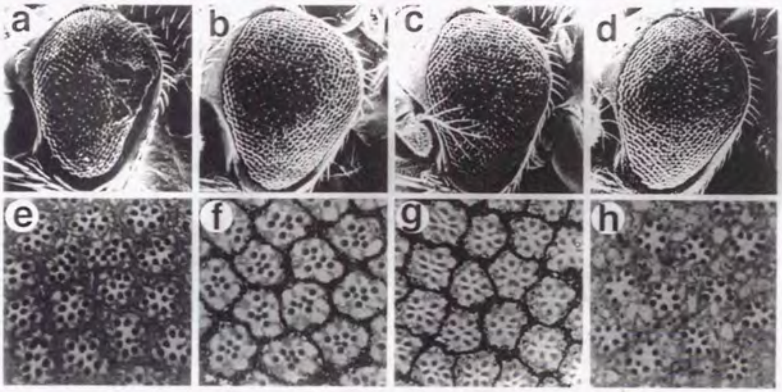

Fig. 5

Ras1, *D-raf* and *Dsor1* act as dominat suppressors of the *argos* loss-of-funciton phenotype. (A-D) SEMs of adult eyes. (E-H) Sections of adult eyes. (A,E) $argos^{257}/argos^{257}$. (B,F) $Ras1^{e2F}argos^{257}/argos^{257}$. (C,G) $D\text{-}raf^{1}$/FM7 ;$argos^{257}/argos^{257}$. (D,H) $Dsor1^{GAP158}$/FM7 ;$argos^{257}/argos^{257}$. In the *argos* mutant eye, regular array of facets are disrupted and characteristic blistering are observed at the posterior region (A). Most of the ommatidia contain extra outer photoreceptor cells in the $argos^{257}/argos^{257}$ eye (E). These defects are considerably suppressed by removal of one copy of *Ras1* (B,F), *Dsor1* (C,G) and *D-raf* (D,H). $Ras1^{e2F}$ (Simon et al., 1991), $D\text{-}raf^{1}$ (Nishida et al., 1988) and $Dsor1^{GAP158}$ (Tsuda et al., 1993) were used as null type alleles.

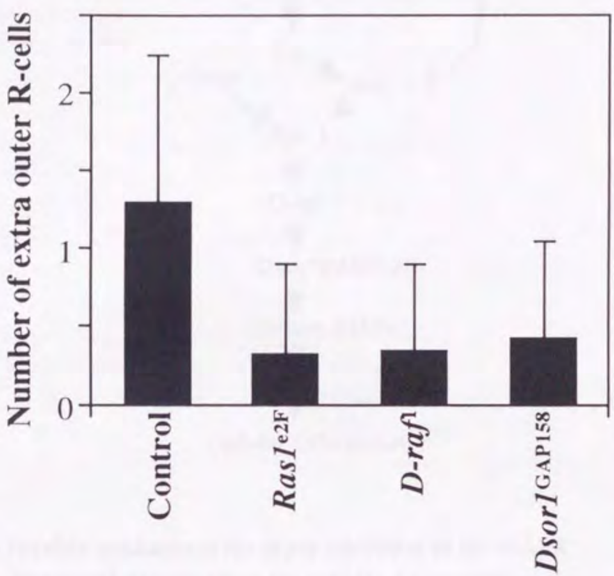

Fig. 6

Effects of loss-of-function mutations of *Ras1*, *D-raf*, and *Dsor1* on the number of extra outer photoreceptor cells in the $argos^{257}$ eyes. The average number of extra outer photoreceptor-cells (R-cells) per ommatidium and the standard deviation were determined in tangential plastic sections of eyes of $argos^{257}/argos^{257}$ (control) animals or $argos^{257}/argos^{257}$ animals that are heterozygous the indicated mutations. The mean number of extra outer photoreceptor cells in the control is distinct from those in *Ras1*, *D-raf*, and *Dsor1* with $P<0.001$ as determined from a t-test. $Ras1^{e2F}$ (Simon et al., 1991), $D\text{-}raf^{1}$ (Nishida et al., 1988) and $Dsor1^{GAP158}$ (Tsuda et al., 1993) were used as null type alleles.

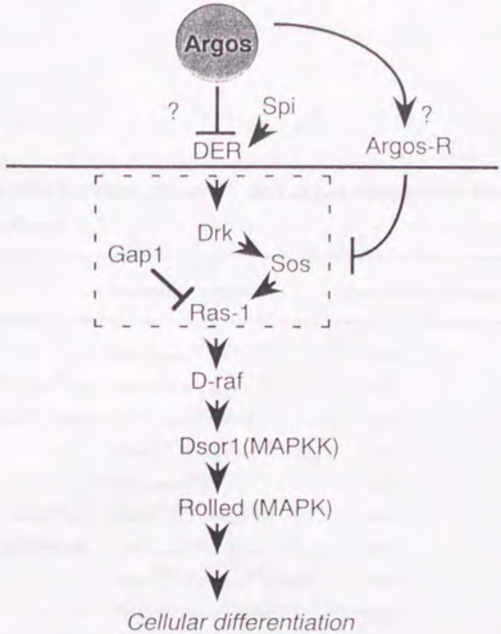

Fig. 7 Possible mechanisms for *argos* inhibition of the MAPK signaling. The signal transducntion for cellular differentiation is triggered by intertaction between the ligands (boss or spi) and the receptors (sev or DER). There are several genetic evidences for involvement of other intracellular components (Ras1, D-raf, Dsor1 and rolled), which act downstream of the receptors in a liner manner (reviewed by Dickson and Hafen, 1993). As argos is secreted protein (Freeman, 1994) and functions non cell-autonomously (Freeman et al., 1992; Ktetzchmar et al., 1992), argos is likely to function as a diffusible ligand. The results presented in this paper suggest argos inhibits the signal transduction of the MAPK cascade. The two major models for argos inhibition of the MAPK signaling cascade are as follows. (1) argos binds to DER and/or sev and inhibits the activation of the receptors by competing with their ligands, spi and/or boss, respectively. (2) argos can bind to another unknown receptor which blocks signal transduction in the MAPK cascade. In this case, the unknown receptor may activate factors negatively regulating the signal transduction such as protein phosphatases or GTPase activating proteins (GAPs).

Table 1.

Genetic interaction between *Dsor1*^{Su1} and *argos* mutants on the embryonic development

Maternal Genotype	Paternal Genotype	% of embryo hatched	N
+/+ ; *argos*^{162}/+	+/Y ; *argos*^{162}/+	97.0	541
Dsor1^{Su1}/Dsor1^{Su1} ; *argos*^{162}/+	*Dsor1*^{Su1}/Y ; *argos*^{162}/+	72.2	338
Dsor1^{Su1}/FM7a ; *argos*^{162}/TM6B	+/Y ; *argos*^{162}/TM3	43.8	715
+/+ ; *argos*^{162}/TM3	*Dsor1*^{Su1}/Y ; *argos*^{162}/TM6B	92.4	171
+/+ ; *argos*^{95}/+	+/Y ; *argos*^{95}/+	99.6	269
Dsor1^{Su1}/Dsor1^{Su1} ; *argos*^{95}/+	*Dsor1*^{Su1}/Y ; *argos*^{95}/+	40.8	120
Dsor1^{Su1}/FM7a ; *argos*^{95}/TM6B	+/Y ; *argos*^{95}/TM3	48.5	355
+/+ ; *argos*^{95}/TM3	*Dsor1*^{Su1}/Y ; *argos*^{95}/TM6B	97.1	344
+/+ ; *argos*^{95}/TM3	FM7a/Y ; *argos*^{95}/TM6B	95.8	552

References

Ambrosio, L., Mahowald, A. P. and Perrimon, N. (1989). Requirement of the *Drosophila raf* homologue for *torso* function. Nature 342, 288-291.

Baker, N. E. and Rubin, G. M. (1989). Effect on eye development of dominant mutations in *Drosophila* homologue of the EGF receptor. Nature 340, 150-153.

Baker, N.E., Mlodzik, M. and Rubin, G.M. (1990). Spacing differentiation in the developing *Drosophila* eye: A fibrinogen-related lateral inhibitor encoded by *scabrous*. Science 250, 1370-1376.

Baker, N. E. and Rubin, G. M. (1992). Ellipse mutations in the *Drosophila* homologue of the EGF receptor affect pattern formation, cell division, and cell death in eye imaginal discs. Dev. Biol. 150, 381-396.

Basler, K., and Hafen, E. (1988). Control of photoreceptor cell fate by the sevenless protein requires a functional tyrosine kinase domain. Cell 54, 299-311.

Bellen, H., O'Kane, C.J., Wilson, C., Grossniklaus, U., Kurth-Pearson, R. and Gehring, W.J. (1989). P-element mediated enhancer detection: a versatile method to study development in *Drosophila*. Genes Dev. 3, 1288-1300.

Belote, J.M., Hoffmann, F.M., McKeown, M., Chorsky, R.L. and Baker, B.S. (1990). Cytogenetic analysis of chromosome region 73AD of *Drosophila melanogaster*. Genetics 125, 783-793.

Bier, E., Ackerman, L., Barbel, S., Jan, L.Y. and Jan, Y.N. (1988). Identification and characterization of a neuron-specific nuclear antigen in *Drosophila*. Science 240, 913-916.

Bier, E., Vaessin, H., Shephererd, S., Lee, K., McCall, K., Barbell, S., Ackerman, L., Carretto, R., Uemura, T., Grell, E.H., Jan, L.Y. and Jan, Y.N. 1989). Searching for pattern and mutations in the *Drosophila* genome with a P-Lac Z vector. Genes Dev. 3, 1273-1287.

Biggs, W.H., Zavitz, K.H., Dickson, B., Straten, A., Brunner, D., Hafen, E. and Zipursky, S.L. (1994) The *Drosophila rolled* locus encodes a MAP kinase required in the sevenless signal transduction pathway. EMBO J. 3, 1628-1635.

Bolwig, N. (1946). Senses and sense organs of the anterior end of the house fly larvae. Vidensk fra Medd Dansk Naturb Foren 109, 81-217.

Boulianne, G.L., de la Concha, A., Campos-Ortega, J.A., Jan, L.Y. and Jan, Y.N. (1991). The *Drosophila* neurogenic gene *neuralized* encodes a novel protein and is expressed in precursors of larval and adult neurons. EMBO J. 10, 2975-2983.

Bowtell, D. D. L., Simon, M. A., and Rubin, G. M. (1988). Nucleotide sequence and structure of the sevenless gene of *Drosophila melanogaster*. Genes Dev. 2, 620-634.

Brunner, A., Twardzik, T. and Schneuwly, S. (1994). The *Drosophila giant lens* gene plays a dual role in eye and optic lobe development: Inhibition of differentiation of ommatidial cells and interference in photoreceptor axon guidance. Mech. Dev. 48, 175-185.

Brunner, D., Oeller, N., Szabad, J., Biggs III, W. H., Zipursky, S. L. and Hafen, E. (1994) A gain-of-function mutation in *Drosophila* MAP kinase activates multiple receptor tyrosine kinase signaling pathways Cell 76, 875-888.

Cagan, R.L. and Ready, D.F. (1989). The emergence of order in the *Drosophila* pupal retina. Dev. Biol. 136, 346-362.

Campbell, G., Görling, H., Lin, T., Spana, E., Anderson, S., Doe, C.Q. and Tomlinson, A. (1994). RK2, a glial-specific homeodomain protein required forembryonic nerve cord condensation and viability in *Drosophila*. Developmant 120, 2957-2966.

Campuzano, S., and Modolell, J. (1992). Patterning of the *Drosophila* nervous system: The *acheate-scute* gene complex. Trends Genet. 8, 202-208.

Cheyette, B.N.R., Green, P.J., Martin, K., Garren, H., Hartenstein, V. and Zipursky, S.L. (1994). The *Drosophila* sine oculis locus encodes a homeodomain-containing protein required for the development of the entire visual system. Neuron 12, 977-996.

Cochet, C., Gill, G. N., Meisenhelder, J., Cooper, J. A. and Hunter, T. (1984). C-kinase phosphorylates the epidermal growth factor receptor and reduces its epidermal growth factor-stimulated tyrosine protein kinase activity. J. Biol. Chem. 259, 2553-2558.

Cooley, L., Kelly, R. and Spradling, A. (1988). Insertional mutagenesis of the *Drosophila* genome with single P-elements. Science. 239, 1121-1128.

Cullen, P.J., Hsuan, J.J., Truong, O., Letcher, A.J., Jackson, T.R., Dawson, A.P. and Irvine, R.F. (1995). Identification of a specific Ins(1,2,4,5)P4-binding protein as a member of the GAP family. Nature 376, 527-530.

Davis, C. G. (1990). The many faces of epidermal growth factor repeats. New Biol. 2, 410-419.

Diaz-Benjumera, F., and García-Bellido, A. (1990). Behavior of cell mutant for an EGF receptor homologue of *Drosophila* in genetic mosaics. Proc. R. Soc. Lond. Biol. Sci. 242, 36-44.

Diaz-Benjumea, F. and Hafen, E. (1994). The sevenless signaling casette mediates *Drosophila* EGF receptor function during epidermal development. Development 120, 569-578.

Dickson, B., Sprenger, F., Morrison, D. and Hafen, E. (1992). Raf functions downstream of Ras1 in the Sevenless signal transduction pathway. Nature 360, 600-603.

Dickson, B. and Hafen, E. (1993). Genetic dissection of eye development in *Drosophila*. In The development of *Drosophila melanogaster*. (ed. Bate, M. and Martinez Ariaz, A.) pp. 1327-1362. Cold Spring Harbor, NY: Cold Spring Harbor Laboratory Press.

Dickson, B. and Hafen, E. (1994). Genetics of signal transduction in invertebrates. Curr. Opin. Genet. Dev. 4, 64-70.

Doe, C.Q., Goodman, C.S. (1985). Early events in insect neurogenesis:II. The role of cell interactions and cell lineage in the determination of neuronal precursor cells. Dev. Biol. 111, 206-219.

Doyle, H. J. and Bishop, J. M. (1993). Torso, a receptor tyrosine kinase required for embryonic pattern formation, shares substrates with the sevenless and EGF-R pathways in *Drosohila*. Genes Dev. 7, 633-646.

Fehon, R.G., Kooh, P.J., Rebay, I., Regan, C.L., Xu, T., Muskavitch, M.A.T. and Artavanis-Tsakonas, S. (1990). Molecular interactions between the protein products of the neurogenic loci *Notch* and *Delta*, two EGF-homologous genes in *Drosophila*. Cell 61, 523-534.

Fischbach, K.F. and Dittrich, A.P.M. (1989). The optic lobe of *Drosophila melanogaster*. I. A Golgi analysis of wild-type structure. Cell Tissue Res. 258, 441-475.

Fortini, M.E. and Rubin, G.M. (1990). Analysis of cis-acting requirements of the Rh3 and Rh4 genes reveals a bipartite organization to rhodopsin promoters in *Drosophila melanogaster*. Genes Dev. 4, 444-463.

Freeman, M., Klämbt, C., Goodman, C., and Rubin, G. (1992a). The *argos* gene encodes a diffusible factor that regulates cell fate decisions in the *Drosophila* eye. Cell 69, 963-975.

Freeman, M., Kimmel, B. E., and Rubin, G. M. (1992b). Identifying targets of the rough homeobox gene of *Drosophila*: evidence that rhomboid functions in eye development. Development 116, 335-346.

Freeman, M. (1994). Misexpression of the *Drosophila argos* gene, a secreted regulator of cell determination. Development 120, 2297-2340.

Freeman, M. (1994b) The *spitz* gene is required for photoreceptor determination in the *Drosophila* eye where it interacts with the EGF receptor. Mech. Dev. 48, 25-33.

Fujita, S., Ziprusky, S.L., Benzer, S., Ferrys, A. and Shotwell, S.L. (1982). Monoclonal antibodies against the *Drosophila* nervous system. Proc. Natl. Acad. Sci. USA 79, 7929-7933.

Furuichi, T., Yoshikawa, S., Miyawaki, A., Wada, K., Maeda, N. and Mikoshiba, K. (1989). Primary structure and functional expression of the inositol 1,4,5-trisphosphate-binding protein P400. Nature 342, 32-38.

Gaul, U., Mardon, G and Rubin, G.M. (1992) A putative Ras GTPase activating protein acts as a negative regulator of signaling by the sevenless receptor tyrosine kinase. Cell 68, 1007-1019.

Gonzárez, F., Romani, S., Cubas, P., Modolell, J. and Campuzano, S. (1989). Molecular analysis of the asense gene, a member of the a*chate-scute* complex of *Drosophila melanogaster*, and its novel role in optic lobe development. EMBO J. 8, 3553-3562.

Green, P., Hartenstein, A.Y. and Hartenstein, V. (1993). The embryonic development of the *Drosophila* visual system. Cell Tissue Res 273, 583-598.

Hafen, E., Basler, K., Edstroem, J. E. and Rubin, G. M. (1987). sevenless, a cell-specific homeotic gene of *Drosophila*, encodes a putative transmembrane receptor with a tyrosine kinase domain. Science 236, 55-63.

Halter, D.A., Urban, J., Rickert, C., Ner, S.S., Ito, K., Travers, A.A. and Technau, G.M. (1995). The homeobox gene *repo* is required for the differentiation and maintenance of glia function in the embryonic nervous system of *Drosophila melanogaster*. Development 121, 317-322.

Hart, A. C., Krämer, H., Van Vactor, Jr., D. L., Paidhungat, M., and Zipursky, S. L. (1990). Induction of cell fate in the *Drosophila* retina: the bride of sevenless protein is predicted to contain a large extracellular domain and seven transmembrane segments. Genes Dev. 4, 1835-1847.

Hartenstein, A.Y., Rugendorff, A.E., Tepass, U. and Hartenstein, V. (1992). The function of neurogenic genes during epithelial development in the *Drosophila* embryo. Development 116, 1203-1220.

Heberlein, U. and Rubin, G.M. (1991). *Star* is required in a subset of photoreceptor cells in the developing *Drosophila* retina and displays dosage sensitive interactions with rough. Dev. Biol. 144, 353-361.

Heberlein, U., Hariharan, I.K. and Rubin, G.M. (1993). Star is required for neuronal differentiation in the *Drosophila* retina and displays dosage-sensitive interactions with ras1. Dev. Biol. 160, 51-63.

Heitzler, P. and Simpson, P. (1991). The choice of cell fate in the epidermis of *Drosophila*. Cell 64, 1083-1092.

Hofbauer, A. and Campos-Ortega, J.A. (1990). Proliferation pattern and early differentiation of the optic lobes in *Drosophila melanogaster*. Roux's Arch Dev. Biol. 198, 264-274.

Holt, C.E., Bertsch, T.W., Ellis, H.M. and Harris, W.A. (1988). Cellular determination in the Xenopus retina is independent of lineage and date of birth. Neuron 1, 15-26.

Hou, X.S., Chou,T.-B., Melnick, M.B. and Perrimon, N. (1995) The Torso receptor tyrosine kinase can activate Raf in a Ras-independent pathway. Cell 81, 63-71.

Hsu, J. and Perrimon, N. (1994) A temperature-sensitive MEK mutation demonstrates the conservation of the signaling pathways activated by receptor tyrosine kinases. Genes Dev. 8, 2176-2187.

Hutchins, J.B. and Casagrande, V.A. (1988). Glial cells develop a laminar pattern before neuronal cells in the lateral geniculate nucleus. Proc. Natl. Acad. Sci. USA. 85, 8316-8320.

Ingham, P.W., Howard, K.R. and Ish-Horowitz, D. (1985). Transcription pattern of the *Drosophila* segmentation gene hairy. Nature 318, 439-445.

Jacobs, J.R. and Goodman, C.S. (1989). Embryonic development of axon pathways in the *Drosophila* CNS. I. A glial scaffold appears before the first growth cones. J. Neurosci. 9, 2402-2411.

Jürgens, G., Lehman, R., Schardin, M. and Nüsslein-Volhard, C. (1986). Segmental organization of the head in the embryo of *Drosophila melanogaster*. A blastoderm fate map of the cuticle structures of larval head. Wilhem Roux's Arch. Dev. Biol. 195, 359-377.

Kaphingst, K. and Kunes, S. (1994). Pattern formation in the visual centers of the Drosophila brain: wingless acts via decapentaplegic to specify the dorsoventral axis. Cell 78, 437-448.

Karess, R. and Rubin, G. M. (1984). Analysis of P transposable element functions in *Drosophila*. Cell 38, 135-146.

Kidd, S., Kelley, M.R. and Young, M.W. (1986). Sequences of the *Notch* locus of *Drosophila melanogaster*: Relationship of the encoded protein to mammalian clotting and growth factors. Mol. Cell. Biol. 6, 3094-3108.

Klingler, M., Erdélyi, M., Szabad, J. and Nüsslein-Volhard, C. (1988). Function of torso in determining the terminal anlagen of the *Drosophila* embryo. Nature 335, 275-277.

Kolodkin, A.L., Pickup, A.T., Lin, D.M., Goodman, C.S. and Banerjee, U. (1994). Characterization of Star and its interactions with sevenless and EGF receptor during photoreceptor cell development in *Drosophila*.. Development 120, 1731-1745.

Kopczynski, C.C., Alton, A.K., Fechtel, K., Kooh, P.J. and Muskavitch, M.A.T. (1988). *Delta*, a *Drosophila* neurogenic gene is transcriptionally complex and encodes a protein related to blood coagulation factors and epidermal growth factor from vertebrates. Gene Dev. 2, 1723-1735.

Krämer, H., Cagan, R. L., and Zipursky, S. L. (1991). Interaction of bride of sevenless membrane-bound ligand and the sevenless tyrosine-kinase receptor. Nature 352, 207-212.

Kretzschmar, D., Brunner, A., Wiersdorff, V., Pflugfelder, G.O., Heisenberg, M and Schnewly, S. *giant lens,* a gene involved in cell determination and axonal guidance in the visual system of *Drosophila melanogaster*. EMBO J. 11, 2531-2539.

Kunes, S. and Steller, H. (1991). Ablation of *Drosophila* photoreceptor cells by conditional expression of a toxin gene. Genes Dev. 5, 970-983.

Kunes, S., Wilson, C., and Steller, H. (1993). Independent guidance of retinal axons in the developing visual system of *Drosophila*. J. Neurosci. 13, 752-767.

Kunes, S. and Steller, H. (1993). Topography in the *Drosophila* visual system. Current Opinion Neurobiol. 3, 53-59.

Kyte, J. and Doolittle, R.F. (1982). A simple method for displaying the hydropathic character of proteins. J. Mol. Biol. 157, 105-132.

Lawrence, P.A., Green, S.M. (1979). Cell lineage in the developing retina of *Drosophila*. Dev. Biol. 71, 142-152.

Lawrence, P.A., Johnston, P. and Morata, G. (1986). Methods of marking cells. In: Roberts, D.B. (ed) *Drosophila*: A Practical Approach. IRL Press, Oxford, pp 229-242.

Le Douarin, N.M. (1980). The ontogeny of neural crest in avian embryo chimeras. Nature 286, 663-669.

Lindsley, D. L., and Zimm, G. G. (1992). "The Genome of *Drosophila melanogaster*." Academic Press, San Diego.

Luskin, M.B., Pearlman, A.L. and Sanes, J.R. (1988). Cell lineage in the cortex of the mouse studied in vivo and in vitro with a recombinant retrovirus. Neuron 1, 635-647.

Markopoulou, K. and Artavanis-Tsakonas, S. (1989). The expression of the neurogenic locus Notch during the postembryonic development of *Drosophila melanogaster* and its relationship to mitotic activity. J. Neurogenet. 6, 11-26.

Mayer, U., and Nüsslein-Volhard, C. (1988). A group of genes required for pattern formation in the ventral ectoderm of the *Drosophila* embryo. Genes Dev. 2, 1496-1511.

Meinertzhagen, I. (1973). Development of the compound eye and optic lobe of insects. In Developmental Neurobiology of arthropods (ed. D. Young), pp. 52-104. Cambridge: Cambridge University Press.

Meinertzhagen, I. and Hanson, T.E. (1993).The development of the optic lobe. In "The Development of *Drosophila melanogaster*." (ed. M. Bate and A. M. Arias), pp. 1363-1505. New York: Cold Spring Harbor Laboratory Press

Meyerowitz, E.M., Kankel, D.R. (1978). A genetic analysis of visual system development in *Drosophila melanogaster*. Dev. Biol. 62, 112-142.

Mlodzik, M. and Hiromi, Y. (1992). The enhancer trap method in *Drosophila*: its application to neurobiology. In : Cann PM (eds) Gene expression in Neural Tissues (Methods in Neuroscience vol 9) Academic Press, Orland, pp. 397-414.

Mlodzik, M., Baker, N. and Rubin, G.M. (1990). Isolation and expression of *scabrous*, a gene regulating neurogenesis in *Drosophila*. Gene Dev. 4, 1848-1861.

Mlodzik, M., Hiromi, Y., Weber, U., Goodman, C.S. and Rubin, G.M. (1990). The *Drosophila seven up* gene, a member of the steroid receptor gene superfamily controls photoreceptor cell fate. Cell 60, 211-224.

Moses, K., Ellis, E. C., and Rubin, G. M. (1989). The glass gene encodes a zinc-finger protein required by *Drosophila* photoreceptor cells. Nature 340, 531-536.

Nishida, Y., Hata, M., Ayaki, T., Ryo, H., Yamagata, M., Shimizu, K. and Nishizuka, Y. (1988) Proliferation of both somatic and germ cells is affected in the *Drosophila* mutants of *raf* proto-oncogene. EMBO J. 7, 775-781.

O'Conell, P. and Rosbash, M. (1984). Sequence, structure, and codon preference of the *Drosophila*.ribosomal protein 49 gene. Nucl. Acid Res. 12, 5495-5513.

O'Kane, C.J. and Gehring, W.J. (1987). Detection in situ of genomic regulatory elements in *Drosophila*. Proc. Natl. Acad. Sci. USA 84, 9123-9127.

Okano, H., Hayashi, S., Tanimura, T., Sawamoto, K., Yoshikawa, S., Watanabe, J., Iwasaki, M., Hirose, S., Mikoshiba, K., and Montell, C. (1992). Regulation of *Drosophila* neural development by a putative secreted protein. Differentiation 52, 1-11.

Olivier, J. P., Raabe, T., Henkemeyer, M., Dickson, B., Mbamalu, G., Margolis, B., Schlessinger, J., Hafen, E. and Pawson, T. (1993). A *Drosophila* SH2-SH3 adaptor protein implicated in coupling the Sevenless tyrosine kinase to an activator of Ras guanine nucleotide exchange, Sos. Cell 73, 179-191.

Pflugfelder, G.O., Roth, H., Poeck, B., Kerscher, S., Schwarz, H., Jonschker, B. and Heisenberg, M. (1992). The *lethal(1)optomoter-blind* gene of *Drosophila melanogaster* is a major organizer of optic lobe development: Isolation and characterization of the gene. Proc. Natl. Acad. Sci. USA 89, 1199-1203.

Puissant, C., Houdebine, L.M. (1990). An improvement of the single-step method of RNA isolation by acid guanidium thiocyanate-phenol-chloroform extraction. BioTechniques 8, 148-149.

Ready, D.F., Hanson, T.E. and Benzer, S. (1976). Development of the *Drosophila* retina, a neurocrystalline lattice. Gene Dev. 53, 217-240.

Ready, D. F., Tomlinson, A., and Lebovits, R. M. (1986). Building an ommatidium: Geometry and genes. In "Development of order in the visual system " (S. R. Hilfer, and J. B. Shejjield, Eds.), pp. 97-125. Springer-Verlag, New York.

Ready, D. (1989). A multifaceted approach to neural development. Trens Neurosci. 12, 102-110.

Rebay, I., Fleming, R.J., Fehon, R.G., Cherbas, P. and Artavanis-Tsakonas, S. (1991). Specific EGF repeats of Notch mediate interactions with Delta and Serrate: implications for Notch as a multifunctional receptor. Cell 67, 687-699.

Rebay, I., Fehon, R. G., and Artavanis-Tsakonas, S. (1993). Specific truncation of *Drosophila* Notch define dominant activated and dominant negative forms of the receptor. Cell 74, 319-329.

Roberts, D.B. (1986). Basic *Drosophila* care and techniques. In: Roberts DB (ed) *Drosophila*: A Practical Approach. IRL Press, Oxford, pp. 1-38.

Robertson, H.M., Preston, C.R., Phillis, R.W., Johnson-Schlitz, D.M., Benz, W.K. and Engels, W.R. (1988). A stable genomic source of P element transposase in *Drosophila melanogaster*. Genetics 118, 461-470.

Rogge, R.D., Kariovich, C.A. and Banerjee, U. (1991). Genetic dissection of a neurodevelopmental pathway: Son of sevenless functions downstream of the sevenless and EGF receptor tyrosine kinases. Cell 64, 39-48.

Rubin, G.M. and Spradling, A.C. (1982). Genetic transformation of *Drosophila* with transposable element vectors. Science 218, 348-353.

Sambrook, J., Fritsch, E.F., Maniatis, T. (1989). Molecular Cloning: A Laboratory Manual, 2nd ed. Cold Spring Harbor Laboratory Press, New York.

Sanger, F., Nicklen, S. and Coulson, A. (1977). DNA sequencing with chain terminating inhibitors. Proc. Natl. Acad. Sci. USA 74, 5463-5467.

Sawamoto, K., Okano, H., Kobayakawa, Y., Hayashi, S., Mikoshiba, K. and Tanimura, T. (1994). The function of *argos* in regulating cell fate decisions during the *Drosophila* eye and wing vein development. Dev. Biol. 164, 267-276.

Sawamoto, K., Okabe, M., Tanimura, T., Hayashi, S., Mikoshiba, K. and Okano, H. (1996) *argos* is required for projection of photoreceptor axons during optic lobe development in *Drosophila*. Dev. Dyn. (in press)

Schnewly, S., Klemenz, R., and Gehring, W. J. (1987). Redesigning the body plan of *Drosophila* by ectopic expression of the homeotic gene Antennapedia. Nature 325, 816-818.

Schüpbach, T. (1987). Germ line and soma cooperate during oogenesis to establish the dorsoventral pattern of the egg shell and embryo in *Drosophila melanogaster*. Cell 49, 699-707.

Schweitzer, R., Shaharabany, M., Seger, R and Shilo, B.-Z. (1995a). Secreted spitz triggers the DER signaling pathway and is a limiting component in embryonic ventral ectoderm determination. Genes Dev. 9, 1518-1529.

Schweitzer, R., Howes, R., Smith, R., Shilo, B.-Z. and Freeman, M. (1995b). Inhibition fo *Drosphila* EGF receptor activation by the secreted protein Argos. Nature 376, 699-702.

Selleck, S.B. and Steller, H. (1991). The influence of retinal innervation on neurogenesis in the first optic ganglion of *Drosophila*. Neuron 6, 83-99.

Selleck, S.B., Gonzalez, C., Glover, D.M. and White, K. (1992). Regulation of the G1-S transition in postembryonic neuronal precursors by axon ingrowth. Nature 355, 253-255.

Serafini, T., Kennedy, T.E., Galko, M.J., Mirzayan, C., Jessel, T.M. and Tessier-Lavigne, M. (1994). The netrins define a family of axon outgrowth-promoting proteins homologous to C. elegans UNC-6. Cell 78, 409-424.

Serikaku, M.A. and O'Tousa, J.E. (1994). *sine oculis* is a homeobox gene required for *Drosophila* visual system development. Genetics 138, 1137-1150.

Simon, M. A., Bowtell, D. D. L., and Rubin, G. M. (1989). Structure and activity of the sevenless protein: A protein tyrosine kinase receptor required for photoreceptor development in *Drosophila*. Proc. Natl. Acad. Sci. USA 86, 8333-8337.

Simon, M. A., Bowtell, D. D., Dodson, G. S., Laverty, T. R. and Rubin, G. M. (1991). Ras1 and a putative guanine nucleotide exchange factor perform crucial steps in signaling by the sevenless protein tyrosine kinase. Cell 67, 701-716.

Simon, M. A., Dodson, G. S. and Rubin, G. M. (1993). An SH3-SH2-SH3 protein is required for p21Ras1 activation and binds to sevenless and Sos proteins in vitro. Cell 73, 169-177.

Spradling, A.C. and Rubin, G.M. (1982). Transposition of cloned P-elements into *Drosophila* chromosomes. Science 218, 341-347.

Spreij, T.E. (1971). Cell death during the development of the imaginal discs of Calliphora erythrocephala. Netherlands J. Zool. 21, 221-264.

Sprenger, F. and Nüsslein-Volhard, C. (1992). Torso receptor activity is regulated by a diffusible ligand produced at the extracellular terminal regions of the *Drosophila* egg. Cell 71, 987-1001.

Steller, H., Fischbach, K.F. and Rubin, G.M. (1987). Disconnected, a locus required for neuronal pathway formation in the visual systems of *Drosophila*. Cell 50, 1139-1153.

Strausfeld, N.J. (1976). Atlas of an Insect Brain. New York: Springer-Verlag.

Sturtevant, M. A., Roark, M., and Bier, E. (1993). The *Drosophila rhomboid* gene mediates the localized formation of wing veins and interacts genetically with components of the EGF-R signaling pathway. Genes Dev. 7, 961-973.

Tautz, D. and Pfeifle, C. (1989). A non-radioactive in situ hybridization method for the localization of specific RNAs in *Drosophila* embryos reveals translational control of the segmentation gene *hunchback*. Chromosoma 98, 81-85.

Tepass, U., Theres, C. and Knust, E. (1990). *crumbs* encodes an EGF-like protein expressed on apical membranes of *Drosophila* epithelial cells and required for organization of epithelia. Cell 61, 787-799.

Thummel, C. S., and Pirrotta, V. (1991). New CaSpeR P-element vectors. *Drosophila* Information News Letter 2.

Tio, M., Ma, C. and Moses, K. (1994) spitz, a *Drosophila* homolog of transforming growth factor-α, is required in the founding photoreceptor cells of the compound eye facets. Mech. Dev. 48,13-23.

Tomlinson, A. and Ready, D. F. (1986). *sevenless*, a cell-specific homeotic mutation of the *Drosophila* eye. Science 231, 400-402.

Tomlinson, A., and Ready, D. F. (1987). Neuronal differentiation in the *Drosophila* ommatidium. Dev. Biol. 123, 264-275.

Trujillo-Cenoz, O. and Melamed, J. (1973). The development of the retina-lamina complex in muscoid flies. J. Ultrastruct. Res. 42, 554-581.

Tsuda, L., Inoue, Y. H., Yoo, M., Mizuno, M., Hata, M., Lim, Y., Adachi-Yamada, T., Ryo, H., Masamune, Y. and Nishida, Y. (1993) A protein kinase similar to MAP kinase activator acts downstream of the raf kinase in *Drosophila*. Cell 72, 407-414.

Turner, D.L. and Cepko, C.L. (1987). A common progenitor for neurons and glia persists in rat retina late in development. Nature 328, 131-136.

Vassein, H., Bremer, K..A, Knust, E. and Campos-Ortega, J.A. (1987). The neurogenic locus Delta of *Drosophila melanogaster* is expressed in neurogenic territories and encodes a putative transmembrane protein with EGF-like repeats. EMBO J. 6, 3431-3440.

Watanabe, T. and Kankel, D.R. (1992). The *l(1)ogre* gene of *Drosophila melanogaster* is expressed in postembryonic neuroblasts. Dev. Biol. 152, 172-183.

Wemmer, T. and Klämbt, C. (1995). A genetic analysis of the *Drosophila* closely linked interacting genes *bulge, argos* and *soba*. Genetics 140, 629-641.

Wharton, K.A., Johansen, R.M., Xu, T. and Artavanis-Tsakonas, S. (1985). Nucleotide sequence from the neurogenic locus Notch implies a gene product that shares homology with proteins containing EGF-like repeats. Cell 43, 567-581.

White, K. and Kankel, D.R. (1978). Patterns of cell division and cell movement in the formation of the imaginal nervous system in *Drosophila melanogaster*. Dev. Biol. 65, 296-321.

Wieschaus, E. and Nüsslein-Volhard, C. (1986). Looking at embryos. In: Roberts DB (ed) *Drosophila*: A Practical Approach. IRL Press, Oxford, pp 199-227.

Wigglesworth, V. B. (1940). Local and general factors in the development of "pattern" in Rhodnius prolixus (Hemiptea). J. Exp. Biol. 17, 180-200.

Winberg, M. L., Perez, S. E. and Steller, H. (1992). Generation and early differentiation of glial cells in the first optic ganglion of *Drosophila melanogaster*. Development 115, 903-911.

Wolff, T., and Ready, D. F.(1991) Cell death in normal and rough eye mutants of *Drosophila*. Development 113, 825-839.

Xiong, W. C., and Montell, C. (1993). tramtrack is a transcriptional repressor required for cell fate determination in the *Drosophila* eye. Genes Dev. 7, 1085-1096.

Xiong, W. C., Okano, H., Patel, N. H., Blendy, J. A., and Montell, C. (1994). *repo* encodes a glial specific homeodomain protein required in the *Drosophila* nervous system. Genes Dev. 8, 981-994.

Xu, T. and Rubin, G. M. (1993). Analysis of genetic mosaics in developing and adult *Drosophila* tissues. Development 117, 1223-1237.

Zipursky, S.L., Venkatesh, T.R., Teplow, D.B. and Benzer, S. (1984). Neuronal development in the *Drosophila* retina: Monoclonal antibodies as molecular probes. Cell 36, 15-26.

Zuker, C.S., Cowan, A.F. and Rubin, G.M. (1985). Isolation and structure of a rhodopsin gene from D. *melanogaster*. Cell 40, 851-858.

Conclusions

The *Drosophila* mutant, *argos*, was isolated as a novel visual system mutant displaying a rough eye phenotype. Mutations in the *argos* gene affect eye development, leading to irregular spacing of ommatidia and an increase in the number of photoreceptor cells. In addition to affecting the visual system, they cause abnormal head involution, an increased number of sensilla in the antenno-maxillary complex in the embryonic stage, and abnormal morphogenesis of labial pulps and the wings in later stages. I examined the expression of the *argos* gene during development in terms of *LacZ* expression from enhancer trap elements inserted within the *argos* gene. During embryogenesis, expression of *LacZ* showed a segmental pattern in the ectoderm and in the nervous system. In the eye imaginal discs, *LacZ* began to be expressed in photoreceptor cells, a few rows posterior to the morphogenetic furrow. It was also expressed in the wing disc. I cloned the *argos* gene by P-element tagging. The sequence of the *argos* cDNA predicted that its product is a secreted peptide with a putative epidermal growth factor (EGF) motif. Ubiquitously expressed *argos* product restored all the loss-of-function phenotypes. Overexpression of *argos* in the wild-type background resulted in the reduced number of photoreceptor cells, cone cells and pigment cells, which are opposite phenotypes to those of the loss-of-function mutants. The *argos* gene is expressed in developing wing veins. Ubiquitous *argos* expression caused loss of veins in a dosage-dependent manner. This phenotype was enhanced by the loss-of-function rhomboid mutation, implying the possibility that *argos* and *rhomboid* play key roles in a common pathway for the normal wing vein formation. These results indicate that *argos* is a diffusible factor negatively regulating the cellular differentiation in multiple developmental processes such as eye and wing morphogenesis.

argos expression was also observed in the optic lobes throughout the developmental stages. In *argos* mutants, neuropiles failed to develop normally during embryonic and larval stages, and photoreceptor axons did not project properly into the lamina. Ubiquitous expression of *argos*, under control of the hsp70 promoter, rescued the defects in optic lobes. I have found that glial cells failed to differentiate in the larval optic lobes of *argos* mutants. Correspondingly, in the loss-of-function repo mutants, whose glial cells also fail to differentiate, photoreceptor axons showed the impaired projection pattern similar to the *argos* phenotype. These results suggest that glial cells play a role for guidance of photoreceptor axons. The loss-of-function Star mutation (*Star*^{X155}) dominantly suppressed the defects in the *argos* optic lobes, suggesting that these two genes act in an antagonistic fashion during optic lobe development.

Finally, to better understand the role of *argos*, I have analyzed genetic interactions of *argos* with other genes involved in the Ras/MAPK signal transduction. Hypomorphic mutation in Star acted as a dominant suppressor of the *argos* null phenotype. Effect of expression of the *hs-argos* transgene was enhanced by the loss-of-function Star mutations. Gain-of-function mutation in the MAPKK gene (*Dsor1*^{Su1}) caused a overproduction of photoreceptor R7 and wing veins. *Dsor1*^{Su1} suppressed the phenotype caused by the *hs-argos* expression. *Dsor1*^{Su1}also enhanced the *argos* loss-of-funtion phenotype. Gain-of-function mutations of rolled, a MAP kinase gene, suppressed the defects caused by the *hs-argos*. These results provide evidences that *argos* negatively regulate the signal transduction in the MAPK cascade for regulation of cellular differentiation.

Acknowledgment

I am deeply grateful to my supervisors, Professors Katsuhiko Mikoshiba and Hideyuki Okano, for their thoughtful advices throughout this study. I thank Yasuyoshi Nishda, Craig Montell, Teiichi Tanimura, Shigeo Hayashi, Yoshitaka Kobayakawa, Yoshitoshi Kasuya, Shingo Yoshikawa, Masayuki Iwasaki and Masataka Okabe for their good collaboration and discussions, Yoshiki Hotta, Daisuke Yamamoto, Yasushi Hiromi, Steve West and Takao Shimizu for valuable comments on the manuscript, Herman Steller, Toyohei Saigusa, Masayuki Miura, Tadashi Uemura, Kei Ito, Takehide Murata, Toshihiko Hosoya, Leo Tsuda, Lim Y.-M., Sharon E. Perez, and Shin-ichi Sakakibara for useful advices, Masato Yasui, Kyoko Fuji, Mariko Yamasaki, Shouko Aoki, Sayaka Satoh, Katsuya Amano and Keiko Kawamatsu for technical assistance, Keiko Okano, Kaori Kawamoto, Nobuko Maeda and Naomi Sawamoto for secretarial jobs and help in preparation of the manuscript, Utpal Banerjee, Andrew Tomlinson, Gerald Rubin, Corey Goodman, Allan Spradling, Matthew Scott, Shinobu C. Fujita, Ernst Hafen, Carl Thummel, Vince Pirrota, Walter Gehring, Bloomington Stock Center and Indiana Stock Center for supplying the fly stocks, vectors, and/or antibodies.

This study was supported by grants from the Ministry of Science, Culture and Education. I am grateful to the research fellowship of the Japan society for the promotion of science for young scientists. Finally, I would like to express my gratitude to all my family for continuous encouragement throughout this study.

January, 1996

澤本和延

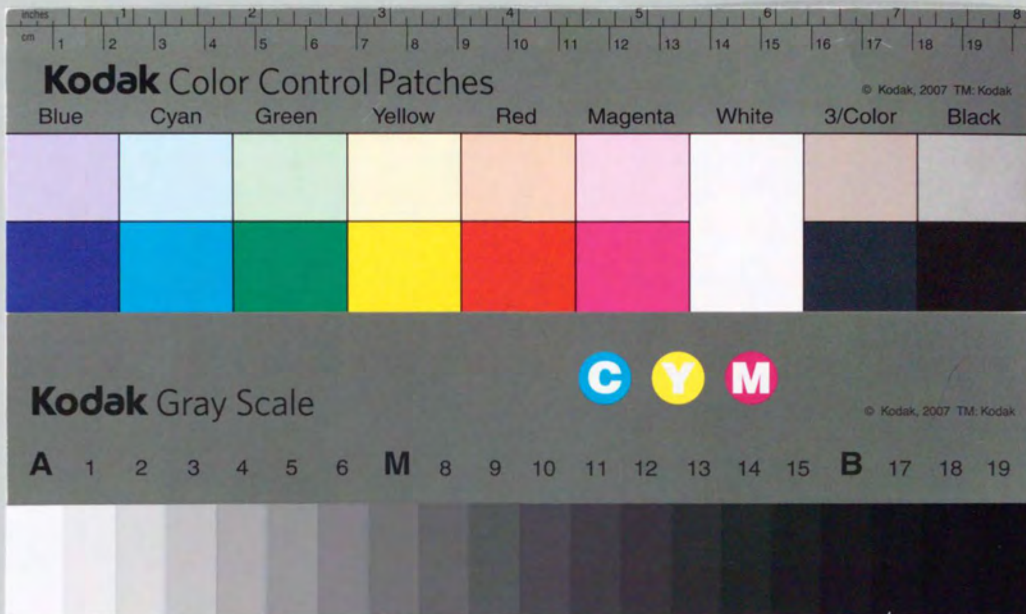
Kodak Color Control Patches
© Kodak, 2007 TM: Kodak
Blue Cyan Green Yellow Red Magenta White 3/Color Black
Kodak Gray Scale
C Y M
© Kodak, 2007 TM: Kodak
A 1 2 3 4 5 6 M 8 9 10 11 12 13 14 15 B 17 18 19